SUPER PRECISION ADAPTIVE ARRAY PROCESSING AND SYSTOLIC ARRAY STRUCTURES

By

© BANDULA WICKRAMARATNA DAHANAYAKE

A thesis

Submitted to the School of Graduate Studies

in Partial Fulfilment of the Requirements

for the Degree

Doctor of Philosophy

McMaster University

1987

DOCTOR OF PHILOSOPHY (1987) McMASTER UNIVERSITY

(Electrical and Computer Engineering) Hamilton, Ontario

TITLE Super Precision Adaptive Array Processing and Systolic Array Structures

AUTHOR Bandula Wickramaratna Dahanayake

B.Sc.Eng. (Hons), University of Sri Lanka, Sri Lanka

M.Eng., Memorial University of Newfoundland, Canada

SUPERVISOR Professor K.M. Wong

NUMBER OF PAGES viii, 201

SUPER PRECISION ARRAY PROCESSING

ABSTRACT

Adaptive array processing is considered as a task of bearing estimation and beamforming.

The use of the subspace decomposition in bearing estimation is studied. Operator decomposition approach is used to provide a more basic and unified framework to the spectrum representation. This unified approach is then utilized to study the geometric relationships between the conventional, high resolution, and super resolution spectrum estimation techniques.

Bearing estimation under coherent signal environment is considered. A methodology is developed to estimate the number of incoming signals and the optimum number of subarrays concurrently.

Beamforming is presented in a more general framework. The concept of beamforming as a process of joint bearing estimation and interference cancellation is proposed.

Finally, a restart to the array processing and digital signal processing problems in general, is initiated.

ACKNOWLEDGEMENTS

I would like to thank Dr. K. M. Wong for his guidance and encouragement as a supervisor, and above all for his friendliness and approachability.

Thanks are also due to Dr. S. Haykin, Dr. P. C. Yip and J. P. Reilly for being supportive as supervisory committee members.

I especially thank Dr. G. P. Madhavan and Dr. P. C. Yip for their help in bringing the thesis into this form.

Finally, I would like to extend my sincere thanks to my friends and colleagues, especially Mr. B. P. Mohanty, Dr. S. Puthenpura, and Miss Yi Zhou for their constant encouragement during the course of study.

TABLE OF CONTENTS

CHAPTER 1

INTRODUCTION TO ARRAY PROCESSING

A set of sensing elements placed in a known spatial pattern is generally referred to as an array. The aim of array processing is to extract the environmental information of interest from the signals received by the array. Array processing has proved to be useful in different disciplines such as radar, sonar, communication, seismology, and astronomy. The information to be extracted may in general be different in different contexts.

In general, the task of array processing can be divided into two major categories, viz:

(a) Bearing estimation : Estimation of the angle of arrival of the signal

(b) Beamforming : Reception of a particular signal of interest while suppressing others.

Beamforming can further be divided into two sub categories, namely:

(1) Reception of a signal coming from a known direction while suppressing other interferences

(2) Reception of all the incoming signals from distinct and unknown directions separately while suppressing the rest of the signals which appear as interferences to the signal chosen to receive.

Adaptive array processing has received a great deal of attention in many areas such as, radar, sonar, communication and seismology as a means of performing the above tasks. One of the primary reasons for this fast growing interest in adaptive array is its capability to automatically perform on-line

processing in a given signal environment. The self adjusting or adaptive capability renders the operation of such systems more reliable and flexible and, more importantly, offers improved reception performance.

An array of sensors operates in the inevitable presence of undesirable interferences which may consist of deliberate electronic countermeasures, nonhostile interferences, clutter scatter returns and natural noise sources. Degradation of the array performance due to such noise may be further aggravated by random sensor motion, poor siting conditions, multipath ray effects and a constantly changing interference environment. Therefore, the suppression of interference is quite important in all applications. Adaptive array system has the ability to automatically sense the presence of interference noise sources and suppress these noise sources while simultaneously enhancing the desired signal reception without a priori knowledge of the signal or noise environment.

After reviewing the tasks of the array processing and the advantages of the adaptive array processing briefly, we next consider the first array processing task: Bearing Estimation.

In bearing estimation, high resolution techniques such as maximum likelihood (ML) [Capon(1969)], and the linear prediction (LP) introduced and developed by Yule, Walker, Wiener and Levinson, and further developed by Burg (1967,1969), McDonough (1974) and many others have been used until the recent development of super resolution techniques. Super resolution techniques such as Pisarenko harmonic decomposition (PHD) [Pisarenko (1972)], Modified forward and backward linear prediction (MFBLP) [Tuft and Kumaresan (1982)], Multiple signal classification (MUSIC) [Schmidt (1979,1982)] and minimum norm (MN) method [Kumaresan and Tuft (1983)] are based on the subspace decomposition of cross spectral density matrix. Out of all the above super resolution techniques, the

MUSIC method introduced by Schmidt has been of great interest to many researchers. The MUSIC method has been developed as a direct consequence of the maximum likelihood (ML) method and can also be considered as a generalized version of the Pisarenko harmonic decomposition.

More recently, another approach to the bearing estimation problem, called the estimation of signal parameters by rotational invariant technique (ESPRIT) was proposed by Paulraj, Roy, and Kailath (1986). ESPRIT makes the assumption that the noise is spatially uncorrelated and the variance of the noise is known. The variance of the noise is not known in practice and hence the applicability of the ESPRIT will be limited. A new approach to the bearing estimation problem with minimum assumption can be found in Dahanayake (1987).

Subspace decomposition of the cross spectral density matrix is generally obtained by using the generalized eigenvalue eigenvector decomposition of the matrix pencil (signal + noise cross spectral density matrix, noise only cross spectral density matrix). Algorithms for generalized eigenvalue eigenvector decomposition can be found in Moler and Stewart (1973), Peters and Wilkinson (1970), Kaufman (1974,1977), Stewart (1972), and Ward (1975). The solution to the generalized eigenvalue eigenvector decomposition problem through the generalized singularvalue singularvector decomposition operated on the matrix pencil (signal + noise data matrix, noise only data matrix) has been of interest recently due to its numerical stability. Algorithms for computing the generalized singularvalue singularvector decomposition can be found in Van Loan (1975,1976), Chan (1982), Luk (1980). A more general and computationally amenable solution has been given by Paige and Saunders (1981). Once the signal and noise space basis vectors are obtained through the generalized eigenvalue eigenvector decomposition or generalized singularvalue singularvector decomposition, signal and noise subspaces

are generally separated based on an information theoretic criterion such as Akaike information theoretic criterion (AIC) or minimum description length criterion (MDLC). In the array processing context, AIC and MDLC had been investigated by Wax and Kailath (1984), Matsuoka and Ulrych (1986), Wang and Kaveh (1986), Kaveh and Wang (1987).

As for beamforming, we find that many criteria have been developed in the past years, out of which the minimum variance distortionless response (MVDR) beamformer due to Capon (1969) has been of interest to many researchers [Monzingo and Miller (1980), Haykin (1985, 1986)]. Surprisingly, to our knowledge all the existing beamformers are capable of receiving signals coming from a known direction while suppressing the rest of the signals and none of the available beamformers are capable of receiving the signal reaching from unknown and distinct directions while suppressing the interferences. Some constructive philosophical thoughts about adaptive array processing beyond the beamforming can be found in Mermoz (1981).

Neither bearing estimation nor beamforming techniques would perform successfully when the incoming signals are coherent. Solution to the difficulties associated with the coherent signal environment has been achieved by spatial smoothing of the cross spectral density matrix [Evans et al (1982)]. Further discussion on the spatial smoothing of the cross spectral density matrix can be found in recent papers by Shan and Kailath (1985), Shan, Wax and Kailath (1985).

Having briefly discussed the adaptive array processing as a whole, now we consider the implementation measures. In general high performance special purpose computer systems are used to meet specific application requirements or to off load computations that are specially taxing on general purpose computers. To achieve this in adaptive array processing, the concept of systolic architec-

tures, a general methodology for mapping high level computations into the hardware structures has been the most recent interest of many disciplines. In a systolic system, data flow from the computer memory in a rhythmic fashion, passing through many processing elements before they return to the memory. Such architecture and algorithms provide modular parallelism, regular data flow, and high efficiency, while using only local interconnections. Since essentially constant efficiency is maintained as the parallelism is increased, they are especially attractive for the intensive, and highly regular computations needed in bearing estimation and beamforming in adaptive array processing. More detailed discussion about the systolic architecture can be found in Kung (1982).

In adaptive array processing, a major portion of the resulting computational load can be reduced to a common set of basic matrix operations including matrix - vector multiplication, matrix - matrix multiplication and addition, linear equation solution and least squares approximate solutions, solution of Hermitian eigensystems and generalized eigensystems, singularvalue decomposition and generalized singularvalue decomposition, and general matrix eigenvalue decomposition. Extensive discussion on the use of systolic architecture in signal processing can be found in Speiser and Whitehouse (1981,1983), Bromley and Whitehouse (1981), Kung, Whitehouse and Kailath (1985), Gentleman and Kung (1981), Mcwhirter (1981), Kailath (1983) and Haykin (1986), Kung (1986). Solution to the singularvalue singularvector decomposition and generalized symmetric eigenvalue eigenvector decomposition on multiprocessor arrays can be found in Brent and Luk (1985).

Up to this point we have briefly presented the task of array processing, advantages of adaptive array processing, bearing estimation techniques, beamforming techniques, use of the systolic architecture in implementation. Therefore,

now it is the time to present our contribution. In this thesis, we introduce new techniques along with more general unification to both bearing estimation and beamforming in adaptive array processing. These techniques are developed in the form of systolic array structures which is suitable for mapping them into hardware structures. This thesis is organized in such a way that each chapter as well as each section within it present some contribution to the field of array processing.

CHAPTER 2

SUBSPACE DECOMPOSITION IN ADAPTIVE ARRAY PROCESSING

Preview An array of sensors, which is excited by narrow band or broad band signals coming from distinct directions is considered. A signal model is suitably formulated to make use of the frequency domain processing in bearing estimation and beamforming in adaptive array processing. Operator decomposition approach is used in solving the array processing problem.

Vectors that represent the signal and noise space are obtained by using the generalized eigenvalue eigenvector decomposition. Significance of the generalized eigenvalues and generalized eigenvectors is studied. Proper orthogonal projection multiple classification (POP-MUSIC) spectrum estimation technique is introduced. It is shown that the POP-MUSIC is a more generalized version of the MUSIC method.

Stationary signal and noise environment is assumed throughout this formulation. Slow varying nonstationary environments can be handled by using a forgetting factor.

2.0 Problem Definition

In the space if we have signals coming from different directions, it is the interest of many disciplines to find out the directions they come from and obtain the information contain in those signals. To receive the incoming signals

and to discriminate against them we use an array of sensors. In general array of sensors can have any arbitrary geometry. But for simplicity we consider a linear array of uniformly spaced sensors. The basic nature of the array is given below.

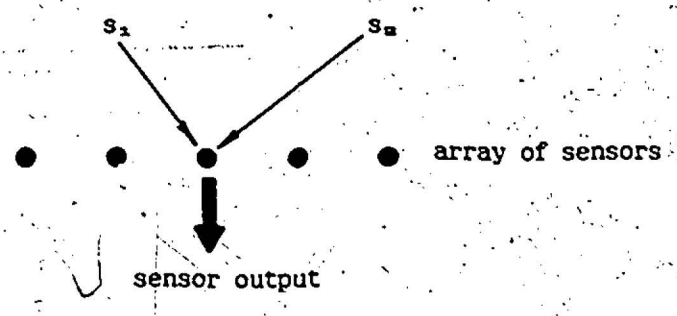

Our task is to obtain the information related to the incoming signals from the sensor output. In our study we only consider the far field sources so that we can assume the incoming signals are planes waves. We further restrict our study to the signals in the plane of the array. In the case where the incoming signals are not in the plane of the array, a set of array that are perpendicular to each other has to be used.

2.1 Signal Model

We consider a linear array consisting of M isotropic sensors with a uniform separation of distance ℓ. A signal model for the case of narrow band signal can be found in Monzingo and Miller (1980), and Haykin (1985). In the case of the broad band signals a signal model has been given in Wang and Kaveh (1985). Suppose we have K signals $s_k(t)$, k=1,2,....,K each being either a narrow-band or a broadband signal the spectrum of which covers the discrete frequencies $\omega_{k0},\omega_{k1},...,\omega_{kL}$. The angle of arrival of the k^{th} signal is θ_k. Then the k^{th} signal received at the m^{th} sensor $s_{km}(t)$ can be expressed as,

$$s_{km}(t) = \sum_{\omega=\omega_{k0}}^{\omega=\omega_{kL}} A_k(\omega)\, \exp[j(\omega t + \frac{2\pi m \ell}{\lambda(\omega)} \sin\theta_k + \psi_k(\omega))] \qquad (2.1.1)$$

where, $\lambda(\omega)$ is the wave length (should not be confused with normalized wavelength) and $\psi_k(\omega)$ is the phase of the k^{th} signal at frequency ω, ω_{k0} and ω_{kL} are the lowest and highest frequency components of the k^{th} signal frequency band, $A_k(\omega)$ is the amplitude of the k^{th} signal at frequency ω and ω represents the discrete frequencies ω_{ki}, i=0,1,2,...,L, for all k.

We assume that $\ell \le 0.5 \min[\lambda(\omega_{k0})]$, k=1,2,...,K and $\psi_k(\omega)$, k=1,2-,...,K are uncorrelated. The output of the m^{th} sensor due to the incoming signals $s_k(t)$, k=1,2,...,K is then given by,

$$x_m(t) = \sum_{k=1}^{K} s_{km}(t) + \upsilon_m(t) \qquad (2.1.2)$$

where, $\upsilon_m(t)$ is the noise at the output of the m^{th} sensor.

The output signal $x_m(t)$ from all the sensors is sampled to facilitate processing. To obtain the frequency information we divide the sampled signal into blocks of I samples and apply the discrete Fourier transform (DFT) which can be realized using the fast Fourier transform (FFT) algorithm or the Winograd Fourier transform (WFT) algorithm, to each block of data. The n^{th} block of data is generally call as the n^{th} snapshot. For the n^{th} block of data $x_m[(n-1)I+i]$, i=-0,1,2,...,I-1, after applying the DFT, the amplitude and phase information of the signal at the frequency ω is contained in $u_m(n)$ where,

$$u_m(n) = \sum_{k=1}^{K} [A_k(n)\, \exp(j\psi_k(n))\, \exp(j \frac{2\pi m \ell}{\lambda} \sin\theta_k)] + \nu_m(n) \qquad (2.1.3)$$

where, $\omega_{min} \le \omega \le \omega_{max}$ and $\omega_{min} = \min[\omega_{k0}]$, $\omega_{max} = \max[\omega_{kL}]$

$\forall$ k, λ is the wave length at frequency ω.

i.e. $$u_m(n) = \sum_{k=1}^{K} s_k(n) z_k^m + \nu_m(n) \qquad (2.1.4)$$

where, $s_k(n) = A_k(n) \exp(j\psi_k(n))$,

$$z_k = \exp\left(j \frac{2\pi\ell}{\lambda} \sin\theta_k\right), \tag{2.1.5}$$

$m = -J,-J+1,\ldots,J$, $J = (M-1)/2$, and $\nu_m(n)$ is the frequency component ω of the Fourier transform of the n^{th} block of the sampled version of $v_m(t)$. M is chosen to be odd.

The quantity $u_m(n)$ at n^{th} snapshot from all the sensors can be arranged into vector form,i.e.,

$$u(n) = (u_{-J}(n),u_{-J+1}(n),\ldots,u_J(n))^T$$

$$= \begin{cases} \sum_{k=1}^{K} d(\theta_k)s_k(n) + \nu(n), & \omega\in[\omega_{min},\omega_{max}] \\ \nu(n), & \omega\notin[\omega_{min},\omega_{max}] \end{cases} \tag{2.1.6}$$

where $d(\theta_k) = M^{-k}(z_k^{-J},z_k^{-J+1},z_k^{-J+2},\ldots,z_k^{J})^T$; (2.1.7)

$\nu(n) = (\nu_{-J}(n),\nu_{-J+1}(n),\ldots,\nu_J(n))^T$, (2.1.8)

and $[.]^T$ denotes the transpose of [.].

Eqn. (2.1.6) can be written into a matrix form so that,

$$u(n) = \begin{cases} D(\theta)s(n) + \nu(n), & \omega\in[\omega_{min},\omega_{max}] \\ \nu(n), & \omega\notin[\omega_{min},\omega_{max}] \end{cases} \tag{2.1.9}$$

where,

$D(\theta) = [d(\theta_1),d(\theta_2),\ldots,d(\theta_K)]$, (2.1.10)

$s(n) = (s_1(n),s_2(n),\ldots,s_K(n))^T$. (2.1.11)

Now, the cross spectral density matrix Φ can be defined as $\Phi=E[u(n)u^H(n)]$, where E denotes the expectation operator. Under the stationary signal and noise environment, expectation operator can be replaced by the time average and therefore we collect the information from the previous snapshots so

that the cross spectral density matrix at a given frequency can be more accurately estimated. Thus using eqn. (2.1.9) we can first form the data matrix, U(n) such that,

$$U(n) = [u(1),u(2),....,u(n)] \tag{2.1.12}$$

$$= \begin{cases} D(\theta)S(n) + N(n) , & \omega\in[\omega_{min},\omega_{max}] \\ N(n) , & \omega\notin[\omega_{min},\omega_{max}] \end{cases} \tag{2.1.13}$$

where, $D(\theta)$ is a Vandermonde matrix determined by, θ_k, k=1,2,3,...,K and the frequency ω,

$$S(n) = [s(1),s(2),....,s(n)] \tag{2.1.14}$$

$$N(n)=[\nu(1),\nu(2),....,\nu(n)] \tag{2.1.15}$$

$U(n) \in C^{M\times n}$, $D(\theta) \in C^{M\times K}$, $S(n) \in C^{K\times n}$, and $N(n) \in C^{M\times n}$,

$C^{i\times j}$ denotes the complex space of dimension (i,j).

The estimate $\Phi(n)$ of the cross spectral density matrix Φ after n snapshots can be obtained as,

$$\Phi(n) = n^{-1} U(n)U^H(n) \tag{2.1.16}$$

$\Phi(n) \in C^{M\times M}$.

Substituting for U(n) in eqn. (2.1.16) from eqn. (2.1.13) we obtain,

$$\Phi(n) = \begin{cases} n^{-1}\{[D(\theta)S(n) + N(n)][D(\theta)S(n) + N(n)]^H\}, & \omega\in[\omega_{min},\omega_{max}] \\ n^{-1} N(n)N^H(n), & \omega\notin[\omega_{min},\omega_{max}] \end{cases} \tag{2.1.17}$$

$$= \begin{cases} n^{-1}\{D(\theta)S(n)S^H(n)D^H(\theta) + D(\theta)S(n)N^H(n) + [D(\theta)S(n)N^H(n)]^H \\ \qquad + N(n)N^H(n)\}, & \omega\in[\omega_{min},\omega_{max}] \\ n^{-1} N(n)N^H(n), & \omega\notin[\omega_{min},\omega_{max}] \end{cases} \tag{2.1.18}$$

where, $[.]^H$ denotes the Hermitian transpose of [.].

Now let,

$$\Phi_{ss}(n) = n^{-1} S(n)S^H(n) \tag{2.1.19}$$

$$\Phi_{\nu\nu}(n) = n^{-1} N(n)N^H(n), \quad \omega\notin[\omega_{min},\omega_{max}] \tag{2.1.20}$$

$$\Phi_{\nu\nu}^{(o)}(n) = n^{-1}\, N(n)N^H(n), \quad \omega\in[\omega_{min},\omega_{max}]$$

$$\Phi_{s\nu}(n) = n^{-1}\, S(n)N^H(n), \tag{2.1.21}$$

then, $\Phi_{ss}(n) \in C^{K\times K}$, $\Phi_{\nu\nu}(n) \in C^{K\times K}$, $\Phi_{s\nu}(n) \in C^{K\times K}$, and $\Phi_{ss}(n)$, $\Phi_{\nu\nu}(n)$, $\Phi_{s\nu}(n)$ are the estimates of the cross spectral density matrices of signal-signal (Φ_{ss}), noise-noise ($\Phi_{\nu\nu}$), and signal-noise ($\Phi_{s\nu}$) given by $\Phi_{ss}=E[s(n)s^H(n)]$, $\Phi_{\nu\nu}=E[\nu(n)\nu^H(n)]$, $\Phi_{s\nu}=E[s(n)\nu^H(n)]$ respectively, where E is the expectation operator.

Eqn.(2.1.18) can be written as,

$$\Phi(n) = \begin{cases} D(\theta)\Phi_{ss}(n)D^H(\theta) + D(\theta)\Phi_{s\nu}(n) + [D(\theta)\Phi_{s\nu}(n)]^H \\ \qquad + \Phi_{\nu\nu}^{(o)}(n), \quad \omega\in[\omega_{min},\omega_{max}] \\ \Phi_{\nu\nu}(n), \quad \omega\notin[\omega_{min},\omega_{max}] \end{cases} \tag{2.1.22}$$

If the signal and noise are uncorrelated asymptotically, for large number of snapshots we can assume,

$$\Phi_{s\nu}(n) = 0, \quad \forall\ \omega \tag{2.1.23}$$

and hence eqn. (2.1.22) reduces to:

$$\Phi(n) = \begin{cases} D(\theta)\Phi_{ss}(n)D^H(\theta) + \Phi_{\nu\nu}^{(o)}(n), & \omega\in[\omega_{min},\omega_{max}] \\ \Phi_{\nu\nu}(n), & \omega\notin[\omega_{min},\omega_{max}] \end{cases} \tag{2.1.24}$$

From eqn. (2.1.24), it is clear that the spatial information about the signals as well as noise is contained in the cross spectral density matrix $\Phi(n)$.

2.2 Structure for systolic array implementation

The data matrix U(n) grows in size with the number of snapshots n and hence its direct use is not suitable for adaptive processing. To overcome this problem, we employ the Jacobi-Givens rotation (Appendix 2a) which premultiplies the matrix $U^H(n) \in C^{n\times K}$ by a unitary matrix, $Q^H(n) \in C^{n\times n}$ resulting in an upper triangular matrix $R^H(n) \in C^{K\times K}$, i.e.

$$Q^H(n)U^H(n) = \begin{bmatrix} R^H(n) \\ \hline 0 \end{bmatrix} \qquad (2.2.1)$$

where, 0 is a null matrix and $0 \in C^{(n-M)\times M}$, $n \geq M$, $R(n) \in C^{M\times M}$.

Since $R^H(n)$ is of constant dimensions, and upper triangular, it can be used much more conveniently. The estimate of the signal plus noise spatial cross spectral density matrix at n^{th} snapshot is then given by,

$$\Phi(n) = n^{-1} R(n)R^H(n) \qquad (2.2.2)$$

In practice, the Jacobi-Givens rotation can be carried out at the end of each snapshot such that the triangularized matrix of the previous snapshots can be recursively utilized. Thus, if we denote R(n) and R(n-1) as the triangularized matrices at n^{th} and $(n-1)^{th}$ snapshots respectively, then we can write,

$$Q^H(n)U^H(n) = Q_n^H(n) \begin{bmatrix} R^H(n-1) \\ \hline 0 \\ \hline u^H(n) \end{bmatrix}$$

$$= \begin{bmatrix} R^H(n) \\ \hline 0 \end{bmatrix} \qquad (2.2.3)$$

where, $Q_n(n)$ is the Jacobi-Givens rotation matrix used to annihilate the n^{th} row of the data matrix.

Eqn. (2.2.3) can be conveniently realized using systolic arrays based on the structure proposed by Gentleman and Kung (1981). The realization is briefly given in Appendix 2a.

In order to obtain the estimate of the spatial cross spectral density matrix $\Phi_{vv}(n)$ for the noise after the n^{th} snapshot for the frequency ω, we assume that spatial noise correlation at the signal frequency band $\Phi_{vv}(n)$, $\omega \in [\omega_{min},\omega_{max}]$ is the same as the spatial correlation at the frequency just outside the signal frequency band. This can be made possible by estimating the frequency band $[\omega_{min},\omega_{max}]$, at the stage where we map the stationary signal

in time domain into the frequency domain.

In general, the complex data matrix $\bar{U}(n)$ which represents the noise data matrix $U_v(n)$ approximately, at n^{th} snapshot can be constructed by using the data vector $\overline{u(n)}$ at frequency $\omega \notin [\omega_{min}, \omega_{max}]$. Again by applying the Jacobi-Givens rotation $Q^H(n)$ to $U^H(n)$, we obtain an upper triangular matrix $R^H(n)$ for the noise, from which we obtain the noise cross spectral density matrix $\Phi_{vv}(n)$ such that,

$$\Phi_{vv}(n) = \Phi(n), \quad \omega \notin [\omega_{min}, \omega_{max}] \tag{2.2.4}$$

$$= n^{-1} R_v(n) R_v^H(n) \tag{2.2.5}$$

where, $\Phi(n) \in C^{M \times M}$ and $R_v(n) \in C^{M \times M}$.

Schematic diagram for the adaptive array processing system is given in Fig. 2.1. At this stage reader may avoid the flipping network which will be explained in the chapter 3.

Now the noise only cross spectral density matrix at a frequency within the frequency band $[\omega_{min}, \omega_{max}]$, $\Phi_{vv}^{(o)}(n)$ can be represented as,

$$\Phi_{vv}^{(o)}(n) = \sigma_v^2 \, \Phi_{vv}(n), \tag{2.2.6}$$

where σ_v^2 is a scalar multiplier, and it represents the variance of the noise when the noise only cross spectral density matrix is normalized.

Therefore, the cross spectral density matrix $\Phi(n)$ can be written as,

$$\Phi(n) = D(\theta)\Phi_{ss}(n)D^H(\theta) + \sigma_v^2 \, \Phi_{vv}(n) \tag{2.2.7}$$

2.3 Solution to the Array Processing Problem by Subspace Decomposition

2.3.0 Introduction

Solution to the array processing problem based on the subspace decomposition had been studied by Schmidt (1979), Bienvenu and Kopp (1980), Johnson

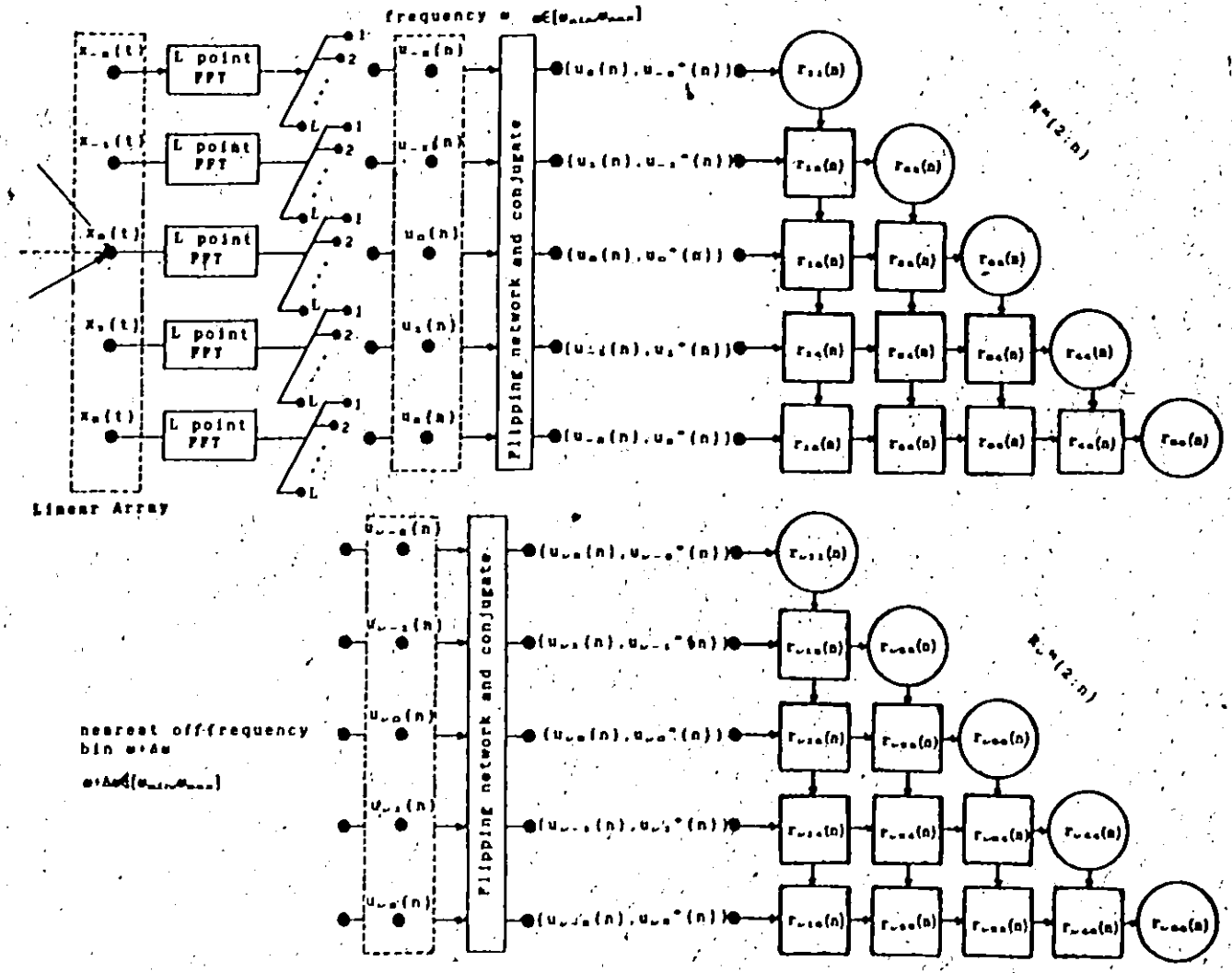

Fig. 2.1 Schematic Diagram for the Adaptive Array Processing Systems

and DeGraaf (1982), Speiser and Van Loan (1984), Orfanidis (1985), and Wang and Kaveh (1985). In general, array processing problem reduces to the generalized eigenvalue eigenvector decomposition or generalized singularvalue singularvector decomposition.

We first formulate the array processing problem as the solution to the generalized eigenvalue eigenvector decomposition. Then we study the significance of the generalized eigenvalues and eigenvectors in the array processing problem. Based on the generalized eigenvalues, we separate the signal subspace generalized eigenvectors and the noise subspace generalized eigenvectors. Using the noise subspace eigenvectors we can form the proper orthogonal projection operator that can be used to project any vector with suitable dimension on to the noise subspace. Noise subspace projection matrix is then used to define the proper orthogonal projection multiple signal classification (POP-MUSIC).

An alternative formulation to the generalized eigenvalue eigenvector decomposition is also considered. Based on this formulation POP-MUSIC spectrum is redefined. It is shown that the POP-MUSIC spectrum reduces to the ordinary MUSIC spectrum when the noise is spatially uncorrelated.

2.3.1 Subspace Decomposition under Correlated Noise

So far it is clear that our signal and noise space can be described by the cross spectral density matrix pencil $(\Phi(n),\Phi_{\nu\nu}(n))$. Array processing problem is to deal with this matrix pencil to extract the information important to the user. The most convenient way to handle the array processing problem is to break the matrix pencil $(\Phi(n),\Phi_{\nu\nu}(n))$ down into smaller spaces. This can generally be achieved as the solution to the constraint minimization problem,

$$\underset{V(n)}{\text{minimize}} \quad \text{trace}\,(V^{H}(n)\Phi(n)V(n)) \qquad (2.3.1)$$

subject to the constraint, $V^H(n)\Phi_{yy}(n)V(n) = I$ (2.3.2)

where $V(n) \in C^{M\times M}$ and I is an identity matrix.

The solution to the above optimization problem can be achieved by introducing the Lagrange multiplier matrix $\Lambda(n)$ given by,

$\Phi(n)V(n) = \Phi_{yy}(n)V(n)\Lambda(n)$ (2.3.3)

where $\Lambda(n) = \text{diag}(\lambda_1(n),\lambda_2(n),....,\lambda_M(n))$, and

$\lambda_1(n)\geq\lambda_2(n)\geq...\geq\lambda_M(n)$,

$V(n) = [v_1(n),v_2(n),....v_M(n)]$. (2.3.4)

Eqn. (2.3.3) represents the generalized eigenvalue eigenvector decomposition of the matrix pencil $(\Phi(n),\Phi_{yy}(n))$. The matrix V(n) contains the generalized eigenvectors as its columns corresponding to the diagonal elements of $\Lambda(n)$ which are the generalized eigenvalues. Computational aspects of the generalized eigenvalue eigenvector decomposition are given in Appendix 2b.

Multiplying the eqn. (2.3.3) by $V^H(n)$ and substituting from eqn. (2.3.2), we obtain,

$V^H(n)\Phi(n)V(n) = \Lambda(n)$ (2.3.5)

Substituting for $\Phi(n)$ from eqn. (2.2.7) in eqn. (2.3.5),

$\Lambda(n) = \sigma_v^2\, V^H(n)\Phi_{yy}(n)V(n) + V^H(n)\Phi_{ss}^{(M)}(n)V(n)$ (2.3.6)

where $\Phi_{ss}^{(M)}(n) = D(\theta)\Phi_{ss}(n)D^H(\theta)$, and $\Phi_{ss}^{(M)}(n) \in C^{M\times M}$, and the $\text{rank}(\Phi_{ss}^{(M)}(n))=K$, $K<M$.

We can combine eqns. (2.3.2) and (2.3.6) to get,

$\Lambda(n) = \sigma_v^2 I + \Lambda_s^{(M)}(n)$, (2.3.7)

where $\Lambda_s^{(M)}(n) = V^H(n)\Phi_{ss}^{(M)}(n)V(n)$, (2.3.8)

$\Lambda_s^{(M)}(n)$ is a diagonal matrix and $\Lambda_s^{(M)}(n) \in C^{M\times M}$.

Since $\Phi_{ss}^{(M)}(n)$ is of rank K,

$$\Lambda_{ss}^{(M)}(n) = \begin{bmatrix} \Lambda_s(n) & | & 0 \\ \hline 0 & | & 0 \end{bmatrix} \tag{2.3.9}$$

where $\Lambda_s(n)$ is a diagonal matrix and $\Lambda_s(n) \in C^{K\times K}$.

The multiplicity of the smallest eigenvalue is equal to M-K from which we can find the number of incoming signals K. Matrix $\Phi_{ss}^{(M)}(n)$ is Hermitian and hence it can be represented as,

$$\Phi_{ss}^{(M)}(n) = Q(n)\Gamma(n)Q^H(n) \tag{2.3.10}$$

where $Q^H(n)Q(n) = I$, $\Gamma(n)$ is a diagonal matrix with I being an identity matrix. The matrix Q(n) used here should not be confused with the matrix Q(n) used in the matrix triangularization.

Since $\Phi_{ss}^{(M)}(n)$ is of rank K,

$$\Gamma(n) = \begin{bmatrix} \Gamma_s(n) & | & 0 \\ \hline 0 & | & 0 \end{bmatrix} \tag{2.3.11}$$

$\Gamma_s(n) \in C^{K\times K}$.

Matrix Q(n) can now be partitioned to obtain the signal subspace orthonormal basis vectors $Q_s(n)$, and the noise subspace orthonormal basis vectors $Q_N(n)$ such that,

$$Q(n) = [Q_s(n), Q_N(n)], \tag{2.3.12}$$

$Q_s(n) \in C^{M\times K}$, $Q_N(n) \in C^{M\times(M-K)}$, and K<M.

Signal subspace basis vectors matrix $Q_s(n)$ corresponds to the eigenvalues $\Gamma_s(n)$ and the noise subspace basis vectors matrix $Q_N(n)$ corresponds to the null space. Null space is also referred to as the noise subspace.

Now we can combine eqns. (2.3.8), (2.3.10), and (2.3.12) so that,

$$\Lambda_{ss}^{(M)}(n) = V^H(n)[Q_s(n), Q_N(n)] \begin{bmatrix} \Gamma_s(n) & | & 0 \\ \hline 0 & | & 0 \end{bmatrix} \begin{bmatrix} Q_s^H(n) \\ \hline Q_N^H(n) \end{bmatrix} V(n) \tag{2.3.13}$$

$$= \begin{bmatrix} V_s^H(n) \\ \hline V_N^H(n) \end{bmatrix} [Q_s(n)\Gamma_s(n)Q_s^H(n)][V_s(n),V_N(n)] \qquad (2.3.14)$$

where, $V_s(n)$ and $V_N(n)$ are given by,

$$V(n) = [V_s(n),V_N(n)], \qquad (2.3.15)$$

$V_s(n) \in C^{M\times K}$, and $V_N(n) \in C^{M\times(M-K)}$.

Comparing eqns. (2.3.9) and (2.3.14), we obtain,

$$\Lambda_s(n) = V_s^H(n)[Q_s(n)\Gamma_s(n)Q_s^H(n)]V_s(n), \qquad (2.3.16)$$

$$V_s^H(n)[Q_s(n)\Gamma_s(n)Q_s^H(n)]V_N(n) = 0, \text{ and} \qquad (2.3.17)$$

$$V_N^H(n)[Q_s(n)\Gamma_s(n)Q_s^H(n)]V_N(n) = 0, \qquad (2.3.18)$$

where 0 is a null matrix with appropriate order.

Eqns. (2.3.17) and (2.3.18) indicate that generalized eigenvectors matrix $V_N(n)$ is orthogonal to the signal subspace orthonormal basis vector matrix $Q_s(n)$, i.e., $V_N(n)$ lies on the noise subspace described by the orthonormal basis $Q_N(n)$.

It is obvious that we do not have the knowledge of the noise subspace orthonormal basis vectors matrix $Q_N(n)$. But now we do have the knowledge of the vectors matrix $V_N(n)$ that lies on the noise subspace or null space. Therefore, we can form the proper orthogonal projection matrix $P_N(n)$ for the noise subspace such that,

$$P_N(n) = V_N(n)[V_N^H(n)V_N(n)]^{-1}V_N^H(n). \qquad (2.3.19)$$

The matrix $P_N(n)$ can be used to project any vector with suitable dimension onto the noise subspace. Now, let us project the direction vector $d(\theta)$ on to the noise subspace so that the noise subspace projection $d_N(\theta)$ is given by,

$$d_N(\theta) = P_N(n)d(\theta) \qquad (2.3.20)$$

Then we define the proper orthogonal projection multiple signal classification (POP-MUSIC) spectrum such that,

$S_{POP-MUSIC}(n,\theta)$ = [some norm of $d_N(\theta)]^{-k}$, where k can be any value.

When we use the Euclidian norm POP-MUSIC spectrum reduces to,

$$S_{POP-EUC}(n,\theta) = |d_N(\theta)|^{-2}$$
$$= [d^H(\theta)P_N(n)d(\theta)]^{-1} \quad (2.3.21)$$

where |.| represents the Euclidian norm of a vector.

2.3.2 An Alternative Formulation of the Array Processing Problem

We have seen that the array processing problem could be expressed as the solution to the generalized eigenvalue eigenvector decomposition of the cross spectral density matrix pencil $(\Phi(n),\Phi_{\downarrow\downarrow}(n))$,

$$\Phi(n)V(n) = \Phi_{\downarrow\downarrow}(n)V(n)\Lambda(n) \quad (2.3.22)$$

As we have done in section 2.2, we can write,

$\Phi(n) = R(n)R^H(n)$ and $\Phi_{\downarrow\downarrow}(n) = R_{\downarrow}(n)R_{\downarrow}^H(n)$.

Eqn. (2.3.22) now becomes,

$$R(n)R^H(n)V(n) = R_{\downarrow}(n)R_{\downarrow}^H(n)V(n)\Lambda(n) \quad (2.3.23)$$

If $\Phi_{\downarrow\downarrow}(n)$ is non singular, eqn. (2.3.23) can be rearranged to obtain,

$$[R_{\downarrow}^{-1}(n)\Phi(n)R_{\downarrow}^{-H}(n)]R_{\downarrow}^H(n)V(n) = R_{\downarrow}^H(n)V(n)\Lambda(n) \quad (2.3.24)$$

where, $R_{\downarrow}^{-H}(n)$ and $R_{\downarrow}^{-1}(n)$ denote the inverse of $R_{\downarrow}^H(n)$ and $R_{\downarrow}(n)$ respectively.

Let, $\Phi'(n) = R_{\downarrow}^{-1}(n)\Phi(n)R_{\downarrow}^{-H}(n)$ (2.3.25)

and $R_{\downarrow}^H(n)V(n) = Y(n)$, (2.3.26)

then eqn. (2.3.24) can be written as,

$$\Phi'(n)Y(n) = Y(n)\Lambda(n), \quad (2.3.27)$$

where, $\Phi'(n)$ is a Hermitian matrix.

Since $R_{\downarrow}^H(n)$ is upper triangular, matrix $\Phi'(n)$ can be constructed simply by using backward substitution (Appendix 2c).

From eqn. (2.3.27), it is now clear that the generalized eigenvalue eigenvector decomposition reduces to the Hermitian eigenvalue eigenvector decomposition of $\Phi'(n)$. Hermitian eigenvectors of $\Phi'(n)$ is related to the generalized eigenvectors of the matrix pencil $(\Phi(n),\Phi_{\cup\cup}(n))$ by the operator $R_{\cup}(n)$. Hermitian eigenvector matrix $Y(n)$ of $\Phi'(n)$ is unitary, i.e.,

$Y^{H}(n)Y(n) = I$, where I is an identity matrix.

The generalized eigenvector matrix $V(n)$ can be obtained from eqn. (2.3.26) and it is given by,

$$V(n) = R_{\cup}^{-H}(n)Y(n) \tag{2.3.28}$$

Now, let us partition the eigenvector matrix $Y(n)$ by using the eigenvalues matrix $\Lambda(n)$ as we did before, to obtain,

$$Y(n) = [Y_{S}(n),Y_{N}(n)], \tag{2.3.29}$$

where $Y_{S}(n) \in C^{M\times K}$, $Y_{N}(n) \in C^{M\times(M-K)}$, and $Y(n) \in C^{M\times M}$.

Then eqn. (2.3.28) can be written as,

$$V(n) = [R_{\cup}^{-H}(n)Y_{S}(n),R_{\cup}^{-H}(n)Y_{N}(n)] \tag{2.3.30}$$

$$= [V_{S}(n),V_{N}(n)] \tag{2.3.31}$$

where, $V_{N}(n) = R_{\cup}^{-H}(n)Y_{N}(n)$, and $V_{S}(n) = R_{\cup}^{-H}(n)Y_{S}(n)$ (2.3.32)

At this point we have the knowledge of the vector matrix $V_{N}(n)$ that lies on the noise subspace. Therefore, we can define the noise subspace projection operator $P_{N}(n)$ such that,

$$P_{N}(n)=R_{\cup}^{-H}(n)Y_{N}(n)Y_{N}^{H}(n)R_{\cup}^{-1}(n) \tag{2.3.33}$$

Now, POP-MUSIC-Euc spectrum estimate can be defined as,

$$S_{POP-Euc}(n,\theta) = |d_{N}(\theta)|^{-2}$$

where, $d_{N}(\theta) = P_{N}(n)d(\theta)$.

It is not necessary to limit ourselves to the Euclidian norm in defining the spectrum estimate, we may also use the k^{th} norm in general, so that,

$S_{POP-Euc}(n,\theta,k) = (|d_N(\theta)|_k)^{-k}$.

where $|.|_k$ denotes the k^{th} norm and k is an integer.

2.3.3 Subspace Decomposition Under Uncorrelated Noise

Let us now consider the subspace decomposition under spatially uncorrelated noise environment. This can be achieved as a special case of the generalized eigenvalue eigenvector decomposition or the alternative formulation given above. When the noise is uncorrelated, normalized noise cross spectral density matrix $\Phi_{vv}(n) = I$ and hence from eqn. (2.3.33), we can obtain the noise subspace projection matrix $P_N(n)$ as,

$$P_N(n) = Y_N(n)[Y_N^H(n)Y_N(n)]^{-1}Y_N^H(n) \qquad (2.3.34)$$

But, since Y(n) is unitary, $Y_N^H(n)Y_N(n) = I$ and hence,

$$P_N(n) = Y_N(n)Y_N^H(n) \qquad (2.3.35)$$

Furthermore, it is obvious that Y(n) is the same as the orthonormal-basis vector matrix Q(n) given in eqn. (2.3.10),

i.e. $Y(n) = Q(n)$ (2.3.36)

Therefore, noise subspace matrix can be written as,

$P_N(n) = Q_N(n)Q_N^H(n)$.

Then, the POP-MUSIC-Euc spectrum can be written as,

$$S_{POP-Euc}(n,\theta) = [d^H(\theta)P_N(n)d(\theta)]^{-1}$$

$$= [d^H(\theta)Q_N(n)Q_N^H(n)d(\theta)]^{-1}$$

$$= \text{MUSIC spectrum [Schmidt (1979)]} \qquad (2.3.37)$$

Therefore, when the noise is spatially uncorrelated, POP-MUSIC spectrum reduces to the well known MUSIC spectrum proposed by Schmidt (1979). Even though the POP-MUSIC spectrum is more general, the underlying subspace decomposition approach used there is due to Schmidt (1979). Therefore, the POP-

MUSIC spectrum is not a new spectrum estimation technique, rather it is a more generalized version of the MUSIC spectrum. To bring this generalized view into the picture, I will refer to the MUSIC as POP-MUSIC in the coming chapters.

At this point it is worth studying the significance of the eigenvalues in the case of spatially uncorrelated noise. Under uncorrelated noise the generalized eigenvalue eigenvector decomposition reduces to Hermitian eigenvalue eigenvector decomposition.

Then the eigenvalue matrix $\Lambda(n)$ can be written as,

$$\Lambda(n) = \sigma_v^2 \cdot I + Q^H(n)D(\theta)\Phi_{ss}(n)D^H(\theta)Q(n) \qquad (2.3.38)$$

with $Q^H(n)Q(n) = I$.

Let, $Q(n) = [q_1(n), q_2(n), \ldots, q_K(n)]$, and $D(\theta) = [d(\theta_1), d(\theta_2), \ldots, d(\theta_K)]$.

We further assume that the incoming signals are uncorrelated so that, $\Phi_{ss}(n) = \text{diag}\,(\sigma_{s1}^2, \sigma_{s2}^2, \ldots, \sigma_{sK}^2)$, where σ_{sK}^2 represents the power of the k^{th} signal, $k = 1,2,\ldots,K$.

Then, $\Lambda(n)$ can be written as,

$$\Lambda(n) = \sigma_v^2 I + \Lambda_s^{(K)}(n), \qquad (2.3.39)$$

where,

$$\Lambda_s^{(K)}(n) = \begin{bmatrix} \Lambda_s(n) & | & 0 \\ \hline 0 & | & 0 \end{bmatrix}$$

$$\Lambda_s(n) = \text{diag}\,(\lambda_{s1}(n), \lambda_{s2}(n), \ldots, \lambda_{sK}(n)),$$

$$\lambda_{sm}(n) = \sum_{k=1}^{K} (\sigma_{sk} \cos \alpha_{mk})^2, \quad m=1,2,\ldots K \qquad (2.3.40)$$

α_{mk} describe the angle between the vector $q_m(n)$ and the direction vector $d(\theta_k)$, i.e. $q_m^H(n)d(\theta_k) = \cos \alpha_{mk} \exp(j\beta_{mk})$ with $|d(\theta_k)| = 1$.

$(\sigma_{sk} \cos \alpha_{mk})^2$ represents the power associated with the projection of the k^{th} signal direction vector on to the m^{th} eigenvector. Therefore, from eqn.

(2.3.40), it is clear that the $\lambda_{ss}(n)$ represents the sum of the power associated with the m^{th} Hermitian eigenvector or m^{th} orthonormal basis vector due to the projection of all the signal components for k=1,2,....,K.

Now it is clear that the Hermitian eigenvalues do not correspond to the power associated with incoming signals. Instead, $\lambda_{ss}(n)$ contains the power associated with the m^{th} basis vector due to the projected components of the incoming signals.

Now let us consider the trace $(\Lambda_s^{(x)}(n))$,

$$\text{trace } (\Lambda_s^{(x)}(n)) = \sum_{m=1}^{K} \lambda_{ss}(n) + \sum 0 \qquad (2.3.41)$$

$$= \sum_{m=1}^{K} \sum_{k=1}^{K} (\sigma_{sk} \cos \alpha_{mk})^2$$

$$= \sum_{k=1}^{K} \sigma_{sk}^2 \sum_{m=1}^{K} (\cos \alpha_{mk})^2 \qquad (2.3.42)$$

But from geometry it is clear that,

$$\sum_{m=1}^{K} (\cos \alpha_{mk})^2 = 1, \quad \forall\, k \text{ and hence}$$

$$\text{trace } (\Lambda_s^{(x)}(n)) = \sum_{k=1}^{K} \sigma_{sk}^2$$

$$= \text{trace } (\Phi_{ss}(n)) \qquad (2.3.43)$$

From eqn. (2.3.39),

$$\Lambda(n) = \sigma_v^2 I + \Lambda_s^{(x)}(n).$$

Taking the trace on both sides and noting the fact that the trace is a linear operator, we obtain,

$$\text{trace } (\Lambda(n)) = \text{trace } (\Lambda_s^{(x)}(n)) + M \sigma_v^2 \qquad (2.3.44)$$

Therefore, the trace of the Hermitian eigenvalue matrix $\Lambda(n)$ represe-

nts the total power of the incoming signals if and only if $\sigma_v^2=0$, i.e. when signal to noise ratio is infinite.

2.3.4 Estimation of the number of signals

Number of signals present at an array is an important parameter that has to be estimated in array processing. If the true cross spectral density matrix is known, from eqn. (2.3.39), it is clear that the multiplicity of the small eigenvalues are equal to (M-K) from which we can estimate the number of signals K. But in practice we are forced to use the estimated cross spectral density matrix due to the non availability of true cross spectral density matrix and hence instead of (M-K) multiple eigenvalues we may end up with (M-K) small and distinct eigenvalues.

Therefore, the number of signals present in an array is generally estimated by using statistical hypothesis and the information theoretic criteria based on the generalized eigenvalue or generalized singularvalues of the matrix pencil $(\Phi(n),\Phi_{vv}(n))$. Information theoretic criteria such as Akaike information theoretic criterion (AIC) [Akaike (1973,1974)] and minimum description length criterion (MDLC) [Wax and Kailath (1984)] have become popular due to the fact that they do not demand any subjective judgement.

We can write the quantities $I_A(k)$ and $L_D(k)$, that are minimized in Akaike information theoretic criterion (AIC) and in minimum description length criterion with different interpretations such that,

$$I_A(k) = 2nH_x(k) + 2k(2M-k) \qquad (2.3.45)$$

$$L_D(k) = nH_x(k) + 0.5k(2M-k)\log n \qquad (2.3.46)$$

where, n is the number of snapshots.

$H_x(k)$ is in turn defined as,

$$H_I(k) = \sum_{i=k+1}^{M} I_{L,i} \qquad (2.3.47)$$

where, M is the number of sensors in the array and $I_{L,i}$ is the information loss of the i^{th} component given by,

$$I_{L,i} = \log(\sigma/\lambda_i) \qquad (2.3.48)$$

with σ being the true noise variance and λ_i being the estimated i^{th} eigenvalue of the noise subspace.

The relationship for $H_I(k)$ given in eqn. (2.3.47) follows the definition of 'height of ignorance' given in section 3.2 of chapter 3. Therefore, $H_I(k)$ is referred to as the height of ignorance when k signals are assumed to be present.

In general, σ is not known and hence an approximate value is used. This is obtained by averaging the noise subspace eigenvalues, i.e.

$$\sigma = (M-k)^{-1} \sum_{i=k+1}^{M} \lambda_i \qquad (2.3.49)$$

The value k corresponding to the minimum value of $I_A(k)$ or $L_D(k)$ will be the number of signals determined by the respective criterion. From eqns. (2.3.45) and (2.3.46) it is clear that both the AIC and MDLC perform equally irrespective of the signal to noise ratio when the number of snapshots equal to some critical value n_c given by $n_c = \log^{-1} 2$. For moderate signal to noise ratios both AIC and MDLC perform equally when the number of snapshots are finite. At low signal to noise ratios, AIC provides better performance compared to MDLC when $n > n_c$ and MDLC provides better performance than the AIC when $n < n_c$. These are some of the observations that can be made from the equations (2.3.45) and (2.3.46). MDLC gives a consistent estimate [Zhao, Krishnaiah and Bai (1987)]. Some of the work on the statistical performance of the AIC and MDLC for finite data can be found in Wang and Kaveh (1986) and Kaveh, Wang and Hung (1987).

2.3.5 Signal and Noise Subspace Projection Operators

We have already obtained the proper orthogonal projection matrix of the noise subspace for both the cases where noise is spatially correlated, and uncorrelated. Our aim in this section is to obtain the relationships between the noise subspace and signal subspace projection matrices when the noise is spatially uncorrelated. These relationships will be exploited in chapter 4.

Once the number of signals K is obtained according to the section 2.3.4, we can partition the space $\Omega(n)$ described by the eigenvectors into the signal subspace $\Omega_s(n)$ and noise subspace $\Omega_N(n)$. The eigenvector matrices $V_s(n)$ and $V_N(n)$ for the signal subspace and noise subspace respectively can be written as,

$$V_s(n) = [v_1(n), v_2(n), \ldots, v_K(n)] \tag{2.3.50}$$

$$V_N(n) = [v_{K+1}(n), v_{K+2}(n), \ldots, v_M(n)] \tag{2.3.51}$$

$$V(n) = [V_s(n), V_N(n)] \tag{2.3.52}$$

$V(n) \in C^{M \times M}$, $V_s(n) \in C^{M \times K}$, $V_N(n) \in C^{M \times (M-K)}$ and $K < M$.

Consider a vector y in the M dimensional space. If we represent y as a linear combination of the noise subspace eigenvectors, we obtain $\hat{y}_N(n)$, the estimate of y on the noise subspace, given by,

$$\hat{y}_N(n) = V_N(n) w(n) \tag{2.3.53}$$

where, w(n) is the weight vector.

If the estimation error of y is denoted by e(n) then,

$$y = \hat{y}_N(n) + e(n). \tag{2.3.54}$$

We can find $y_N(n)$, the best estimate y in the least squares sense, by minimizing the quantity $|e(n)|^2$ with respect to w(n) with the result,

$$y_N(n) = P_N(n) y \tag{2.3.55}$$

and

$$y = y_N(n) + e_s(n) \tag{2.3.56}$$

where,

$$P_N(n) = V_N(n)[V_N^H(n)V_N(n)]^{-1}V_N^H(n) \quad (2.3.57)$$

Under this condition, the minimum error vector $e_s(n)$ is orthogonal to the vector $y_N(n)$.

Similarly, the best estimate of y on the signal subspace using the signal subspace eigenvectors can be written as,

$$y_s(n) = P_s(n)y \quad (2.3.58)$$

where,

$$P_s(n) = V_s(n)[V_s^H(n)V_s(n)]^{-1}V_s^H(n) \quad (2.3.59)$$

such that,

$$y = y_s(n) + e_N(n), \quad (2.3.60)$$

with $e_N(n)$ being orthogonal to $y_s(n)$.

$P_N(n)$ and $P_s(n)$, that are given by eqns. (2.3.57) and (2.3.59) can be shown to have the following properties:

1. They are idempotent, i.e.

$$P(n)P(n) = P(n) \quad (2.3.61)$$

2. They are Hermitian, i.e.

$$P(n) = P^H(n) \quad (2.3.62)$$

3. $$P_N(n) = I - P_s(n) \quad (2.3.63)$$

where I is an identity matrix.

4. $$P_N(n)P_s(n) = P_s(n)P_N(n) = 0 \quad (2.3.64)$$

where 0 is a null matrix.

Since $P_N(n)$ and $P_s(n)$ are idempotent and Hermitian they represent the projection operators so that $y_N(n)$, and $y_s(n)$ represent the orthogonal projection of the vector y onto the noise, and signal subspaces respectively. Since the signal and noise subspaces are mutually orthogonal, the residual vectors $e_s(n)$,

and $e_N(n)$ in eqns. (2.3.56), and (2.3.60) lie in the signal, and noise subspaces respectively.

Substituting eqn. (2.3.55) in eqn. (2.3.56) and using the property given in eqn. (2.3.63), we obtain,

$$P_S(n)y = e_S(n) \tag{2.3.65}$$

Hence, $e_S(n)$ represents the projection of y onto the signal subspace. Similarly, substituting eqn. (2.3.58) in (2.3.60) and using the property 3, we obtain,

$$P_N(n)y = e_N(n) \tag{2.3.65}$$

Therefore, $e_N(n)$ represent the projections of y onto the noise subspace. Further, it is also noteworthy that for the case of the orthonormal eigenvectors, the proper orthogonal projection matrices reduce to,

$$P_N(n) = V_N(n)V_N^H(n) \tag{2.3.66}$$

$$P_S(n) = V_S(n)V_S^H(n) \tag{2.3.67}$$

2.4 Discussion

Generalized eigenvalue eigenvector decomposition provides a general framework for subspace decomposition in adaptive array processing. Proper orthogonal projection multiple signal classification (POP-MUSIC) can be considered as a generalized version of the MUSIC method. POP-MUSIC reduces to MUSIC when the noise is spatially uncorrelated. Generalized singularvalue singularvector decomposition gives a numerically more stable solution compared to the generalized eigenvalue eigenvector decomposition. The use of the upper triangularized data matrices based on the Jacobi-Givens rotation in place of the data matrices provides a computationally efficient way of solving the generalized eigenvalue eigenvector decomposition or generalized singularvalue singularvector decomposition in adaptive array processing. Matrix triangularization based on the

Jacobi-Givens rotation can generally be carried out by using systolic array architecture. The foundation of bearing estimation and beamforming can be laid using the proper orthogonal projection matrices of the signal subspace, and noise subspace.

CHAPTER-3

FLIPPING TECHNIQUE IN ADAPTIVE ARRAY PROCESSING

Preview The use of the forward and backward technique has a very long history. Forward and backward techniques have been used in sequential processing as well as parallel processing. Lattice structures are generally used in implementing the forward and backward techniques. But until now there had not been a simple technique for the parallel implementation of forward and backward techniques in adaptive array processing.

We introduce 'flipping technique' in implementing the forward and backward techniques in adaptive array processing. Flipping technique is not limited to linear arrays. But for successful application of flipping technique the array geometry must be symmetric. For a given input vector at the n^{th} snapshot, flipping technique produces two vectors, one the conjugate reverse of the input vector and the other the same as the input, as its output. It is shown that the input vector at n^{th} snapshot and its conjugate reverse are two distinct vectors that have the same spatial coherence relationship through the array. Any vector that has the same spatial coherence relationship can be used in constructing the input data matrix.

The data matrix that is constructed by using flipping technique is then used to obtain the cross spectral density matrix estimate.

'Height of ignorance' and 'K-perturbation' are introduced as a measure of performance for the estimated cross spectral density matrix. A small value of height of ignorance and K-perturbation indicates that the cross spectral density matrix estimate is closer to the true cross spectral density matrix estimate. The cross spectral density matrix obtained by using the flipping technique provides a smaller value of height of ignorance and K-perturbation compared to the cross spectral density matrix estimate obtained without flipping. Simulation is performed for a known signal and noise environment. Through simulation it is found that the height of ignorance of the cross spectral density matrix estimate obtained by using flipping technique is one half of the height of ignorance of the unflipped cross spectral density matrix estimate.

3.1 Flipping Technique

We have already assumed that the signal and noise environment is stationary. Under this assumption, we make use of the vector u(n) to construct a new data vector $u^{r}(n)$ which represents the conjugate reverse of u(n) at n^{th} snapshot, i.e.,

$$u^{r}(n) = (u_J^{*}(n), u_{J-1}^{*}(n), \ldots, u_{-J}^{*}(n))^{T}, \qquad (3.1.1)$$

where, $J = (M-1)/2$, M is odd, $[.]^{r}$ denotes the conjugate reverse of [.], and $[.]^{*}$ denotes the complex conjugate of [.].

The formation of new data vector, $u^{r}(n)$ at each snapshot is named as 'flipping' while the network that produces the vector pair $(u^{r}(n), u(n))$ as the output for a given input u(n) is named as the 'flipping network'. Flipping network is shown as a part of the Fig. 2.1. The pair of vectors $(u^{r}(n), u(n))$ is shown to have the following property:

Property 3.1

The vectors u(n) and $u^*(n)$ have the same spatial coherence relationship through the array.

The statement of the property 3.1 can be justified as follows:

Rewriting the eqn. (2.1.9),

$$u(n) = \begin{cases} D(\theta)s(n) + \nu(n), & \omega \in [\omega_{min}, \omega_{max}] \\ \nu(n), & \omega \notin [\omega_{min}, \omega_{max}] \end{cases} \quad (3.1.2)$$

We observe that the conjugate reverse $u^*(n)$ of vector u(n) at n^{th} snapshot is given by,

$$u^*(n) = \begin{cases} D(\theta)s^*(n) + \nu^*(n), & \omega \in [\omega_{min}, \omega_{max}] \\ \nu^*(n), & \omega \notin [\omega_{min}, \omega_{max}] \end{cases} \quad (3.1.3)$$

Spatial correlation through the array depends only on the direction vector matrix $D(\theta)$ and it is the same for both u(n) and $u^*(n)$. Therefore, two distinct vectors, u(n) and its conjugate reverse $u^*(n)$ have the same spatial correlation through the array. Here, we consider spatially uncorrelated noise in order to make our analysis simpler.

By making use of the vector pair $(u^*(n),u(n))$, we can construct a new data matrix U(2:n) such that,

$$U(2:n) = [u^*(1),u(1),u^*(2),u(2),\ldots,u^*(n),u(n)] \quad (3.1.4)$$

where, $U(2:n) \in C^{M \times 2n}$.

Then the new cross spectral density matrix $\Phi(2:n)$ at n^{th} snapshot can be written as,

$$\Phi(2:n) = (2n)^{-1} U(2:n)U^H(2:n) \quad (3.1.5)$$

where, $\Phi(2:n) \in C^{M \times M}$.

Using eqn. (2.1.13), the data matrix U(2:n) can also be written as,

$$U(2:n) = \begin{cases} D(\theta)S(2:n) + N(2:n), & \omega \in [\omega_{min}, \omega_{max}] \\ N(2:n), & \omega \notin [\omega_{min}, \omega_{max}] \end{cases} \quad (3.1.6)$$

where, $D(\theta)$ is a Vandermonde matrix determined by the angle of arrival θ_i, $i = 1,2,\ldots,K$,

$S(2:n) = [s^H(1), s(1), s^H(2), s(2), \ldots, s^H(n), s(n)]$

$N(2:n) = [\nu^H(1), \nu(1), \nu^H(2), \nu(2), \ldots, \nu^H(n), \nu(n)]$,

$S(2:n) \in C^{K \times 2n}$, and $N(2:n) \in C^{M \times 2n}$.

Under the assumption that the signals and noise are uncorrelated, eqn. (3.1.5) can be written as,

$$\Phi(2:n) = \begin{cases} D(\theta)\Phi_{ss}(2:n)D^H(\theta) + \Phi_{\nu\nu}(2:n), & \omega \in [\omega_{min}, \omega_{max}] \\ \Phi_{\nu\nu}(2:n), & \omega \notin [\omega_{min}, \omega_{max}] \end{cases} \quad (3.1.7)$$

where, $\Phi_{ss}(2:n) = (2n)^{-1} S(2:n)S^H(2:n)$ (3.1.8)

$\Phi_{\nu\nu}(2:n) = (2n)^{-1} N(2:n)N^H(2:n)$, (3.1.9)

$\Phi_{ss}(2:n) \in C^{K \times K}$, $\Phi_{\nu\nu}(2:n) \in C^{M \times M}$.

Eqns. (3.1.8) and (3.1.9) can easily be shown to have the following relationships,

$$\Phi_{ss}(2:n) = .5[\Phi_{ss}(n) + \Phi_{ss}^H(n)] \quad (3.1.10)$$

$$\Phi_{\nu\nu}(2:n) = .5[\Phi_{\nu\nu}(n) + \Phi_{\nu\nu}^H(n)] \quad (3.1.11)$$

where, the ij^{th} element $\phi_{\nu\nu(ij)}^H(n)$ of the matrix $\Phi_{\nu\nu}^H(n)$ is related to the ij^{th} element $\phi_{\nu\nu(ij)}(n)$ of the matrix $\Phi_{\nu\nu}(n)$ by the relationship,

$$\phi_{\nu\nu(ij)}^H(n) = \phi_{\nu\nu(M-i+1, M-j+1)}(n), \quad (3.1.12)$$

$\Phi_{ss}(n) \in C^{K \times K}$, and $\Phi_{\nu\nu}(n)$, $\Phi_{\nu\nu}^H(n) \in C^{M \times M}$.

Let the true cross spectral density matrix be $\Phi \in C^{M \times M}$. True cross spectral density matrix can be obtained with the knowledge of the signals and noise environment. We now have two matrices $\hat{\Phi}(n)$ and $\Phi(2:n)$ as the estimate of the cross spectral density matrix Φ. Out of these two cross spectral density

matrix estimates we have to find out the one which is the closer to the true cross spectral density matrix Φ. A performance measure has to be defined in achieving this.

3.2 A performance measure

Let us first consider the cross spectral density matrix pair $(\Phi,\Phi(2:n))$. Since both Φ and $\Phi(2:n)$ matrices are Hermitian there exist unitary matrices Q and Q(2:n) such that,

$$Q\Phi Q^{H} = \Lambda, \text{ and} \tag{3.1.13}$$

$$Q(2:n)\Phi(2:n)Q^{H}(2:n) = \Lambda(2:n), \tag{3.1.14}$$

where,

$$\Lambda = \mathrm{diag}(\lambda_1,\lambda_2,\ldots,\lambda_M) \tag{3.1.15}$$

$$\Lambda(2:n) = \mathrm{diag}(\lambda_1(2:n),\lambda_2(2:n),\ldots,\lambda_M(2:n)), \tag{3.1.16}$$

diagonal elements in matrices Λ and $\Lambda(2:n)$ are in descending order,

$$QQ^{H} = I,\ Q(2:n)Q^{H}(2:n) = I, \tag{3.1.17}$$

I is an identity matrix and

$$Q, Q(2:n) \in C^{M\times M} \text{ and} \tag{3.1.18}$$

$$\Lambda, \Lambda(2:n) \in C^{M\times M}. \tag{3.1.19}$$

The columns of the matrices Q and Q(2:n) also represent the eigenvectors of the cross spectral density matrices Φ and $\Phi(2:n)$ respectively whereas the diagonal matrices Λ and $\Lambda(2:n)$ consist of the eigenvalues of the matrices Φ and $\Phi(2:n)$ respectively as the diagonal elements.

As we have shown in the chapter 2, the largest K diagonal elements of the matrices Λ and $\Lambda(2:n)$ correspond to the power associated with the signal subspace basis vectors while the M-K eigenvalues represent the power associated with the noise subspace basis vectors. We can now obtain the dominant mode or

the M^{th} order signal cross spectral density matrix $\Phi_{ss}^{(M)}$, and an estimate of it, $\Phi_{ss}^{(M)}(2:n)$ by removing the noise from the cross spectral density matrices Φ and $\Phi(2:n)$ respectively. This noise suppression can be achieved by substituting zeros in the place of M-K smallest eigenvalues. The signal cross spectral density matrices $\Phi_{ss}^{(M)}$ and $\Phi_{ss}^{(M)}(2:n)$ can therefore be written as,

$$\Phi_{ss}^{(M)} = Q^H \Lambda_s^{(M)} Q \quad \text{and} \tag{3.1.20}$$

$$\Phi_{ss}^{(M)}(2:n) = Q^H(2:n)\Lambda_s^{(M)}(2:n)Q(2:n) \tag{3.1.21}$$

$$\text{where, } \Lambda_s^{(M)} = \begin{bmatrix} \Lambda_s & | & 0 \\ \text{---} & & \text{---} \\ 0 & | & 0 \end{bmatrix} \tag{3.1.22}$$

$$\Lambda_s^{(M)}(2:n) = \begin{bmatrix} \Lambda_s(2:n) & | & 0 \\ \text{---------} & & \text{---} \\ 0 & | & 0 \end{bmatrix} \tag{3.1.23}$$

$$\Lambda_s = \text{diag}(\lambda_1, \lambda_2, \ldots, \lambda_K) \tag{3.1.24}$$

$$\Lambda_s(2:n) = \text{diag}(\lambda_1(2:n), \lambda_2(2:n), \ldots, \lambda_K(2:n)) \tag{3.1.25}$$

K is the number of signals, $\Phi_{ss}^{(M)}$, $\Phi_{ss}^{(M)}(2:n), \Lambda_s^{(M)}, \Lambda_s^{(M)}(2:n) \in C^{M \times M}$, $\Lambda_s, \Lambda_s(2:n) \in C^{K \times K}$.

Under the assumption that u(n) is Gaussian distributed, the information content (I_c) of the true cross spectral density matrix Φ and estimated cross spectral density matrix $\Phi(2:n)$ are proportionately given by,

$$I_c(\Phi) = \log |\Phi_{ss}^{(M)}|, \text{ and} \tag{3.1.26}$$

$$I_c(\Phi(2:n)) = \log |\Phi_{ss}^{(M)}(2:n)| \tag{3.1.27}$$

where, $|.|$ denotes the pseudo determinant defined as the largest value of the determinant of the minors of the cross spectral density matrix. $I_c(\Phi)$ and $I_c(\Phi(2:n))$ denote the information content of the matrices Φ and $\Phi(2:n)$ respectively.

The difference between $I_c(\Phi)$ and $I_c(\Phi(2:n))$ describes the amount of ignorance we have about the system and hence it can be used as a performance

measure of a estimated cross spectral density matrix.

Definition 3.1

We define a term 'height of ignorance (H_I)' between the cross spectral density matrix pair ($\Phi,\Phi(2:n)$) as,

$$H_I(\Phi,\Phi(2:n)) = \log \frac{|\Phi_{ss}^{(x)}|}{|\Phi_{ss}^{(x)}(2:n)|} \tag{3.1.28}$$

Theorem 3.1

The height of ignorance (H_I) has the relationship,

$$H_I(\Phi,\Phi(2:n)) = \sum_{k=1}^{K} I_{L(k)}(\Phi_{ss}^{(x)},\Phi_{ss}^{(x)}(2:n)) \tag{3.1.29}$$

where, $I_{L(k)}(\Phi_{ss}^{(x)},\Phi_{ss}^{(x)}(2:n))$ is the information loss of the k^{th} signal subspace component given by,

$$I_{L(k)}(\Phi_{ss}^{(x)},\Phi_{ss}^{(x)}(2:n)) = \log \frac{\lambda_k}{\lambda_k(2:n)} \tag{3.1.30}$$

Proof

By taking pseudo determinant on both sides of the eqns. (3.1.20) and (3.1.21) and using the fact that the unitary transformations are norm preserving, we obtain,

$$|\Phi_{ss}^{(x)}| = \prod_{k=1}^{K} \lambda_k \quad \text{and} \tag{3.1.31}$$

$$|\Phi_{ss}^{(x)}(2:n)| = \prod_{k=1}^{K} \lambda_k(2:n). \tag{3.1.32}$$

Then, H_I can be written as,

$$H_I(\Phi,\Phi(2:n)) = \log \frac{\prod_{k=1}^{K} \lambda_k}{\prod_{k=1}^{K} \lambda_k(2:n)} \tag{3.1.33}$$

$$= \sum_{k=1}^{K} \log \frac{\lambda_k}{\lambda_k(2:n)} \qquad (3.1.34)$$

Let,

$$I_{\Sigma(k)}(\Phi_{ss}^{(k)},\Phi_{ss}^{(k)}(2:n)) = \log \frac{\lambda_k}{\lambda_k(2:n)} \qquad (3.1.35)$$

Then, $I_{\Sigma(k)}(\Phi_{ss}^{(k)},\Phi_{ss}^{(k)}(2:n))$ represents the information loss of the k^{th} signal subspace component of the matrix pair $(\Phi_{ss}^{(k)},\Phi_{ss}^{(k)}(2:n))$. Eqn. (3.1.34) now becomes,

$$H_I(\Phi,\Phi(2:n)) = \sum_{k=1}^{K} I_{\Sigma(k)}(\Phi_{ss}^{(k)},\Phi_{ss}^{(k)}(2:n))$$

If the estimated cross spectral density matrix $\Phi(2:n)$ is equal to the true cross spectral density matrix Φ, then, the height of ignorance (H_I) becomes zero indicating that there is no ignorance about the system. On the other hand, if the estimated dominant mode cross spectral density matrix is zero, H_I becomes infinite and hence there is absolutely no information available about the system, i.e. total ignorance about the system. Therefore, the lower is the value of H_I, the better is the estimated cross spectral density matrix. Hence the height of ignorance provides a reasonable way of comparing the two estimates $\Phi(n)$ and $\Phi(2:n)$. The height of ignorance (H_I) for $\Phi(n)$ and $\Phi(2:n)$ can therefore be written as,

$$H_I(\Phi,\Phi(n)) = \sum_{k=1}^{K} \log \frac{\lambda_k}{\lambda_k(n)} \quad \text{, and} \qquad (3.1.36)$$

$$H_I(\Phi,\Phi(2:n)) = \sum_{k=1}^{K} \log \frac{\lambda_k}{\lambda_k(2:n)} \qquad (3.1.37)$$

The height of ignorance itself may not be sufficient to obtain the closeness of a cross spectral density matrix to the true cross spectral density matrix. We should also consider the perturbation of the estimated signal subspace

$Q_m(2:n)$ from the true signal subspace Q_N. In order to analyze the deviation of the estimated signal subspace from the true signal subspace we make the following definition in the light of the work by Wang and Kaveh (1986).

Definition 3.2

K-Perturbation $(\alpha_K(\Phi,\Phi(2:n))$ is defined as,

$$\alpha_K(\Phi,\Phi(2:n))=\cos^{-1}[|\{q_K^{(m)}\}^H q_K^{(m)}(2:n)|],$$

where K is the number of signals, $q_K^{(m)}(2:n)$ and $q_K^{(m)}$ are the K^{th} columns of the matrices $Q_m(2:n)$ and Q_m respectively, $|.|$ denotes the absolute value.

We know the fact that the eigenvector corresponding to the smallest eigenvalue is the most perturbed eigenvector compared to the rest of the eigenvectors. Therefore $\alpha_K(\Phi,\Phi(2:n))$ will be the largest perturbation angle that can exist in the estimated signal subspace. If the estimated signal subspace is in coincidence with the true subspaces, then the K-perturbation angle is zero. Therefore, the lower the is the K-perturbation angle the better the estimated cross spectral density matrix. Hence the K-perturbation angle provide a reasonable measure to compare the closeness of the estimated cross spectral density matrix to the true cross spectral density matrix. K-Perturbation angles for the estimated cross spectral density matrices $\Phi(n)$ and $\Phi(2:n)$ can therefore be written as,

$$\alpha_K(\Phi,\Phi(n))=\cos^{-1}[|\{q_K^{(m)}\}^H q_K^{(m)}(n)|],$$

$$\alpha_K(\Phi,\Phi(2:n))=\cos^{-1}[|\{q_K^{(m)}\}^H q_K^{(m)}(2:n)|].$$

3.3 Simulation Results

For the purpose of simulation we consider two narrow band signals

reaching an array consisting of five equally separated sensors, in distinct directions. The target signal and the interference are assumed to be coming from the directions $\sin^{-1}(0.2)$ and $\sin^{-1}(-0.4)$ respectively. We further assume that the incoming signals are uncorrelated and the signals and noise are uncorrelated. We consider the cases where signal to noise ratio (SNR) is 20 dB and interference to noise ratios are 40 dB, 30 dB and 20 dB.

We consider one hundred snapshots. After averaging over 200 independent realizations, the height of ignorance and the K-Perturbation of the cross spectral density matrices $\Phi(n)$and $\Phi(2:n)$ are tabulated in the Tables 3.1 and 3.2 respectively for three different interference to noise ratio (INR) values. It can be seen that the height of ignorance and the K-Perturbation of the cross spectral density matrix $\Phi(2:n)$ are smaller than the height of ignorance of the cross spectral density matrix $\Phi(n)$. Therefore, the cross spectral density matrix $\Phi(2:n)$ provides a better estimate for the cross spectral density matrix Φ than the cross spectral density matrix $\Phi(n)$. The exact relationship of height of ignorance for the estimated cross spectral density matrices $\Phi(n)$ and $\Phi(2:n)$ is not clear.

Therefore, the forward and backward techniques should provide an improved performance in adaptive array processing. The performance of the flipping as applied to the minimum variance distortionless response (MVDR) beamformer will be given in chapter 6.

3.4 Discussion

Flipping technique provides a suitable structure for systolic array implementation of forward and backward techniques in adaptive array processing. The cross spectral density matrix obtained by using the flipping technique is a better estimate compared to the unflipped cross spectral density matrix. There-

fore the use of the flipping technique should provide improved performance in adaptive array processing for symmetric arrays. Flipping technique cannot be used with asymmetric arrays.

Table 3.1

Height of Ignorance (H_x) for $\Phi(n)$ and $\Phi(2:n)$

INR dB	$H_x(\Phi,\Phi(n))$	$H_x(\Phi,\Phi(2:n))$
40	0.0051	0.0021
30	0.0041	0.0023
20	0.0045	0.0030

Table 3.2

K-Perturbation

INR dB	$\alpha_K(\Phi,\Phi(n))$	$\alpha_K(\Phi,\Phi(2:n))$
40	0.011	0.0071
30	0.029	0.0194
20	0.124	0.0075

CHAPTER 4

BEARINGS ESTIMATION IN ADAPTIVE ARRAY PROCESSING

Preview Bearing estimation in adaptive array processing means the estimation of the number of signals and their angles of arrivals. Super resolution techniques based on subspace decomposition are considered in this chapter.

Limitations of the modified forward and backward linear prediction (MFBLP) is studied. It is shown that the MFBLP is sensitive to the eigenvalue spread of the signal cross spectral density matrix for finite number of snapshots. Further MFBLP can provide an unbiased estimate only at infinite signal to noise ratio.

To overcome these limitations we introduce a modification to the modified forward and backward linear prediction(M-MFBLP). This improvement is achieved by using the normal equation with noise removed in place of the normal equation with noise only partially removed as in MFBLP. In MFBLP, a noisy vector is projected on to the column space of the noise partially removed signal only cross spectral density matrix whereas in M-MFBLP, a noise removed vector is projected on to the column space of the noise removed signal cross spectral density matrix. On the other hand, in linear prediction a noisy vector is projected on to the column space of the cross spectral density matrix. For smaller number of snapshots, M-MFBLP provides improved

performance and it is robust to the eigenvalue spread of the signal cross spectral density matrix. Furthermore, M-MFBLP provides asymptotically unbiased estimate.

Spectral estimate derived by using either MFBLP or M-MFBLP depends, not only on the perturbation of eigenvectors of the cross spectral density matrix but also on the perturbation of the eigenvalues. Since the eigenvectors are asymptotically not affected by the signal to noise ratio, we could also obtain a bearing estimate which is independent of the signal to noise ratio by defining a bearing estimate which depend only on the eigenvectors.

The techniques which depend only on the eigenvectors are unaffected by the signal to noise ratio provided the true cross spectral density matrix is known(Appendix 4a). Of course the knowledge of the true cross spectral density matrix is not available in practice and hence the estimated cross spectral density matrix is used. The use of estimated cross spectral density matrix makes the bearing estimation techniques based on eigenvectors alone, such as proper orthogonal projection multiple signal classification (POP-MUSIC) family, depend on the signal to noise ratio. But this dependence will not be severe as it is in MFBLP or any other conventional, and high resolution techniques.

Two spectral estimates named POP-MUSIC-Euc and POP-MUSIC-Elem are derived based on the 'proper orthogonal projection' which provide a deeper insight into the MUSIC method. Geometric relationship between the POP-MUSIC-Euc and POP-MUSIC-Elem is given. It is shown that POP-MUSIC-Elem provides sharper peaks compared to the POP-MUSIC-Euc. At this point, it is worthwhile to

mention that the sharpness of the peaks itself is not a criterion for analyzing the performance of the spectral estimates. POP-MUSIC-Euc does not give rise to any dominant spurious peaks even though theoretically one may expect them in the POP-MUSIC-Elem spectrum. But to our knowledge the occurrence of dominant spurious peaks in POP-MUSIC-Elem is very rare in practice. If the true cross spectral density matrix is known, neither POP-MUSIC-Euc estimate nor POP-MUSIC-Elem estimate is affected by the signal to noise ratio. This is mainly because in both POP-MUSIC-Euc and POP-MUSIC-Elem, eigenvectors that are not affected by the signal to noise ratio are used. But in practice, estimated cross spectral density matrix is generally used in the place of the true cross spectral density matrix and hence the POP-MUSIC bearing estimates are affected by the signal to noise ratio. Further, it is shown that the minimum norm method used in bearing estimation is a special case of the POP-MUSIC-Elem. Additionally, the generalized minimum norm technique is introduced.

As was mentioned earlier, theoretically there is no limitation to the resolution capabilities of the MUSIC method if the true cross spectral density matrix is known. But in practice due to the errors in the estimated cross spectral density matrix, the resolution capabilities of the MUSIC method will be limited. The errors in the cross spectral density matrix causes a rotation of the subspaces from the true subspaces and that leads to the limitation in the resolution capabilities of the POP-MUSIC method. Rotational correction multiple signal classification (ROC-MUSIC) is introduced in correcting the errors in the estimated subspaces and hence improved resolution capabilities over the

rest of the spectra. The rotational correction is performed using the plane rotation. In ROC-MUSIC, due to the non-existence of an unique criterion in guiding the rotation we could not achieve the expected ideal performance. However, it is observed that the ROC-MUSIC spectrum is capable of providing improved resolution over the rest of the spectra if a suitable criterion is found in guiding the rotation. Additionally, computer simulation results are presented.

The spectral estimation techniques such as high resolution and super resolution techniques which are based on the eigenstructure of the cross spectral density matrix will fail to perform under the coherent signal environment. In the presence of coherent signal environment, the signal cross spectral density matrix become rank deficient. In general, the rank of the cross spectral density matrix is recovered by using the spatial smoothing preprocessing of the cross spectral density matrix. To our knowledge existing literature consider only the case where all the incoming signals are coherent. Further, in selecting the number of subarrays it is assumed that the number of incoming signals are known, which is not a valid assumption in practice. Even with this assumption there does not exist a methodology for estimating the optimal number of subarrays since the number of signals that are coherent is not known.

Here we study the effect of spatial smoothing in a more general framework where two or more signals are coherent. A methodology is formulated to estimate the number of incoming signals and the optimal number of subarrays concurrently.

We also present the 'adaptive spatial data smoothing preproc-

essing (ASDSP)' scheme in recovering the rank of the data matrix adaptively and hence the rank of the cross spectral density matrix. In ASDSP, cross spectral density matrices for each subarray are not constructed and hence it is computationally more stable and efficient compared to the spatial smoothing of the cross spectral density matrix. Both ASDSP and the spatial cross spectral density matrix smoothing perform under the same principle. A suitable systolic array structure is presented for VLSI implementation of the adaptive spatial data smoothing preprocessing scheme. Computer simulation results are presented.

4.1 Modification to the Modified Forward and Backward Linear Prediction (M-MFBLP)

4.1.1 Introduction

We consider the case where the noise is spatially uncorrelated. The basic nature of the M-MFBLP can be found in Tuft and Kumaresan (1982), and Haykin (1986). In general, forward and backward linear prediction (FBLP) finally reduces to the solution of the normal equation.,

$\Phi(2:n)a = b(2:n)$

where, $\Phi(2:n) \in C^{M \times M}$,

$\Phi(2:n)$ is the estimated cross spectral density matrix and it contains the elements

$\phi_{ij}(2:n)$, $i,j = 0,1,2,\ldots,M-1$,

$b^T(2:n) = (\phi_{01}(2:n),\phi_{02}(2:n),\ldots,\phi_{0M}(2:n))$, and a is the prediction filter vector, notation (2:n) follows the definition given in chapter 3.

In the MFBLP, the solution of the normal equation is performed in several steps.,

step 1 ; A large aperture size prediction filter is used

step 2 : In the place of $\Phi(2:n)$, noise removed cross spectral density matrix $\Phi_{ss}^{(\infty)}(2:n)$ is used. The noise removed cross spectral density matrix $\Phi_{ss}^{(\infty)}(2:n)$ is obtained by using the Hermitian eigenvalue eigenvector decomposition of the matrix $\Phi(2:n)$ and can be written as,

$\Phi_{ss}^{(\infty)}(2:n) = V_s(2:n)\Lambda_s(2:n)V_s^H(2:n)$

where $\Lambda_s(2:n)$ represents the estimated signal space eigenvalue matrix and $V_s(2:n)$ is the corresponding eigenvector matrix, and

$\Lambda_s(2:n)=\mathrm{diag}(\lambda_1(2:n),\lambda_2(2:n),....,\lambda_K(2:n))$.

step 3 : The prediction filter vector a is obtained as the minimum norm solution to the normal equation and it is given by,

$a = [\Phi_{ss}^{(\infty)}(2:n)]^{\#}b(2:n)$, where $[.]^{\#}$ denotes the pseudo inverse of $\{.\}$.

MFBLP provide a biased estimate due to the remaining noise in the signal eigenvalues. It can easily be made asymptotically unbiased by subtracting the smallest eigenvalue from the rest of the eigenvalues, i.e. we modify the step 2 such that,

$\Lambda_s(2:n)=\mathrm{diag}(\lambda_1(2:n),\lambda_2(2:n),....,\lambda_K(2:n))-\lambda_M(2:n)I$

where, λ_i, i=1,2,...M are the eigenvalues of $\Phi(2:n)$, I is an identity matrix, and $\lambda_M(2:n)$ is the smallest eigenvalue.

The vector b(2:n) that is used in MFBLP contains the elements of the cross spectral density matrix $\Phi(2:n)$, and it is a noisy vector. This will deteriorate the performance of the modified forward and backward linear prediction depending on the amount of noise perturbation in the vector b(2:n) and more importantly, when the perturbation is not orthogonal to the column space of the signal cross spectral density matrix. Perturbation vector of this nature may

specially be observed at small number of snapshots.

We propose a modification to the modified forward and backward linear prediction (M-MFBLP). In M-MFBLP, we first form the cross spectral density matrix $\Phi^{(M-1)}(n)$ of order (M+1) and, then removing the noise and by partitioning we obtain a noise removed vector b(2:n) and the asymptotically noise free cross spectral density matrix $\Phi^{(M)}(n)$ of order M which will later be used in the normal equation.

4.1.2 Effect of signal eigenvalue spread on MFBLP

Let the noise perturbation of vector b(2:n) at n^{th} snapshot be $\delta b(2:n)$. It is now important to study the effect of the perturbation vector $\delta b(2:n)$ on the vector a. To do this we formulate the following Theorem.

Theorem 4.1

Let consider the noise free normal equation

$$\Phi_{ss}^{(M)}(2:n)a = b(2:n). \tag{4.1.1}$$

The relative change of b(2:n) by $\delta b(2:n)$ produces a change in a by δa, and the relative change of a is bounded by the relative change of b(2:n) such that,

$$\sup \frac{|\delta a|}{|a|} = c(\Phi_{ss}^{(M)}(2:n)) \frac{|\delta b(2:n)|}{|b(2:n)|} \tag{4.1.2}$$

where,

$c(\Phi_{ss}^{(M)}(2:n))$ = signal eigenvalue spread (4.1.3)

Proof

If the vector b(2:n) in the noise free normal eqn.,

$$\Phi_{ss}^{(M)}(2:n)a = b(2:n), \tag{4.1.4}$$

is perturbed by the amount $\delta b(2:n)$, the vector a will also be perturbed by the

amount δa given by,

$$\Phi_{ss}^{(\infty)}(2:n)(a+\delta a) = b(2:n)+\delta b(2:n). \tag{4.1.5}$$

Eqns. (4.1.4) and (4.1.5) simplified to

$$\Phi_{ss}^{(\infty)}(2:n)\delta a = \delta b(2:n). \tag{4.1.6}$$

Eqn. (4.1.6) can also be written as,

$$\delta a = [\Phi_{ss}^{(\infty)}(2:n)]^{*}\delta b(2:n). \tag{4.1.7}$$

Dividing the eqn. (4.1.7) by $|a|$, we obtain,

$$\frac{\delta a}{|a|} = [\Phi_{ss}^{(\infty)}(2:n)]^{*} \frac{\delta b(2:n)}{|a|} \tag{4.1.8}$$

where, $|.|$ denotes a suitable norm of a vector or a matrix.

Using Schwartz inequality in eqn. (4.1.4), we obtain,

$$|b(2:n)| \le |\Phi_{ss}^{(\infty)}(2:n)|\,|a| \tag{4.1.9}$$

i.e. $|a| \ge |\Phi_{ss}^{(\infty)}(2:n)|^{-1}|b(2:n)|$. (4.1.10)

Eqns. (4.1.8) and (4.1.10) can be used to obtain the relationship,

$$\frac{\delta a}{|a|} \le |\Phi_{ss}^{(\infty)}(2:n)|\,[\Phi_{ss}^{(\infty)}(2:n)]^{*} \frac{\delta b(2:n)}{|b(2:n)|} \tag{4.1.11}$$

Using Schwartz inequality in eqn. (4.1.11) we obtain,

$$\frac{|\delta a|}{|a|} \le c(\Phi_{ss}^{(\infty)}(2:n)) \frac{|\delta b(2:n)|}{|b(2:n)|}, \tag{4.1.12}$$

where, $c(\Phi_{ss}^{(\infty)}(2:n)) = |\Phi_{ss}^{(\infty)}(2:n)|\,|[\Phi_{ss}^{(\infty)}(2:n)]^{*}|$ (4.1.13)

i.e. $$\sup \frac{|\delta a|}{|a|} = c(\Phi_{ss}^{(\infty)}(2:n)) \frac{|\delta b(2:n)|}{|b(2:n)|}$$

If we use the spectral norm,

$c(\Phi_{ss}^{(\infty)}(2:n)) = \lambda_1/\lambda_K$

=signal eigenvalue spread,

where, λ_1 and λ_K are the largest and smallest signal eigenvalues respectively.

Let the projection of $\delta b(2:n)$ on the column space of the matrix $\Phi_{ss}^{(\infty)}(2:n)$ be $\delta b_s(2:n)$; then, from eqns. (4.1.6) and (4.1.7) we obtain,

$\delta b_s(2:n) = P_s(2:n)\delta b(2:n)$

where, $P_s(2:n) = \Phi_{ss}^{(\infty)}(2:n)[\Phi_{ss}^{(\infty)}(2:n)]^{*}$

$P_s(2:n)$ denotes the signal subspace projection matrix. Additionally, $P_s(2:n)$ also has the relationship,

$P_s(2:n) = V_s^{(\infty)}(2:n)[V_s^{(\infty)}(2:n)]^{H}$.

We have assumed that the signals and noise are asymptotically uncorrelated. Therefore, for larger number of snapshots, noise perturbation vector $\delta b(2:n)$ is orthogonal to the signal subspace $P_s(2:n)$, and hence $\delta b_s(2:n)$ will be a null vector. But for small number of snapshots $\delta b_s(2:n)$ may not be perpendicular to the signal subspace. From the Theorem 3.1 it is clear that the larger is the eigenvalue spread of the signal cross spectral density matrix the larger is the variance of the bearing estimate for finite number of snapshots. Since we have no control over the eigenvalue spread, this problem can be overcome by removing the perturbation vector $\delta b_s(2:n)$.

4.1.3 Formulation of the M-MFBLP

We start with a brief introduction to the division of array elements into subarrays. We consider a linear array consisting of M_T even number of sensors. The input vector at n^{th} snapshot $u_T(n)$ is given by,

$u_T(n) = (u_1(n), u_2(n), \ldots, u_{MT}(n))^{T}$.

(please note that $_{MT}$ is the same as M_T)

where [.] denotes the transpose of [.].

In forward and backward linear prediction, we divide the array of M_T elements into J overlapping subarrays such that each subarray consist of M

elements where M will be the length of the prediction filter. The division of the subarray is done such that they overlap, i.e. sensors {1,2,...,M} form the first subarray, sensors {2,3,...M+1} form the second subarray and so on. Hence the number of subarrays is given by,

$$J = M_T - M + 1 \tag{4.1.14}$$

In modified forward and backward linear prediction, the size of the subarray or the order of the prediction filter is chosen such that [Tuft and Kumaresan (1982), Haykin (1986)],

$$M = \lfloor 0.75M_T \rfloor_{odd}. \tag{4.1.15}$$

where $\lfloor . \rfloor_{odd}$ denotes the nearest odd number.

Combining eqns. (4.1.14) and (4.1.15), we obtain,

$$J = \lfloor 0.25M_T+1 \rfloor. \tag{4.1.16}$$

$\lfloor . \rfloor$ denotes the nearest lower integer.

For the j^{th} subarray, the data vector at the n^{th} snapshot is given by,

$$u_j(n) = (u_j(n),u_{j-1}(n),...,u_{j-M}(n))^T. \tag{4.1.17}$$

We now form the data matrix $U_m(2:n)$ for the n^{th} snapshot such that,

$$U_m(2:n) = [u_1(n),u_1^*(n),u_2(n),u_2^*(n),...,u_J(n),u_J^*(n)] \tag{4.1.18}$$

$$U_m(2:n) \in C^{M \times 2J}.$$

Then, the complete data matrix U(2:n) after n^{th} snapshot can be constructed so that,

$$U(2:n) = [U_m(2:1),U_m(2:2),...,U_m(2:n)] \tag{4.1.19}$$

$$U(2:n) \in C^{M \times 2nJ}.$$

We employ the Jacobi-Givens rotation by premultiplying the matrix $U^H(2:n)$ by a unitary matrix, $Q^H(2:n) \in C^{2nJ \times 2nJ}$ resulting in an upper triangular matrix $R^H(2:n) \in C^{M \times M}$.

Matrix $R^H(2:n)$ can be obtained adaptively using the flipping network and

the matrix triangularization systolic array structure. The implementation is the same as the adaptive spatial data smoothing preprocessing scheme that will be given in section 4.4. Due to this inherent adaptive spatial data smoothing, MFBLP or M-MFBLP can be used even when the incoming signals are coherent.

The estimated signal and noise cross spectral density matrix $\Phi(2:n)$, can now be written as,

$$\Phi(2:n) = U(2:n)U^{H}(2:n)$$
$$= R(2:n)R^{H}(2:n),\ \Phi(2:n) \in C^{M\times M}. \tag{4.1.20}$$

Now in developing the M-MFBLP, we first consider a subarray of size M+1 and generate the cross spectral density matrix $\Phi^{(M+1)}(2:n)$ given by,

$$\Phi^{(M+1)}(2:n) = R^{(M+1)}(2:n)[R^{(M+1)}(2:n)]^{H} \tag{4.1.21}$$

$$\Phi^{(M+1)}(2:n) \in C^{(M+1)\times(M+1)}. \tag{4.1.22}$$

Then, performing the Hermitian eigenvalue eigenvector decomposition on the matrix $\Phi^{(M+1)}(2:n)$, we obtain the estimated signal cross spectral density matrix $\Phi_{ss}^{(M+1)}(2:n)$,

$$\Phi_{ss}^{(M+1)}(2:n) = V_s^{(M+1)}(2:n)\Lambda_s^{(M+1)}(2:n)[V_s^{(M+1)}(2:n)]^{H} \tag{4.1.23}$$

where,

$$\Lambda_s^{(M+1)}(2:n)=\mathrm{diag}(\lambda_1^{(M+1)}(2:n),\lambda_2^{(M+1)}(2:n),$$
$$\ldots,\lambda_K^{(M+1)}(2:n))-\lambda_M^{(M+1)}(2:n)I,$$

$\lambda_i^{(M+1)}(2:n)$, i = 1,2,...M denotes the eigenvalues in descending order, $V_s^{(M+1)}(2:n)$ is the matrix that contains the signal subspace basis vectors as its columns, and notation (2:n) is used to show that they are derived using the cross spectral density matrix estimate obtained by flipping (chapter 3).

$V_s^{(M+1)}(2:n) \in C^{(M+1)\times K}$, $\Lambda_s^{(M+1)}(2:n) \in C^{K\times K}$,

$\Phi_{ss}^{(M+1)}(2:n) \in C^{(M+1)\times(M+1)}$, and K is the number of signals.

Now we partition the signal subspace basis vector matrix $V_s(2:n)$ such

that,

$$V_{ss}^{(M-1)}(2:n) = \begin{bmatrix} [v_{ss}^{(M-1)'}(2:n)]^T \\ \hline V_{ss}^{(M-1)'}(2:n) \end{bmatrix} \tag{4.1.24}$$

where $v^{(M-1)'}(2:n)$ is the vector that contains the first row of the matrix $V_{ss}^{(M-1)}(2:n)$, $V_{ss}^{(M-1)'}(2:n)$ is the matrix obtained by deleting the first row of the matrix $V_{ss}^{(M-1)}(2:n)$, and $V_{ss}^{(M-1)'}(2:n) \in C^{M\times K}$.

Substituting eqn. (4.1.24) in eqn. (4.1.23), we get,

$$\Phi_{ss}^{(M-1)}(2:n) = \begin{bmatrix} \phi(0) & | & b^T(2:n) \\ \hline b^*(2:n) & | & \Phi^{(M)}(2:n) \end{bmatrix} \tag{4.1.25}$$

where,

$$b(2:n) = [V_{ss}^{(M-1)'}(2:n)]^* \Lambda_{ss}^{(M-1)}(2:n) v^{(M-1)'}(2:n) \tag{4.1.26}$$

$$\Phi^{(M)}(2:n) = V_{ss}^{(M-1)'}(2:n) \Lambda_{ss}^{(M-1)}(2:n) [V_{ss}^{(M-1)'}(2:n)]^H \tag{4.1.27}$$

$$\phi(0) = [v^{(M-1)'}(2:n)]^T \Lambda_{ss}^{(M-1)}(2:n) [v^{(M-1)'}(2:n)]^* \tag{4.1.28}$$

$\Phi^{(M)}(2:n) \in C^{M\times M}$, $[.]^*$ denotes the complex conjugate of $[.]$.

Once again we use the eigenvalue eigenvector decomposition on $\Phi^{(M)}(2:n)$ to obtain,

$$\Phi^{(M)}(2:n) = V^{(M)}(2:n) \Lambda^{(M)}(2:n) [V^{(M)}(2:n)]^H, \tag{4.1.29}$$

where, $\Lambda^{(M)}(2:n) = \mathrm{diag}(\lambda_1^{(M)}(2:n), \lambda_2^{(M)}(2:n), \ldots, \lambda_M^{(M)}(2:n))$,

The estimated M^{th} order signal cross spectral density matrix $\Phi_{ss}^{(M)}(2:n)$ can be written as,

$$\Phi_{ss}^{(M)}(2:n) = V_{ss}^{(M)}(2:n) \Lambda_{ss}^{(M)}(2:n) [V_{ss}^{(M)}(2:n)]^H \tag{4.1.30}$$

$$\Lambda_{ss}^{(M)}(2:n) = \mathrm{diag}(\lambda_1^{(M)}(2:n), \lambda_2^{(M)}(2:n), \ldots, \lambda_K^{(M)}(2:n)) - \lambda_M^{(M)}(2:n))I,$$

where, I is an identity matrix, $V_{ss}^{(M)}(2:n)$ is the estimated signal subspace basis vector matrix,

$V^{(M)}(2:n) = [V_{ss}^{(M)}(2:n), V_N^{(M)}(2:n)]$, $V^{(M)}(2:n) \in C^{M\times M}$, $V_{ss}^{(M)}(2:n) \in C^{M\times K}$, $V_N^{(M)}(2:n) \in C^{M\times(M-K)}$, and K is the number of signals.

Using the noise removed M^{th} order cross spectral density matrix $\Phi_{aa}^{(M)}(2:n)$ given in eqn. (4.1.30) and the noise removed vector b(2:n) given in eqn. (4.1.26), we can write the normal equation,

$$\Phi_{aa}^{(M)}(2:n)a = b(2:n) \tag{4.1.31}$$

where, a is the prediction filter.

Eqn. (4.1.31) can also be written as,

$$a = [\Phi_{aa}^{(M)}(2:n)]^{\#}b(2:n) \tag{4.1.32}$$

where, $[.]^{\#}$ represent the pseudoinverse of [.].

$[\Phi_{aa}^{(M)}(2:n)]^{\#}$ can be obtained by using eqn. (4.1.30) and it is given by,

$$[\Phi_{aa}^{(M)}(2:n)]^{\#} = V_a^{(M)}(2:n)[\Lambda_a^{(M)}(2:n)]^{-1}[V_a^{(M)}(2:n)]^{H} \tag{4.1.33}$$

Using eqns. (4.1.32) and (4.1.33), and substituting for vector b(2:n) from eqn. (4.1.26), we obtain,

$$a = V_a^{(M)}(2:n)[\Lambda_a^{(M)}(2:n)]^{-1}[V_a^{(M)}(2:n)]^{H} \cdot [V_a^{(M-1)'}(2:n)]^{-}\Lambda_a^{(M-1)}(2:n)v^{(M-1)'}(2:n) \tag{4.1.34}$$

Therefore, the modified - modified forward and backward linear prediction spectrum, $S_M(2:n,\theta)$ can be written as,

$$S_M(2:n,\theta) = |H(z)|^{-2} \tag{4.1.35}$$

where, $H(z) = (a')^{H}d(\theta)$, (4.1.36)

$$a' = \begin{bmatrix} 1 \\ -a \end{bmatrix}, \tag{4.1.37}$$

$d(\theta)$ is the direction vector given by,

$$d(\theta) = (z^{-J}, z^{-J+1}, z^{-J+2}, \ldots, z^{J}), \tag{4.1.38}$$

$J = 0.5(M-1)$ and $z = \exp(j \frac{2\pi\ell}{\lambda} \sin\theta)$.

Based on computer simulation, it has been shown by Reilly (1986), and Wong (1987) that the M-MFBLP provides improved performance over the MFBLP.

4.1.4 Discussion

MFBLP is sensitive to the eigenvalue spread of the signal cross spectral density matrix and it can not provide an asymptotically unbiased estimate. MFBLP can be made asymptotically unbiased by subtracting the smallest eigenvalue from the rest of the eigenvalues. The proposed M-MFBLP is less sensitive to the eigenvalue spread of the signal cross spectral density matrix and it also provides an asymptotically unbiased estimate. Therefore, M-MFBLP provides improved performance irrespective of the number of snapshots. M-MFBLP requires the eigenvalue decomposition twice and that is the cost one has to pay for the proposed improvement.

4.2 Proper Orthogonal Projection Multiple Signal Classification (POP-MUSIC)

4.2.1 Introduction

For finite number of snapshots both MFBLP and M-MFBLP provide bearing estimates that are perturbed by the errors due to both eigenvalues and eigenvectors. This may result larger bias and larger variance in the MFBLP and M-MFBLP spectrum estimates. Since the proper orthogonal projection multiple signal classification (POP-MUSIC) is derived based on the eigenvectors alone, POP-MUSIC family is less perturbed for the finite number of snapshots compared to the rest of the spectra. This fact increases the superiority of the POP-MUSIC family over the rest of the bearing estimation techniques.

In chapter 2, we have introduced the proper orthogonal projection multiple signal classification (POP-MUSIC) as a generalization of the MUSIC method. Here, we derive two spectral estimates, POP-MUSIC-Euc and POP-MUSIC-Elem based on the Euclidian norm and the elemental norm. Geometrical

relationship between POP-MUSIC-Euc and the POP-MUSIC-Elem are developed. It is shown theoretically that the POP-MUSIC-Elem leads to sharper peaks compared to the POP-MUSIC-Euc. POP-MUSIC-Euc does not give any dominant spurious peaks and hence it is unambiguous whereas the POP-MUSIC-Elem may give rise to dominant spurious peaks theoretically, even though to our knowledge such cases are very rare in practice.

Minimum norm (MN) spectrum is rediscovered as a special case of the POP-MUSIC-Elem spectrum. The relationship between the POP-MUSIC and the minimum norm (MN) method is developed. Generalized minimum norm (GMN) method is introduced. Computer simulation results are presented.

Further, geometrical relationship between the maximum likelihood (ML) method and the linear prediction (LP) method is developed based on the proper orthogonal projection (POP-MUSIC) (Appendix 4b). General consideration of the geometric relationships between the spectrum estimation techniques will be given in chapter 5.

4.2.2 POP-MUSIC-Euc

In section 2.3.5, we have obtained the proper orthogonal projection matrices $P_N(2:n)$ and $P_s(2:n)$ for noise subspace and signal subspace respectively. Now we obtain the projection of M dimensional vector $d(\theta)$ onto the noise subspace, $d_N(\theta)$,

$$d_N(\theta) = P_N(2:n)d(\theta) \tag{4.2.1}$$

Now we define a spatial spectral estimate $S_{POP-Euc}(2:n,\theta)$ as,

$$S_{POP-Euc}(2:n,\theta) = |d_N(\theta)|^{-a} \tag{4.2.2}$$

where, $|.|$ denotes the Euclidian norm.

Definition 4.2.1

Dominant Peaks

The peaks that correspond to the infinite amplitude of the spectrum are referred to as the dominant peaks

If the direction vector $d(\theta)$ lies in the signal subspace, $d_N(\theta) = 0$, and therefore dominant peaks of the spectrum $S_{POP-Euc}(2:n,\theta)$ occur at the angles corresponding to the direction of the incoming signals. Eqn. (4.2.2) can also be written as,

$$S_{POP-Euc}(2:n,\theta) = [d_N^H(\theta)d_N(\theta)]^{-1}, \tag{4.2.3}$$

$$= [\{P_N(2:n)d(\theta)\}^H\{P_N(2:n)d(\theta)\}]^{-1},$$

$$= [d^H(\theta)P_N(2:n)d(\theta)]^{-1} \tag{4.2.4}$$

If we replace the matrix $P_N(2:n)$ of eqn. (4.2.4) by $\Phi^{-1}(2:n)$, it is the same as the maximum likelihood spectral estimate. In view of the similarity between the maximum likelihood spectral estimate (maximum likelihood spectrum estimate can be found in [Haykin (1985)]),

$$S_{ML}(2:n,\theta) = [d^H(\theta)\Phi^{-1}(2:n)d(\theta)]^{-1}, \tag{4.2.5}$$

and the $S_{POP-Euc}(2:n,\theta)$ given in eqn. (4.2.4), the $S_{POP-Euc}(2:n,\theta)$ can also be named as POP-MUSIC-ML.

POP-MUSIC-Euc spectrum $S_{POP-Euc}(2:n,\theta)$ can alternatively be expressed as the reciprocal of the polynomial G(z) such that,

$$S_{POP-Euc}(2:n,\theta) = [G(z)]^{-1} \tag{4.2.6}$$

where, $$G(z) = \sum_{m=-M+1}^{M-1} g_m(2:n)z^m \tag{4.2.7}$$

and $g_m(2:n)$ is given by,

$$g_{m-1}(2:n) = \sum_{j=1}^{M-m+1} p_{N(j,m-j-1)}(2:n), \quad 1 \le m \le M \tag{4.2.8}$$

$$g_{-m}(2:n) = g_m^*(2:n), \quad m > 0 \tag{4.2.9}$$

$[.]^*$ denotes the complex conjugate of $[.]$, $p_{N(m,j)}(2:n)$ is the $(m,j)^{th}$ element of the matrix $P_N(2:n)$, and eqn. (4.2.9) holds since $P_N(2:n)$ is Hermitian.

Polynomial G(z) given in eqn. (4.2.7) is symmetric, and hence it has 2(M-1) roots which occur in conjugate reciprocal pairs, i.e. if z_k is a root of G(z), the $(z_k^*)^{-1}$ is also a root of G(z). If the estimated cross spectral density matrix $\Phi(2:n)$ is equal to the true cross spectral density matrix Φ, and if there is no source of errors in computing the noise subspace projection matrix P(2:n), the polynomial G(z) will have K double roots on the unit circle, i.e.

$$z_k = \exp(j \frac{2\pi\ell}{\lambda} \sin \theta_k) \tag{4.2.10}$$

corresponding to the K signals arriving from the directions θ_k, k = 1,2,...,K.

Theorem 4.2.1

The number of dominant peaks in the POP-MUSIC-Euc spectrum is equal to the number of incoming signals and they occur at the angles corresponding to the incoming signals if the true cross spectral density matrix is known.

Proof:

We first consider the case where the noise is spatially uncorrelated. Then the generalized eigenvalue eigenvector decomposition becomes Hermitian eigenvalue eigenvector decomposition. For Hermitian eigenvectors noise subspace projection matrix $P_N(2:n)$ can be written as,

$$P_N(2:n) = [v_{K+1}(2:n), v_{K+2}(2:n), \ldots, v_M(2:n)] \cdot [v_{K+1}(2:n), v_{K+2}(2:n), \ldots, v_M(2:n)]^H \tag{4.2.11}$$

Then the noise subspace projection of $d_N(\theta)$ of $d(\theta)$ can be written as,

$$d_N(\theta) = P_N(2:n)d(\theta) \tag{4.2.12}$$

$$= V_N(2:n)\begin{bmatrix} v_{K+1,1}^*(2:n), v_{K+2,2}^*(2:n), \ldots, v_{K+1,M}^*(2:n) \\ v_{K+2,1}^*(2:n), v_{K+2,2}^*(2:n), \ldots, v_{K+2,M}^*(2:n) \\ v_{K+3,1}^*(2:n), v_{K+3,2}^*(2:n), \ldots, v_{K+3,M}^*(2:n) \\ \vdots \\ v_{M,1}^*(2:n), \quad v_{M,2}^*(2:n) \quad , \ldots, v_{M,M}^*(2:n) \end{bmatrix} d(\theta) \tag{4.2.13}$$

$$= \begin{bmatrix} v_{1,K+1}(2:n), v_{1,K+2}(2:n), \ldots, v_{1,M}(2:n) \\ v_{2,K+1}(2:n), v_{2,K+2}(2:n), \ldots, v_{2,M}(2:n) \\ v_{3,K+1}(2:n), v_{3,K+2}(2:n), \ldots, v_{3,M}(2:n) \\ \vdots \\ v_{M,K+1}(2:n), v_{M,K+2}(2:n), \ldots, v_{M,M}(2:n) \end{bmatrix} \begin{bmatrix} \cos(\alpha_{K+1})\exp(j\beta_{K+1}) \\ \cos(\alpha_{K+2})\exp(j\beta_{K+2}) \\ \cos(\alpha_{K+3})\exp(j\beta_{K+3}) \\ \vdots \\ \cos(\alpha_M)\exp(j\beta_M) \end{bmatrix} \tag{4.2.14}$$

where, $\cos(\alpha_m)\exp(j\beta_m) = v_m^*(2:n)d(\theta)$, (4.2.15)

α_m and β_m denote the angular separation of two vectors, $[.]^*$ denotes the complex conjugate of $[.]$, $v_m(2:n)$ and $d(\theta)$, $m = K+1, K+2, \ldots, M$.

Geometrically, α_m denotes the angle between the vectors $v_m(2:n)$ and $d(\theta)$, and β_m denotes the angle between the vector $v_m(2:n)$ and the real axis.

Let $d_N(\theta) = (d_{N(1)}(\theta), d_{N(2)}(\theta), \ldots, d_{N(mo)}(\theta), \ldots, d_{N(M)}(\theta))^T$, (4.2.16)

then, the $d_{N(mo)}(\theta)$, i.e. the m_o^{th} element of the vector $d_N(\theta)$ can be written using eqn. (4.2.14) as (please note subscript $_{mo}$ is the same as m_o),

$$d_{N(mo)}(\theta) = v_{mo,K+1}(2:n)\cos(\alpha_{K+1})\exp(j\beta_{K+1}) + v_{mo,K+2}(2:n)\cos(\alpha_{K+2})\exp(j\beta_{K+2}) + \ldots + v_{mo,M}(2:n)\cos(\alpha_M)\exp(j\beta_M). \tag{4.2.17}$$

Hence, the Euclidian norm $\|d_N(\theta)\|$ can be written as,

$$\|d_N(\theta)\|^2 = \sum_{m_o=1}^{M} |d_{N(mo)}(\theta)|^2 \tag{4.2.18}$$

Since the POP-MUSIC-Euc spectrum is defined as,

$$S_{POP-Euc}(2:n,\theta) = \|d_N(\theta)\|^{-2}, \tag{4.2.19}$$

the dominant peaks of $S_{POP-Euc}(2:n,\theta)$ occur when

$$\|d_N(\theta)\| = 0. \tag{4.2.20}$$

Since $|d_{N(mo)}(\theta)|^2$ is always positive, $\|d_N(\theta)\|^2$ can be zero provided,

$|d_{N(m_o)}(\theta)|^H = 0$ for all $m_o = 1,2,...,M.$ (4.2.21)

i.e.

$$a_{K+1}v_{m_o,K+1}(2:n) + a_{K+2}v_{m_o,K+2}(2:n) + ... + a_M v_{m_o,M}(2:n) = 0 \quad \text{for all } m_o = 1,2,...M, \tag{4.2.22}$$

where, $a_m = \cos(\alpha_m)\exp(j\beta_m)$; $m = K+1,K+2,...,M.$

Eqn. (4.2.22) can be written in the matrix form as follows,

$$[v_{K+1}(2:n),v_{K+2}(2:n),....,v_M(2:n)]a = 0 \tag{4.2.23}$$

where, $a = (a_{K+1},a_{K+2},....,a_M)^T$. (4.2.24)

Since the noise subspace vector $v_m(2:n)$, $m = K+1,K+2,...,M$ are linearly independent, the relationship given in eqn.(4.2.23) can only be true provided that $a_m = 0$, for all $m = K+1,K+2,...,M$. The coefficients a_m represent the angular separation parameters α_m and β_m of the noise subspace eigenvector $v_m(2:n)$ and the direction vector $d(\theta)$. Therefore, $a_m = 0$ for all $m = K+1,K+2,...,M$ can only be true when and only when the direction vector $d(\theta)$ lies in the signal subspace by making $\alpha_m = \pi/2$ for all $m = K+1,K+2,....,M$.

Now let us consider the case where the noise is spatially correlated. In this case the noise subspace projection matrix can be written as,

$$P_N(2:n) = V_N(2:n)[V_N^H(2:n)V_N(2:n)]^{-1}V_N^H(2:n) \tag{4.2.25}$$

Let $B = V_N^H(2:n)V_N(2:n)$, where $B \in C^{M-K\times M-K}$.

Matrix B is Hermitian and hence using eigenvalue eigenvector decomposition we can write,

$$B = Q\Gamma Q^H \tag{4.2.26}$$

where $\Gamma = \text{diag}(\tau_1,\tau_2,....,\tau_K)$, and $QQ^H = I$, with I being an identity matrix, $Q \in C^{M-K\times M-K}$, (Q should not be confused with the rotation matrix used in chapter 2).

Now the matrix $P_N(2:n)$ becomes,

$$P_N(2:n) = V_N(2:n)Q\Gamma^{-1}Q^H V_N^H(2:n) \tag{4.2.27}$$

and hence the POP-MUSIC-Euc spectrum is given by,

$$S_{POP-Euc}(2:n,\theta) = [d^H(\theta)V_N(2:n)Q\Gamma^{-1}Q^H V_N^H(n)d(\theta)]^{-1} \tag{4.2.28}$$

Using eqn. (4.2.14), we can write,

$$V_N^H(2:n)d(\theta) = \begin{bmatrix} \cos(\alpha_{K-1})\exp(j\beta_{K-1}) \\ \cos(\alpha_{K-2})\exp(j\beta_{K-2}) \\ \vdots \\ \cos(\alpha_K) \quad \exp(j\beta_K) \end{bmatrix} = \alpha_p \tag{4.2.29}$$

where, $v_m^H(2:n)d(\theta) = \cos(\alpha_m)\exp(j\beta_m)$, and α_m, β_m denotes the angular separation of two vectors $v_m(2:n)$ and $d(\theta)$, $m = K+1,K+2,\ldots,M$.

Then eqn. (4.2.28) can be written as,

$$S_{POP-Euc}(2:n,\theta) = [\alpha_p^H Q\Gamma^{-1}Q^H\alpha_p]^{-1} \tag{4.2.30}$$

It is clear that $|q_m| = 1$, and hence

$$\alpha_p^H q_m = |\alpha_p|\cos(\psi_m)\exp(j\phi_m) \tag{4.2.31}$$

where, q_m is the m^{th} column vector of Q, ψ_m and ϕ_m represent the angular separation between the vectors α_p and q_m, $m = K+1,K+2,\ldots,M$.

Then eqn. (4.2.30) can be written as,

$$S_{POP-Euc}(2:n,\theta) = [\sum_{m=K+1}^{M} \tau_m^{-1}|\alpha_p|^2(\cos(\psi_m))^2]^{-1} \tag{4.3.32}$$

Under the assumption that τ_m, $m=K+1,K+2,\ldots,M$ are finite, it is clear from eqn. (4.2.32) that the dominant peaks of the POP-MUSIC-Euc spectrum occur when $\psi_m=\pi/2$ or $|\alpha_p|=0$. Let us first consider the case $\psi_m=\pi/2$, i.e., α_p is orthogonal to q_m, $m = K+1,K+2,\ldots,M$. But both vectors α_p and q_m are M-K dimensional. Therefore, this situation is possible if and only if α_p is a null vector, i.e. $\alpha_p = 0$. From eqn. (4.2.29), α_p can be a null vector when $\alpha_{K-m}=\pi/2$, $m = 1,2,\ldots,M-K$, i.e., when the direction vector $d(\theta)$ is orthogonal to the noise

subspace. Now it is also clear that the conditions $\psi_m=\pi/2$ and $|\alpha_p|=0$ satisfy simultaneously. Therefore, the dominant peaks of the POP-MUSIC-Euc can occur when and only when the direction vector d(θ) lies on the signal subspace.

Therefore, the dominant peaks of POP-MUSIC-Euc correspond to the angles of arrival of signals and the number of dominant peaks correspond to the number of incoming signals. It can be concluded that dominant peaks cannot exist in a direction other than the direction from which the signals are arriving.

4.2.3 POP-MUSIC-Elem

M dimensional space can be expressed by a set of basis vectors e_i, i = 1,2,....,M given by,

$$[e_1,e_2,....,e_M] = I \tag{4.2.33}$$

where, I is an identity matrix and $I \in C^{M\times M}$.

Any vector in the M dimensional space can be represented as a linear combination of the basis vectors e_i, i = 1,2,....,M. Therefore the vector $d_N(\theta)$ given in eqn. (4.2.16) can be written as,

$$d_N(\theta) = \sum_{m_o=1}^{M} d_{N(mo)}(\theta)e_{mo} \tag{4.2.34}$$

(please note that the $_{mo}$ is same as m_o)

Therefore, $d_{N(mo)}(\theta)$ represents the m_o^{th} element $d_N(\theta)$ or the projection of $d_N(\theta)$ on to the m_o^{th} basis vector given by eqn. (4.2.33). Utilizing the m_o^{th} coefficient $d_{Nmo}(\theta)$ of $d_N(\theta)$ or the elemental norm of $d_N(\theta)$, we can define another spectral estimate $S_{POP-Elem}(2:n,\theta)$ such that,

$$S_{POP-Elem}(2:n,\theta,m_o) = |d_{N(mo)}(\theta)|^{-2}. \tag{4.2.35}$$

Eqn. (4.2.35) can also be written as,

$$S_{POP-Elem}(2:n,\theta,m_o) = |e_{mo}^T d_N(\theta)|^{-2}$$

$$= |e_{m_o}^T P_N(2:n) d(\theta)|^{-2} \tag{4.2.36}$$

where, e_{m_o} is the m_o^{th} basis vector given by eq. (4.2.33).

If we replace the matrix $P_N(2:n)$ of eqn. (4.2.36) by $\Phi^{-1}(2:n)$, then $S_{POP-Elem}(2:n,\theta,m_o)$ is the same as the linear prediction spectrum $S_{LP}(2:n,\theta,m_o)$ (linear prediction spectrum can be found in [Haykin (1986)]),

$$S_{LP}(2:n,\theta,m_o) = |e_{m_o}^T \Phi^{-1}(2:n) d(\theta)|^{-2} \tag{4.2.37}$$

obtained by predicting the output of the m_o^{th} element of the array using output of the rest of the elements. Again, in view of the similarity between the two expressions, the spectrum $S_{POP-Elem}(2:n,\theta,m_o)$ can also be named as the POP-MUSIC-LP.

POP-MUSIC-Elem can alternatively be expressed as the reciprocal of the polynomial H(z) such that,

$$S_{POP-Elem}(2:n,\theta,m_o) = |H(z)|^{-2} \tag{4.2.38}$$

where, $$H(z) = \sum_{m=1}^{M} h_m(2:n,m_o) z^{m-1} \tag{4.2.39}$$

with $h_m(2:n,m_o)$ being the m^{th} element of the vector $h(2:n,m_o)$ which is the m_o^{th} row of the matrix $P_N(2:n)$.

If $P_N(2:n)$ is infinitely accurate, then H(z) has (M-1) roots out of which K roots at,

$$z_k = \exp\left(j \frac{2\pi \ell}{\lambda} \sin \theta_k \right) \tag{4.2.40}$$

correspond to the K signals from θ_k, k = 1,2,...,K. Thus from the roots of H(z), the bearing angles θ_k of the incoming signals can be determined. The dominant peaks of the spectrum $S_{POP-Elem}(2:n,\theta,m_o)$ occur when $d_{N(m_o)}(\theta) = 0$, i.e. when the eqn. (4.2.22),

$$a_{K-1} v_{m_o,K-1}(2:n) + a_{K-2} v_{m_o,K-2}(2:n) + \ldots + a_K v_{m_o,K}(2:n) = 0 \tag{4.2.41}$$

is satisfied. We can consider two cases where the eqn. (4.2.41) is satisfied.

case 1 When the direction vector $d(\theta)$ lies in the signal subspace, $a_m = 0$ for all $m = K+1,K+2,\ldots,M$ and hence the eqn. (4.2.41) is satisfied and the dominant peaks correspond to the angle of arrival of the signals.

case 2 Even when $d(\theta)$ is not in the signal subspace, there may exist some θ such that the eqn. (4.2.41) is satisfied causing dominant spurious peaks.

Since it is theoretically possible that the case 2 can occur, there may be situations giving rise to dominant spurious peaks in the POP-MUSIC-Elem spectrum.

4.2.4 Relationship between the POP-MUSIC-ML and POP-MUSIC-Elem

Because of the simple geometric relationship,

$$|d_{N(m_0)}(\theta)| \leq |d_N(\theta)| \qquad (4.2.42)$$

we obtain,

$$|d_{N(m_0)}(\theta)|^{-2} \geq |d_N(\theta)|^{-2} \qquad (4.2.43)$$

Hence, $S_{POP-Elem}(2:n,\theta,m_0) \geq S_{POP-Euc}(2:n,\theta)$. (4.2.44)

Therefore, from eqn. (4.2.44), it is clear that the POP-MUSIC-Elem method can give rise to sharper peaks than the POP-MUSIC-Euc method.

Further, it is noteworthy that estimates based on both dominant spectral peaks and polynomial roots provide the same results provided the signal roots are exactly on the unit circle and infinitesimal spatial angle discretization has been considered in plotting the spectrum.

4.2.5 Minimum norm (MN) spectrum

Here we consider the case where the noise is spatially uncorrelated. The

vector $h(2:n,m_o)$ which provides the polynomial coefficients for the POP-MUSIC-Elem has the property given by Theorem 4.2.2 when $m_o = 1$:

Recall that the orthonormal eigenvector matrices for the signal and noise subspaces are given by,

$$V_s(2:n) = [v_1(2:n), v_2(2:n), \ldots, v_K(2:n)]$$

$$= \begin{bmatrix} [v_s'(2:n)]^T \\ \hline V_s'(2:n) \end{bmatrix} \qquad (4.2.45)$$

and, $V_N(2:n) = [v_{K+1}(2:n), v_{K+2}(2:n), \ldots, v_M(2:n)]$

$$= \begin{bmatrix} [v_N'(2:n)]^T \\ \hline V_N'(2:n) \end{bmatrix} \qquad (4.2.46)$$

where, $v_s'(2:n)$ is a K dimensional vector containing the elements of the first row of $V_s(2:n)$, and $v_N'(2:n)$ is a (M-K) dimensional vector containing the elements of the first row of $V_N(2:n)$; $V_s'(2:n)$ and $V_N'(2:n)$ are the submatrices obtained by eliminating the first row of $V_s(2:n)$ and $V_N(2:n)$ respectively.

Then we have,

Theorem 4.2.2

For the case of spatially uncorrelated noise the POP-MUSIC-Elem polynomial coefficient vector $h(2:n,m_o)$ has the following relationship when $m_o = 1$,

$$h(2:n,1) = \|v_N'(2:n)\|^2 \begin{bmatrix} 1 \\ \hline \|v_N'(2:n)\|^{-2}[V_N'(2:n)]^* v_N'(2:n) \end{bmatrix} \qquad (4.2.47)$$

$$= (1-\|v_s'(2:n)\|^2) \begin{bmatrix} 1 \\ \hline -(1-\|v_s'(2:n)\|^2)^{-1}[V_s'(2:n)]^* v_s'(2:n) \end{bmatrix} \qquad (4.2.48)$$

where $[.]^*$ denotes the complex conjugate of $[.]$.

Proof

Since we are considering the Hermitian eigenvectors, the noise subspace projec-

tion matrix $P_N(2:n)$ reduces to the form,

$$P_N(2:n) = V_N(2:n)V_N^H(2:n)$$

$$= \begin{bmatrix} \{v_N'(2:n)\}^T \\ \hline V_N'(2:n) \end{bmatrix} [\{v_N'(2:n)\}^* \mid \{V_N'(2:n)\}^H] \tag{4.2.49}$$

$$= \begin{bmatrix} \{v_N'(2:n)\}^T\{v_N'(2:n)\}^* \mid \{v_N'(2:n)\}^T\{V_N'(2:n)\}^H \\ \hline V_N'(2:n)\{v_N'(2:n)\}^* \mid V_N'(2:n)\{V_N'(2:n)\}^H \end{bmatrix} \tag{4.2.50}$$

Recalling eqn. (4.2.36), POP-MUSIC-Elem is given by,

$$S_{POP-Elem}(2:n,\theta,m_o) = |e_{m_o}^T P_N(2:n)d(\theta)|^{-a} \tag{4.2.51}$$

Let,

$$e_{m_o}^T P_N(2:n) = h^T(2:n,m_o) \tag{4.2.52}$$

i.e. the m_o^{th} row of the noise subspace projection matrix $P_N(2:n)$, then,

$$S_{POP-Elem}(2:n,\theta,m_o) = |h^T(2:n,m_o)d(\theta)|^{-a}. \tag{4.2.53}$$

For the case $m_o = 1$, POP-MUSIC-Elem is given by,

$$S_{POP-Elem}(2:n,\theta,1) = |h^T(2:n,1)d(\theta)|^{-a} \tag{4.2.54}$$

Since $h^T(2:n,1)$ is the first row of the matrix P(2:n), from eqn. (4.2.50) we obtain,

$$h^T(2:n,1) = [\{v_N'(2:n)\}^T\{v_N'(2:n)\}^* \mid \{v_N'(2:n)\}^T\{V_N'(2:n)\}^H] \tag{4.2.55}$$

i.e. $$h(2:n,1) = \begin{bmatrix} \{v_N'(2:n)\}^H v_N'(2:n) \\ \hline \{V_N'(2:n)\}^* v_N'(2:n) \end{bmatrix} \tag{4.2.56}$$

$$= |v_N'(2:n)|^a \begin{bmatrix} 1 \\ \hline |v_N'(2:n)|^{-a}\{V_N'(2:n)\}^* v_N'(2:n) \end{bmatrix} \tag{4.2.57}$$

where, $|v_N'(2:n)|^a = \{v_N'(2:n)\}^H v_N'(2:n)$.

Further h(2:n,1) can also be represented as follows:

As we have shown in section 2.3.5, when the noise is spatially uncorrelated, we have the relationship $P_N(2:n) = I - P_s(2:n)$ and hence the POP-MUSIC-Elem spectrum can also be written as,

$$S_{POP-Elem}(2:n,\theta,m_o) = |e_{mo}^T(I - P_s(2:n))d(\theta)|^{-a} \quad (4.2.58)$$

where, I is an identity matrix and $P_s(2:n)$ is the signal subspace projection matrix.

Therefore, the vector h(2:n,1) can also be written as,

$$h(2:n,1) = e_{mo}^T(I - P_s(2:n)) \quad (4.2.59)$$

Since we are again considering orthonormal eigenvectors, the signal subspace projection matrix $P_s(2:n)$ reduces to the following form:

$$P_s(2:n) = V_s(2:n)V_s^H(2:n)$$

$$= \begin{bmatrix} \{v_s'(2:n)\}^T \\ \hline V_s'(2:n) \end{bmatrix} [\{v_s'(2:n)\}^* \mid \{V_s'(2:n)\}^H] \quad (4.2.60)$$

$$= \begin{bmatrix} \{v_s'(2:n)\}^T\{v_s'(2:n)\}^* \mid \{v_s'(2:n)\}^T\{V_s'(2:n)\}^H \\ \hline V_s'(2:n)\{v_s'(2:n)\}^* \mid V_s'(2:n)\{V_s'(2:n)\}^H \end{bmatrix} \quad (4.2.61)$$

From eqn. (4.2.59), $h^T(2:n,1)$ is the first row of the matrix $(I - P_s(2:n))$ and hence by using eqn. (4.2.61) we obtain,

$$h^T(2:n,1) = [1 - \{v_s'(2:n)\}^T\{v_s'(2:n)\}^* \mid -\{v_s'(2:n)\}^T\{V_s'(2:n)\}^H] \quad (4.2.62)$$

i.e.,

$$h(2:n,1) = \begin{bmatrix} 1 - \{v_s'(2:n)\}^H v_s'(2:n) \\ \hline -\{V_s'(2:n)\}^* v_s'(2:n) \end{bmatrix}$$

$$= (1 - \|v_s'(2:n)\|^2) \begin{bmatrix} 1 \\ \hline -(1 - \|v_s'(2:n)\|^2)^{-1}\{V_s'(2:n)\}^* v_s'(2:n) \end{bmatrix}$$

Eqns. (4.2.47) and (4.2.48) bear resemblance to the coefficient vector of the minimum norm method proposed by Kumaresan and Tuft (1983) except for a scaling factor. Therefore we conclude that the minimum norm method is a special case of the POP-MUSIC-Elem method such that the minimum norm spectrum $S_{MN}(2:n,\theta)$ is given by,

$$S_{MN}(2{:}n,\theta) = S_{POP\text{-}Elem}(2{:}n,\theta,1) \tag{4.2.64}$$

$$= |d_{N(1)}(\theta)|^{-2}. \tag{4.2.65}$$

where, $d_{N(1)}(\theta)$ is the first element of the vector $d_N(\theta)$.

4.2.6 Generalized Minimum Norm (GMN) Spectrum

We refer to the minimum norm spectrum under spatially correlated noise environment as the generalized minimum norm (GMN) spectrum. For the case of spatially correlated noise, the noise projection matrix $P_N(2{:}n)$ is given by,

$$P_N(2{:}n) = V_N(2{:}n)[V_N^H(2{:}n)V_N(2{:}n)]^{-1}V_N^H(2{:}n) \tag{4.2.66}$$

Therefore, for the correlated noise the Theorem 4.2.2 can be restated as follows.

Theorem 4.2.3

For the case of spatially correlated noise the POP-MUSIC-Elem polynomial coefficient vector $h(2{:}n,m_o)$ has the following relationship when $m_o=1$,

$$h(2{:}n,1)=|v_{NB}'(2{:}n)|^2 \begin{bmatrix} 1 \\ |v_{NB}'(2{:}n)|^{-2}\{V_N'(2{:}n)\}^H B v_N'(2{:}n) \end{bmatrix} \tag{4.2.67}$$

where, $B = [V_N^H(2{:}n)V_N(2{:}n)]^{-1}$, and

$|v_{NB}'(2{:}n)|^2 = \{v_N'(2{:}n)\}^H B v_N'(2{:}n)$.

The proof follows the same procedure given for the Theorem 4.2.2 except the fact that the distance measures are now taken in domain B.

4.3 Rotational Correction Multiple Signal Classification (ROC-MUSIC)

4.3.1 Introduction

Here we consider the case where the noise is spatially uncorrelated. If the true cross spectral density matrix is known, there is no limitation on the

resolution capabilities of the MUSIC method. But in practice one does not have the knowledge of the true cross spectral density matrix and hence the estimated cross spectral density matrix is generally used. The errors associated with the estimated cross spectral density matrix cause a rotation of the true signal and noise subspaces, leading to limitations on the resolution capabilities of the MUSIC method.

If one can bring the estimated signal and noise subspaces back to the true signal and noise subspaces, the limitations on the resolution capabilities of the MUSIC method can be overcome. We introduce the rotational correction multiple signal classification (ROC-MUSIC) in bringing the estimated signal and noise subspaces back to the true signal and noise subspaces approximately. ROC-MUSIC may provide improved resolution capabilities over the rest of the spectrum estimation techniques. The rotation is performed using the Jacobi-Givens rotation.

4.3.2 Effects and the correction of errors in the cross spectral density matrix

In estimation of the cross spectral density matrix and formation of the noise subspace projection matrices, errors occur due to various causes,

1. The number of snapshots, n is finite and therefore the estimated cross spectral density matrix $\Phi(2:n)$ may not be same as the true cross spectral density matrix Φ.
2. The sensors are constantly perturbed by random disturbance and thus the sensor alignment and the distance between two sensors may not be constant. The effect of random sensor motion on the cross spectral density matrix and hence the eigenvectors is given in Appendix 4c.

3. Finite wordlength is used in the calculation of the cross spectral density matrix and thus random round off errors are introduced.

The errors are assumed to be independent of each other and we can relate the estimated cross spectral density matrix $\Phi(2:n)$ to the true cross spectral density matrix, Φ as,

$$\Phi(2:n) = \Phi + \Delta\Phi_n + \Delta\Phi_s + \Delta\Phi_q \tag{4.3.1}$$

$$= \Phi + \Delta\Phi \tag{4.3.2}$$

where, $\Delta\Phi_n$, $\Delta\Phi_s$, $\Delta\Phi_q$, $\in C^{m\times m}$ are matrices representing the errors introduced by finite snapshots, sensor perturbation and round off effects, and $\Delta\Phi$ represents the combined effect of these errors, i.e.

$$\Delta\Phi = \Delta\Phi_n + \Delta\Phi_s + \Delta\Phi_q \ , \quad \Delta\Phi \in C^{m\times m}. \tag{4.3.3}$$

Since the errors are assumed to be independent and $\Phi(2:n)$ and Φ are Hermitian, we can conclude that $\Delta\Phi_n$, $\Delta\Phi_s$, $\Delta\Phi_q$ and $\Delta\Phi$ are Hermitian.

If the error perturbation matrix $\Delta\Phi$ is diagonal, the orthonormal eigenvectors of the estimated cross spectral density matrix $\Phi(2:n)$ and the true cross spectral density matrix Φ are the same and hence the estimated signal and noise subspaces will be same as the true signal and noise subspaces. Since the spatial spectrum estimates $S_{POP-Euc}(2:n,\theta)$ and $S_{POP-Elem}(2:n,\theta,m_o)$ are obtained by projecting the directional vector onto the noise subspace which is invariant if the perturbation matrix $\Delta\Phi$ is diagonal, we can conclude that the POP-MUSIC is unaffected by the perturbations which give rise to diagonal perturbation error matrix $\Delta\Phi$.

In general, however, the combined effect of errors gives rise to a Hermitian matrix $\Delta\Phi$ which is not necessarily diagonal. The effect of this total error matrix is such that the set of eigenvectors of the estimated cross spectral density matrix $\Phi(2:n)$ is a rotated version of the true cross spectral density

matrix Φ, and hence the estimated subspaces calculated from $\Phi(2:n)$ will be the rotated version of the subspace obtained from the exact cross spectral density matrix Φ. The amount of rotation depends on the matrix $\Delta\Phi$. Thus, if we denote the orthonormal eigenvectors of Φ and $\Phi(2:n)$ by v_m and $v_m(2:n)$ respectively, m = 1,2,....,M, then we have,

$$V(2:n) = VQ \tag{4.3.4}$$

where, $V(2:n) = [v_1(2:n), v_2(2:n), \ldots, v_M(2:n)]$ (4.3.5)

$V = [v_1, v_2, \ldots, v_M]$, (4.3.6)

and $Q \in C^{M\times M}$ is a norm preserving unitary transformation matrix.

The M dimensional space Ω can be partitioned into estimated signal and noise subspaces $\Omega_s(2:n)$ and $\Omega_N(2:n)$ or into true signal and noise subspaces Ω_s and Ω_N where $\Omega_s(2:n)$ and $\Omega_N(2:n)$ are spanned by $\{v_k(2:n), k = 1,2,\ldots,K\}$ and $\{v_k(2:n), k = K+1,K+2,\ldots,M\}$, respectively, and Ω_s and Ω_N are spanned by $\{v_k, k = 1,2,\ldots K\}$ and $\{v_k, k = K+1,K+2,\ldots,M\}$ respectively.

Now, any vector y in the M dimensional space Ω can be expressed as a linear combination of the Hermitian eigenvectors $\{v_m\}$ or of the eigenvectors $\{v_m(2:n)\}$, i.e.

$$y = \sum_{m=1}^{M} a_m v_m$$

$$y = \sum_{m=1}^{M} a_m(2:n) v_m(2:n) \tag{4.3.7}$$

The M tuples a and a(2:n) are related to each other by,

$$a(2:n) = Ga \tag{4.3.8}$$

where, $a(2:n) = (a_1(2:n), a_2(2:n), \ldots, a_M(2:n))^T$, $a = (a_1, a_2, \ldots, a_M)^T$, and g_{km}, the km^{th} element of the matrix $G \in C^{M\times M}$ is given by,

$$g_{km} = v_m^H v_k(2:n), \quad k,m = 1,2,\ldots,M. \tag{4.3.9}$$

Replacing the vector y by the array manifold $d(\theta)$ in eqn. (4.3.7), and in

particular, if $d(\theta) \in \Omega_s$, then,

$$a_{K+1} = a_{K+2} = \ldots = a_M = 0 \qquad (4.3.10)$$

If the estimated projection matrix $P_N(2:n)$ is to project $d(\theta)$ onto the true noise subspace Ω_N, and if $P_N(2:n)$ contains no error, then,

$$a_m(2:n) = 0, \quad m = K+1, K+2, \ldots, M \qquad (4.3.11)$$

$$v_m^H v_k(2:n) = 0, \quad m = K+1, K+2, \ldots, M, \quad k = 1, 2, \ldots K. \qquad (4.3.12)$$

If eqn. (4.3.12) is satisfied, then POP-MUSIC-Euc and POP-MUSIC-Elem will have K poles situated on the unit circle, i.e.,

$$z = \exp\left(j \frac{2\pi \ell}{\lambda} \sin \theta_k\right), \quad k = 1, 2, \ldots, K,$$

resulting in K peaks each of infinite magnitude or K roots of the corresponding polynomials G(z) and H(z) exactly on the unit circle according to the direction θ_k from which the K signals arrive. However, due to various errors mentioned above, eqn. (4.3.12), in general, is not satisfied by the estimated eigenvectors $v_k(2:n)$. These errors cause the roots of the polynomials G(z) and H(z) to migrate away from the unit circle resulting in errors of bearing estimation and deterioration of sharpness of the peaks, and hence uncertainties in the angle of arrival and the deterioration of resolution. If the errors are too large, then signals from different directions may not be sufficiently resolved.

4.3.3 ROC-MUSIC

To correct the errors, we propose the rotation of the basis vectors $\{v_m(2:n), m = 1, 2, \ldots, M\}$ of the estimated signal and noise subspaces so that eqn. (4.3.12) is satisfied. Eqn. (4.3.12) states that the K basis vectors $\{v_k(2:n), k = 1, 2, \ldots K\}$ of the estimated signal subspace must be orthogonal to the M-K basis vectors $\{v_m, m = K+1, K+2, \ldots, M\}$ of the true noise subspace Ω_N for an optimum

spatial spectral estimate. But since the M-K basis vectors $\{v_m(2:n),\ m = K+1,K+2,\ldots,M\}$ of the estimated noise subspace must be always orthogonal to $\{v_k(2:n),\ k = 1,2,\ldots,K\}$ we can conclude that when eqn. (4.3.12) is satisfied $\{v_m(2:n),\ m = K+1,K+2,\ldots,M\}$ will also span the true noise subspace Ω_N. Thus, the rotation of the basis vectors $\{v_m(2:n),\ m = 1,2,\ldots,M\}$ should be performed by rotating one by one, the planes formed by $\{v_m(2:n),\ m = 1,2,\ldots,K\}$ and $\{v_m(2:n),\ m = K+1,K+2,\ldots,M\}$. The procedure of this rotation can be formulated as follows:

Let $v_m(2:n)$ be the Hermitian eigenvector corresponding to the eigenvalue $\lambda_m(2:n)$ where,

$$\lambda_1(2:n) \geq \lambda_2(2:n) \geq \ldots \geq \lambda_K(2:n) \geq \lambda_{K+1}(2:n) \geq \ldots \geq \lambda_M(2:n).$$

If we have decided that there are K signals, then the first K eigenvectors $v_1(2:n), v_2(2:n), \ldots, v_K(2:n)$ will be the basis vectors of the estimated signal subspace whereas $v_{K+1}(2:n), v_{K+2}(2:n), \ldots, v_M(2:n)$ will be the basis vectors of the estimated noise subspace. Since the eigenvectors $v_m(2:n)$ and $\bar{v}_m$ are complex, their inner products are complex, i.e.,

$$v_m^H v_k(2:n) = \cos\alpha \exp(j\beta). \tag{4.3.13}$$

In order to correct the errors introduced by the rotation of the estimated eigenvectors, the readjustment has to be carried out by modifying both the angles α and β. Now we first rotate the plane formed by $v_1(2:n)$ and $v_{K+1}(2:n)$ by the amount α_{11} and β_{11}. This results in a new eigenvector matrix $V_1^{(1)}(2:n)$ given by,

$$V_1^{(1)}(2:n) = V(2:n)Q_{11} \tag{4.3.14}$$

where, $Q_{11} \in C^{M\times M}$ and the km^{th} element q_{km} of Q_{11} is given by,

$$q_{km} = \begin{cases} 1 & k = m,\ k \neq 1,\ m \neq K+1 \\ \cos\alpha_{11} & k = m = 1,\ k = m = K+1 \\ -\sin\alpha_{11}\exp(-j\beta_{11}) & k = 1,\ m = K+1 \\ \sin\alpha_{11}\exp(j\beta_{11}) & k = K+1,\ m = 1 \\ 0 \quad \text{otherwise,} & \text{for } k,m = 1,2,\ldots,M. \end{cases} \tag{4.3.15}$$

$V_1^{(1)}(2:n)$ now consists of M column vectors,

$\{v_1^{(1)}(2:n), v_2(2:n), \ldots, v_K(2:n), v_{K+1}^{(1)}(2:n), v_{K+2}(2:n), \ldots, v_M(2:n)\}$.

Note that only the vectors associated with the rotated plane have been changed from the original eigenvector matrix.

Then, we rotate the plane formed by $v_1^{(1)}(2:n)$ and $v_{K+2}(2:n)$ by the amount α_{12} and β_{12} resulting another eigenvector matrix $V_1^{(2)}(2:n)$ such that,

$$V_1^{(2)}(2:n) = [v_1^{(2)}(2:n), v_2(2:n), \ldots, v_K(2:n), v_{K+1}^{(1)}(2:n), v_{K+2}^{(1)}(2:n), v_{K+3}(2:n), \ldots, v_M(2:n)] \quad (4.3.16)$$

$$= V_1^{(1)}(2:n)Q_{12} \quad (4.3.17)$$

$$= V(2:n)Q_{11}Q_{12} \quad (4.3.18)$$

where, $Q_{12} \in C^{M \times M}$ and the km^{th} element q_{km} of Q_{12} is given by,

$$q_{km} = \begin{cases} 1 & k = m,\ k \neq 1,\ m \neq K+2 \\ \cos \alpha_{12} & k = m = 1,\ k = m = K+2 \\ -\sin \alpha_{12} \exp(-j\beta_{12}) & k = 1,\ m = K+2 \\ \sin \alpha_{12} \exp(j\beta_{12}) & k = K+2,\ m = 1 \\ 0 \quad \text{otherwise,} & \text{for } k,m = 1,2,\ldots,M. \end{cases} \quad (4.3.19)$$

Such rotation continues until we have rotated the plane formed by $v_1^{(M-K-1)}(2:n)$ and the last vector of the noise subspace $v_M(2:n)$ resulting $v_1^{(M-K)}(2:n)$ and $v_M^{(1)}(2:n)$. The resulting eigenvector matrix $V_1(2:n)$ is given by,

$$V_1(2:n) = V_1^{(M-K)}(2:n) \quad (4.3.20)$$

$$= V(2:n)\left\{ \prod_{k=1}^{M-K} Q_{1k} \right\} \quad (4.3.21)$$

where, $Q_{1k} \in C^{M \times M}$ and the im^{th} element q_{im} of Q_{1k} is given by,

$$q_{im} = \begin{cases} 1 & i = m,\ i \neq 1,\ m \neq K+k \\ \cos \alpha_{1k} & i = m = 1,\ i = m = K+k \\ -\sin \alpha_{1k} \exp(-j\beta_{1k}) & i = 1,\ m = K+k \\ \sin \alpha_{1k} \exp(j\beta_{1k}) & i = K+k,\ m = 1 \\ 0 \quad \text{otherwise,} & \text{for } i,m = 1,2,\ldots,M. \end{cases} \quad (4.3.22)$$

The new eigenvector matrix $V_1(2:n)$ contains column vectors,

$\{v_1^{(M-K)}(2:n), v_2(2:n), \ldots, v_K(2:n), v_{K+1}^{(1)}(2:n), v_{K+2}^{(1)}(2:n), \ldots, v_M^{(1)}(2:n)\}$. The superscript in parentheses associated with a vector denotes the number of times

the vector has been rotated from its initial position. If the rotation angle pairs (α_{1m},β_{1m}), $m = 1,\ldots,M-K$ are chosen correctly, the first column vector $v_1^{(M-K)}(2:n)$ will be orthogonal to the noise subspace and satisfy the eqn. (4.3.12).

The above procedure is then repeated for the planes formed by $v_2(2:n)$ and each of the eigenvectors $v_m^{(1)}$, $m = K+1,K+2,\ldots,M$ of the noise subspace resulting in a new eigenvector matrix $V_2(2:n)$ such that,

$$V_2(2:n) = [v_1^{(M-K)}(2:n),v_2^{(M-K)}(2:n),v_3(2:n),\ldots,v_K(2:n),$$
$$v_{K-1}^{(2)}(2:n),\ v_{K-2}^{(2)}(2:n),\ldots,v_M^{(2)}(2:n)] \tag{4.3.23}$$

$$= V_1(2:n)\{\prod_{m=1}^{M-K} Q_{2m}\} \tag{4.3.24}$$

where, $v_2^{(M-K)}(2:n)$ will be orthogonal to the true noise subspace if the rotation angle pairs (α_{2m},β_{2m}), $m = 1,2,\ldots,M-K$ have been chosen correctly.

We continue this procedure until we complete the rotations involving K eigenvectors of the signal subspace so that the final eigenvector matrix is obtained as,

$$V_K(2:n) = [v_1^{(M-K)}(2:n),v_2^{(M-K)}(2:n),\ldots,v_K^{(M-K)}(2:n),v_{K+1}^{(K)}(2:n),$$
$$\ldots,v_M^{(K)}(2:n)] \tag{4.3.25}$$

$$= V(2:n)\{\prod_{k=1}^{K}\prod_{m=1}^{M-K} Q_{km}\} \tag{4.3.26}$$

where, $v_k^{(M-K)}(2:n)$, $k = 1,2,\ldots,K$ satisfy the eqn. (4.3.12) for the choice of rotation angle pairs (α_{km},β_{km}), $k = 1,2,\ldots,K$, $m = 1,2,\ldots,M-K$.

The procedure described above preceded by POP-MUSIC will be referred to as the rotational correction multiple signal classification (ROC-MUSIC).

In practice, the true cross spectral density matrix Φ is unknown and thus v_m, $m = 1,2,\ldots,M$, are also unknown so that we cannot make use of eqn. (4.3.12) to guide the angle of rotation pairs (α_{km},β_{km}), $m = 1,2,\ldots,M-K$, $k =$

1,2,...,K. A criterion has to be established so that the basis vectors of the estimated noise subspace can be realigned with the unknown basis vectors of the true noise subspace in order to resolve two closely separated signals. There is no unique choice of such a criterion, but if a suitable choice is found, we may be able to resolve two signals with sufficient accuracy. Since we know that the rotation of the estimated subspaces from the true subspaces results in the departure of the signal roots of G(z) and H(z) from the unit circle, we may choose the criterion to be the distance of these signal roots from the unit circle. One suitable measure is to minimize the distance of the most deviated signal root at each discrete rotation. The rotation operation is performed by a real matrix operating on a real and an imaginary axes separately.

4.4 Array Processing Under Coherent Signal Environment

4.4.1 Introduction

The application of high resolution super resolution array processing techniques encounters difficulties when the two or more incoming signals are coherent (perfectly correlated). Such cases occurs, for example, in multipath propagation or in jamming. The reasons for such difficulties is that the coherency of the signals causes rank deficiency in the signal correlation matrix $\Phi_{ss}(2{:}n)$ given in eqn. (2.1.19).

As a result, the number of detectable signals and the number of resolvable directions of arrivals are reduced. Under the correlated signal environment, the rank of the cross spectral density matrix is generally recovered by using the spatial cross spectral density matrix smoothing preprocessing scheme [Evans, Johnson and Sun (1982), Shan and Kailath (1985)]. Most of the available

literature consider the cases where all the incoming signals are coherent. The knowledge of the number of incoming signals are also assumed in selecting the number of subarrays for successful spatial smoothing. Even with the knowledge of the number of signals it is not possible to obtain the number of optimal subarrays since the number of coherent signals are not known. By the number of optimal subarrays we mean the minimum number of subarrays required to recover the rank of the cross spectral density matrix. The use of the term optimal can be justified as follows. We know that the aperture size plays an role in the resolution capabilities of the bearing estimation techniques. reduction of aperture size may case deterioration in the resolution capabilities of the bearing estimation techniques. Spatial smoothing reduces the aperture size. Therefore it is important to choose the minimum number of subarrays required to reconstruct the effective rank in order to maintain the maximum possible aperture size. Therefore, the minimum number of subarrays can be called as optimum number of subarrays.

Here, we consider a more general case where two or more incoming signals are coherent. A methodology is given to estimate the number of incoming signals and the optimal number of subarrays concurrently.

We also propose a method to recover the rank of the input data matrix by directly applying the spatial smoothing preprocessing scheme to the input data matrix U(2:n). In this way computation of several data matrices associated with the spatial cross spectral density matrix smoothing can be avoided. Further, the adaptive spatial data smoothing preprocessing scheme has a systolic array structure which is suitable for implementation in VLSI form.

Both spatial cross spectral density matrix smoothing and adaptive spatial data smoothing preprocessing scheme perform under high signal to noise ratio.

Spatial smoothing techniques fail to perform under the low signal to noise ratio.

4.4.2 Signal Model

Let us divide our linear array of M_T elements into J overlapping subarrays such that each subarray consist of M elements. Hence the number of subarrays is,

$$J = M_T - M + 1 \tag{4.4.1}$$

where $M \leq M_T$.

The division of the subarray is done such that they overlap, i.e. sensors {1,2,...,M} form the first subarray, sensors {2,3,...,M+1} form the second subarray and so on. Then the data vector $u^{(k)}(n)$ for the k^{th} subarray at n^{th} snapshot can be written as,

$$u^{(k)}(n) = D(\theta)A^{k-1}s(n) + \nu^{(k)}(n) \tag{4.4.2}$$

where $D(\theta) = [d(\theta_1),d(\theta_2),....,d(\theta_K)]$, $D(\theta) \in C^{M\times K}$,

$s(n) = (s_1(n),s_2(n),....,s_K(n))^T$,

$\nu^{(k)}(n) = (\nu_1{}^{(k)}(n),\nu_2{}^{(k)}(n),....,\nu_M{}^{(k)}(n))^T$, and

$A = diag(\tau_1,\tau_2,....,\tau_K)$,

$\tau_k = \exp(j\frac{2\pi\ell}{\lambda}\sin\theta_k)$, k=1,2,....,K, K<M, and ℓ is the separation between the sensors.

Now we can form the cross spectral density matrix $\Phi^{(k)}$ for the k^{th} subarray,

$$\begin{aligned}\Phi^{(k)} &= E[u^{(k)}(n)u^{(k)H}(n)] \\ &= D(\theta)A^{k-1}\Phi_{ss}(A^{k-1})^H D^H(\theta)+D(\theta)A^{k-1}\Phi_{s\nu}{}^{(k)}+[D(\theta)A^{k-1}\Phi_{s\nu}{}^{(k)}]^H+\Phi_{\nu\nu}{}^{(k)}\end{aligned} \tag{4.4.3}$$

where, $E[s(n)s^H(n)] = \Phi_{ss}$, $E[s(n)\nu^{(k)H}(n)] = \Phi_{s\nu}{}^{(k)}$, and

$E[\nu^{(k)}(n)\nu^{(k)H}(n)] = \Phi_{\nu\nu}{}^{(k)}$.

By making the assumption that signals and noise are uncorrelated, i.e. $\Phi_{ss}^{(k)} = 0$, we obtain,

$$\Phi^{(k)} = D(\theta)A^{k-1}\Phi_{ss}(A^{k-1})^{H}D^{H}(\theta) + \Phi_{vv}^{(k)} \tag{4.4.4}$$

Once we obtain the cross spectral density matrix $\Phi^{(k)}$, k=1,2,...,J, the spatially smoothed cross spectral density matrix $\Phi_{sm}^{(J)}$ can be obtained by averaging the matrix $\Phi^{(k)}$ over all the J subarrays such that,

$$\Phi_{sm}^{(J)} = J^{-1}\sum_{k=1}^{J}\Phi^{(k)} \tag{4.4.5}$$

Our aim here is to study the effective rank of the cross spectral density matrix due to the spatial smoothing and hence we can disregard the noise cross spectral density matrix without loss of generality.

Combining eqns. (4.4.4) and (4.4.5), we obtain,

$$\begin{aligned}\Phi_{sm}^{(J)} &= J^{-1}\sum_{k=1}^{J} D(\theta)A^{k-1}\Phi_{ss}(A^{k-1})^{H}D^{H}(\theta) \\ &= D(\theta)\bar{\Phi}_{ss}D^{H}(\theta),\end{aligned} \tag{4.4.6}$$

where, $\bar{\Phi}_{ss} = J^{-1}\sum_{k=1}^{J} A^{k-1}\Phi_{ss}(A^{k-1})^{H}$. (4.4.7)

4.4.3 Spatial Smoothing Under a General Framework

So far we have not made any assumption about the coherence of the incoming signals. Signal environment may be such that;

1. **All the incoming signals may be coherent:** this situation may be very rare in practice since the signals are coming from highly unknown sources. This is the case that has been considered in the present literature, example, Shan and Kailath (1985).
2. **Some of the incoming signals may be coherent:** this is the most expected situation due to the presence of smart jammers and/or multipath environme-

nt. To our knowledge this situation has not been treated so far.

To study the effect of coherence on the array processing techniques, we have to understand the effect of the coherence on the rank of the matrix $\Phi_{sx}^{(J)}$. We study the variation of the rank of the matrix $\Phi_{sx}^{(J)}$ with the number of subarrays J and the number of coherent signals K_c, where $K_c \leq K$, with K being the number of signals. To obtain more insight into the matrix $\Phi_{sx}^{(J)}$, we formulate the following Theorems.

Theorem 4.4.1

The rank of the matrix $\Phi_{sx}^{(1)}$ is given by the relationship,

$$\text{rank}\,[\Phi_{sx}^{(1)}] = r_1 = K-K_c+1, \quad K_c \leq K$$

Proof

Since the number of subarrays J=1, $\Phi_{sx}^{(1)}$ can be written as,

$$\Phi_{sx}^{(1)} = D(\theta)\Phi_{ss}D^H(\theta),$$

$$r_1 = \text{rank}\,[\Phi_{sx}^{(1)}] = \text{rank}\,[D(\theta)\Phi_{ss}D^H(\theta)] = \min[\text{rank}(D(\theta)),\text{rank}(\Phi_{ss})] \quad (4.4.8)$$

But it is obvious that,

$$\text{rank}\,(\Phi_{ss}) = K-K_c+1 \quad (4.4.9)$$

Since $1 \leq K_c \leq K$,

$$r_1 = K-K_c+1$$

Theorem 4.4.2

Let the rank of the matrix $\Phi_{sx}^{(J)}$ is r_J, then r_J is given by the relationship,

$$r_J = \min[K, r_1 J] \quad (4.4.10)$$

Proof

We decompose the matrix Φ_{ss} into subspaces which can easily be handled. This can be achieved by using the eigenvalue eigenvector decomposition, i.e.,

$$\Phi_{ss} = V\Lambda V^H \tag{4.4.11}$$

where $V^HV = I$, and

$$\Lambda = \begin{bmatrix} \Lambda_o & 0 \\ \hline 0 & 0 \end{bmatrix}, \quad \Lambda_o = \mathrm{diag}(\lambda_1,\lambda_2,\ldots,\lambda_{r_1}),$$

$r_1 = \mathrm{rank}(\Phi_{sM}^{(1)})$, $V = [v_1,v_2,\ldots,v_K]$, and Φ_{ss} , V , $\Lambda \in C^{K\times K}$.

Eqn. (4.4.11) can be written as,

$$\Phi_{ss} = \sum_{m=1}^{r_1} \lambda_m v_m v_m^H. \tag{4.4.12}$$

By combining eqns. (4.4.7) and (4.4.12), we obtain,

$$\bar{\Phi}_{ss} = J^{-1} \sum_{k=1}^{J} [A^{k-1}(\sum_{m=1}^{r_1} \lambda_m v_m v_m^H)(A^{k-1})^H] \tag{4.4.13}$$

$$= J^{-1} \sum_{k=1}^{J} \sum_{m=1}^{r_1} \lambda_m (A^{k-1}v_m)(A^{k-1}v_m)^H$$

$$= J^{-1} (\Omega\bar{V})(\Omega\bar{V})^H \tag{4.1.14}$$

where, $\Omega = [A^0,A^1,\ldots,A^{J-1}]$,

$$\bar{V} = [\bar{V}_1,\bar{V}_2,\ldots,\bar{V}_{r_1}],$$

$$\bar{V}_m = [\bar{v}_{m1},\bar{v}_{m2},\ldots,\bar{v}_{mJ}]$$

$$= (\lambda_m)^{1/2}[v_m,z^{-K}v_m,z^{-2K}v_m,\ldots,z^{-K(J-1)}v_m], \quad m=1,2,\ldots,r_1, \tag{4.4.15}$$

z^{-K} is a delay operator which provides a delay of K units.

Matrix $\bar{V}_m$ can also be written as,

$$\bar{V}_m = (\lambda_m)^{1/2} \begin{bmatrix} v_m & 0 & 0 & \cdots & 0 \\ 0 & v_m & 0 & \cdots & 0 \\ 0 & 0 & v_m & \cdots & 0 \\ \vdots & \vdots & \vdots & \ddots & \vdots \\ 0 & 0 & 0 & \cdots & v_m \end{bmatrix}_J \qquad (4.4.16)$$

$\bar{V}_m \in C^{(K,J)\times(J)}$, $\bar{V} \in C^{(K,J)\times(r_1,J)}$, $\Omega \in C^{(K)\times(K,J)}$.

Substituting eqn. (4.4.14) in eqn. (4.4.6), we obtain the rank of the cross spectral density matrix $\Phi_{xx}^{(J)}$, so that,

$$\text{rank}\,(\Phi_{xx}^{(J)}) = \min\,[K, \text{rank}(\bar{\Phi}_{ss})] \qquad (4.4.17)$$

Using eqn. (4.4.14), we obtain,

$$\text{rank}\,(\bar{\Phi}_{ss}) = \min\,[\text{rank}(\Omega), \text{rank}(\bar{V})]. \qquad (4.4.18)$$

But, it is obvious that,

rank (Ω) = K and hence,

$$\text{rank}\,(\Phi_{xx}^{(J)}) = \min\,[K, \text{rank}\,(\bar{V})] \qquad (4.4.19)$$

Now, let us consider the rank of the matrix $\bar{V}$. In determining the rank of the matrix $\bar{V}$, we first consider the rank of the matrix $\bar{V}_m$, $m=1,2,\ldots r_1$.

It can easily be seen from eqns. (4.4.15) and (4.4.16), that the column vectors of the matrix $\bar{V}_m$ are orthonormal, i.e.,

$$\bar{v}_{mj}^{*T}\bar{v}_{mk} = 0, \; j \neq k$$
$$= 1, \; j = k \qquad (4.4.20)$$

where $\bar{v}_{mj}$ is the j^{th} column vector of the matrix $\bar{V}_m$.

Therefore, rank $(\bar{V}_m)$ = J. (4.4.21)

Since the eigenvectors of a symmetric matrix Φ_{ss} are orthogonal, we can also write,

$\bar{V}_i^H \bar{V}_j = 0, \; i \neq j$

$= I, \; i = j$ (4.4.22)

where, $I, 0 \in C^{J \times J}$.

Therefore, from eqn. (4.4.22), we can conclude that the matrix $\bar{V}$ contains linearly independent columns and hence,

$\text{rank}\,(\bar{V}) = \min\,[KJ, r_s J]$. (4.4.23)

But, we know that $r_s \leq K$, so that,

$\text{rank}\,(\bar{V}) = r_s J$. (4.4.24)

Substituting eqn. (4.4.24) in eqn. (4.4.19), we get,

$\text{rank}\,(\Phi_{SM}^{(J)}) = \min\,[K, r_s J]$ (4.4.25)

Definition 4.4.1

Optimal Number of Subarrays

Optimal number of subarrays, J_{opt} is defined as the minimum number of subarrays required to recover the rank of the matrix $\Phi_{SM}^{(J)}$.

Corollary 4.4.1

Optimal number of subarrays J_{opt} is given by the relationship,

$J_{opt} = K/r_s$ (4.4.26)

Proof

From eqn. (4.4.25), it is obvious that the rank of the matrix $\Phi_{SM}^{(J)}$ will be equal to the number of incoming signals provided that,

$r_s J \geq K$,

i.e., $J_{opt} = K/r_s$ (4.4.27)

From this result it is clear that the smaller the number of coherent signals, the smaller is the number of optimal subarrays.

Propositions

1. $J_{opt} = K$ when $r_1 = 1$, i.e., all the incoming signals are coherent. This is in agreement with the results given by Shan and Kailath (1985).

2. $J_{opt} = 1$, when $r_1 = K$, i.e., all the incoming signals are independent.

After observing the properties of the cross spectral density matrix $\Phi_{SM}^{(J)}$, let us now try to formulate a methodology for obtaining the number of signals K, and the optimal number of subarrays J_{opt} concurrently.

4.4.4 A Methodology for Obtaining the Number of Signals and the Optimal Number of Subarrays Concurrently

Let, r_J = rank $(\Phi_{SM}^{(J)})$,

then, $r_J = \min [K, r_1 J]$. (4.4.28)

In this relationship, we do not have any control over the number of signals K, and it is the quantity we have to determine. But, we do have control over the number of subarrays J, and hence r_J, J=1,2,..... . This is the property we are going to exploit in estimating the number of incoming signals K and the optimal number of subarrays J_{opt} concurrently.

Differentiating r_J with respect to J, we obtain,

$$\frac{\partial r_J}{\partial J} = \begin{cases} r_1 & , \ r_1 J < K \\ 0 & , \ r_1 J > K \end{cases} \qquad (4.4.29)$$

where, $1 \leq r_1 \leq K$.

According to eqns. (4.4.28) and (4.4.29), r_J increases linearly w.r.t. J with the gradient r_1 until it reaches the steady value K. Based on this property, a methodology for estimating the number of signals K and the optimal number subarrays J_{opt} concurrently, can be formulated in the following steps:

step 1 Obtain the cross spectral density matrix $\Phi_{mx}(J)$ and its effective rank r_J for J=1,2,....., using AIC or MDLC as outlined in chapter 2.

step 2 Plot r_J versus J : plot reaches a steady value with a constant gradient of r_1, where $1 \leq r_1 \leq K$.

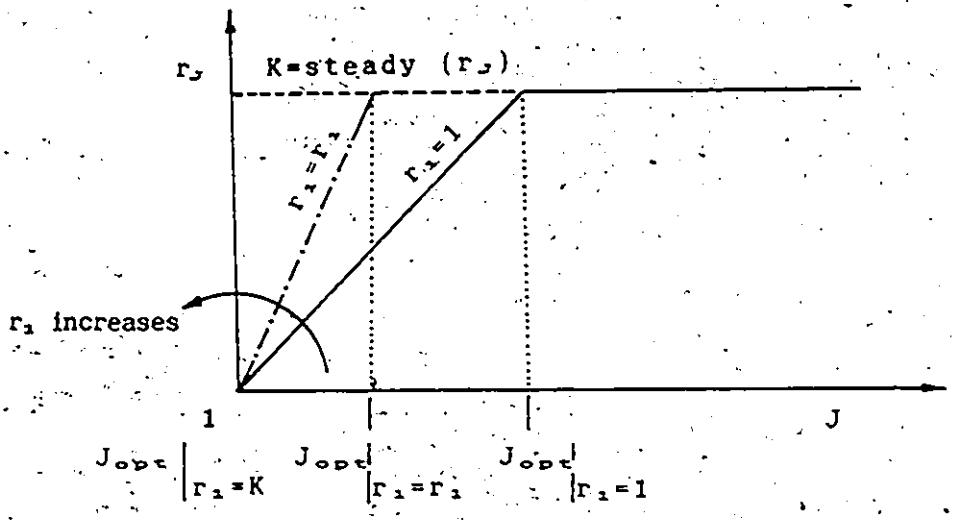

step 3 i. The number of incoming signals K is given by the steady value of r_J; i.e., K = steady (r_J)

ii. The value of J at which r_J enters steady state is the optimal number of subarrays J_{opt}.

iii. The number of correlated signals K_c is given by,

$$K_c = K+1-r_1$$

$$= \text{steady}(r_J)+1-r_1$$

4.4.5 Adaptive Spatial Data Smoothing Preprocessing (ASDSP) Scheme

In general, it has been the custom to construct the cross spectral density matrices for each of the subarrays separately and then take the average to obtain the spatially smoothed cross spectral density matrix. The matrix matrix multiplication associated with the construction of the cross spectral density matrix may result in numerical instability.

Here, we propose a method to recover the rank of the input data matrix by directly applying the spatial smoothing preprocessing scheme to the input data matrix U(2:n). In this way not only we can avoid the numerical instability due to the matrix matrix multiplication, but also we can bypass the computation of several cross spectral density matrices associated with the spatial smoothing of the cross spectral density matrix.

To do that we obtain a data vector at n^{th} snapshot so that for the j^{th} subarray, the data vector at n^{th} snapshot is given by,

$$u_j(n) = [u_j(n),u_{j+1}(n),....,u_{j+M-1}(n)]^T, \quad \text{for } j = 1,2,....,J. \tag{4.4.30}$$

We can now form a data submatrix $U_{sm}(2:n,J) \in C^{M\times 2J}$ for the n^{th} snapshot such that,

$$U_{sm}(2:n,J) = [u_1^H(2:n),u_1(2:n),u_2^H(2:n),u_2(2:n),....,u_J^H(2:n),u_J(2:n)] \tag{4.4.31}$$

The complete data matrix $U_c(2:n,J)$ can be constructed so that,

$$U_c(2:n,J) = [U_{sm}(2:1,J),U_{sm}(2:2,J),....,U_{sm}(2:n,J)], \tag{4.4.32}$$

where, $U_c(2:n,J) \in C^{M\times 2nJ}$.

Since the matrix $U_c(2:n,J)$ increases in dimensions with n, we employ the Jacobi-Givens rotation by premultiplying the matrix $U_c^H(2:n,J)$ by a unitary matrix $Q^H(2:n,J)$, resulting an upper triangular matrix $R_c^H(2:n,J)$,

$U_c^H(2:n,J) \in C^{2nJ\times M}$, $Q^H(2:n,J) \in C^{2nJ\times 2nJ}$, $R_c^H(2:n,J) \in C^{M\times M}$.

Then the spatially smoothed cross spectral density matrix $\Phi_{sm}(2:n,J)$ is given by,

$$\Phi_{sm}(2:n,J) = (2nJ)^{-1}R_c(2:n,J)R_c^H(2:n,J) \tag{4.4.33}$$

Similarly, by considering J subarrays for the frequency bin just outside the signal frequency band one could obtain the noise data matrix $U_{cv}(2:n,J)$ which finally could be used to obtain the noise cross spectral density matrix

$\Phi_{cc}(2:n,J)$ such that,

$$\Phi_{cc}(2:n,J) = (2nJ)^{-1}R_{cc}(2:n,J)R_{cc}^{H}(2:n,J). \qquad (4.4.34)$$

$R_{cc}(2:n,J)$ is an unitary triangular matrix,

$R_{cc}(2:n,J) \in C^{M\times M}$, $\Phi_{cc}(2:n,J) \in C^{M\times M}$.

The cross spectral density matrix $\Phi_{mm}(2:n,J)$ obtained by eqn. (4.4.33) can be easily seen to be the average over the cross spectral density matrices obtained by the J subarrays as well as an average over the n snapshots. This spatial data smoothing procedure can be obtained adaptively by using a suitable systolic array structure.To obtain the optimal number of subarrays we can still use the procedure given in section 4.4.4. In this case, r_J is the effective rank of the upper triangular matrix $R_c^H(2:n,J)$. We know that the eigenvalues of $R_c^H(2:n,J)$ are the diagonal elements of it. Therefore, to obtain the effective rank r_J, we can use MDLC or AIC with the diagonal elements of $R_c^H(2:n,J)$ that are arranged in descending order.

4.4.6 Systolic Array Structure for ASDSP

We consider the case M = 5, K = 2 and J = 3 for simplicity. The basic nature of the systolic array structure is presented below:

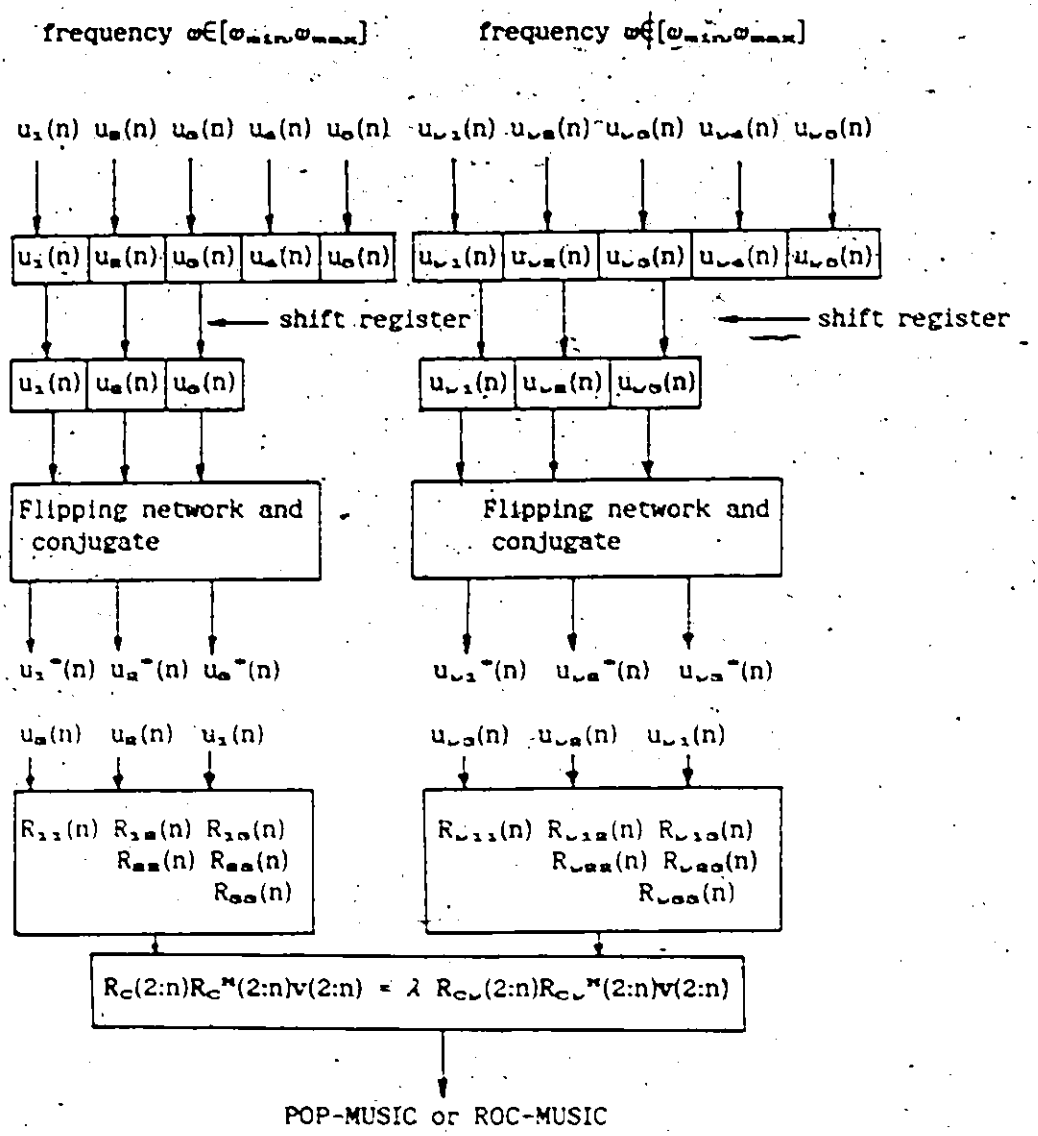

4.5 Simulation Results

In this section we present some of the results of bearing estimation using some of the methods described above.

(a) **Noncoherent Signals**

We consider the case where two uncorrelated narrowband signals of equal strength are approaching an array consisting of five omni-directional elements. We further assume that the sensor noise is uncorrelated and the separation of array elements is 0.5λ.

Example 1

The direction of the signals are assumed to be $\sin^{-1}(0.0)$ and $\sin^{-1}(0.2)$. The POP-MUSIC-Euc spectral estimate $S_{POP-Euc}(n,\theta)$, and POP-MUSIC-Elem spectral estimate $S_{POP-Elem}(n,\theta,m_o)$ for $m_o = 5$ after one hundred snapshots are shown in Figure 4.1 and 4.2 respectively. The locations of poles of G(z) and H(z) are shown in Table 4.1. Bearing estimates based on the roots of the polynomials G(z), H(z) and the spatial spectra $S_{POP-Euc}(n,\theta)$, and $S_{POP-Elem}(n,\theta,m_o)$ are shown in Table 4.2. The results for both AIC and MDLC are shown in Table 4.3. In general, we are not in a position to know a priori whether the two signals are coherent. Thus, the spatial data smoothing preprocessing is applied as a safeguard. The POP-MUSIC-Euc spectrum preceded by adaptive spatial data smoothing scheme is shown in Fig. 4.3. Three signal to noise ratios, SNR = 20,10 and 0 dB are considered in the simulation.

Remarks

It can be seen that both POP-MUSIC-Euc and POP-MUSIC-Elem could resolve the two signals. The POP-MUSIC-Euc spectrum provides a very smooth noise spectra whereas the POP-MUSIC-Elem spectrum contains some spurious peaks of small amplitude. This is because of the fact that when $d(\theta)$ lies outside the signal subspace, it results in a reasonably constant magnitude projection

$d_w(\theta)$ as this example shows, the projection of $d_w(\theta)$ on to the m_o^{th} axis, $d_{w(m_o)}(\theta)$ may vary with θ and may sometimes be small resulting in the spurious peaks. As we expected theoretically, POP-MUSIC-Elem gives rise to sharper peaks than POP-MUSIC-Euc. The bearing estimates obtained by plotting $S_{POP-Euc}(n,\theta)$, and $S_{POP-Elem}(n,\theta,m_o)$ spectra can be computationally intensive due to the necessity of a large number of look directions. Furthermore, we cannot provide infinitesimally discretized step size of θ, and the location of the peaks by interpolation may result in a biased bearing estimate. Thus, the roots of the corresponding polynomial is an attractive alternative and the results obtained are shown in Table 4.2. However, bias can also occur in the bearing estimates obtained by spatial spectrum and the roots of the polynomials G(z) and H(z), when the signal roots departs from the unit circle.

When we use the adaptive spatial data smoothing preprocessing under non-coherent signal environment, it results in sharper peaks. This is mainly due to the improved cross spectral density matrix estimate achieved as a result of adaptive spatial data smoothing preprocessing.

It can also be observed that the minimum of the AIC and MDLC correspond to the number of signals and both AIC and MDLC perform equally for finite number of snapshots.

Example 2

We consider the case where two signals are closer together than those in Example 1. The direction of arrival of the two signals are chosen to be $\sin^{-1}(0.16)$ and $\sin^{-1}(0.2)$. TO obtain ROC-MUSIC spectrum, we perform the rotation so that the most deviated signal root from the unit circle is a minimum in every discrete rotation. The POP-MUSIC-Euc spectrum, $S_{POP-Euc}(n,\theta)$, and

ROC-MUSIC spectrum, $S_{ROC-MUSIC}(n,\theta)$ are shown in Fig. 4.4. The signal to noise ratio is chosen to be 20 dB. The POP-MUSIC-Euc spatial spectral estimate under ideal conditions with a priori knowledge of the signal and noise environment is shown in Fig. 4.5. The direction of arrival of the signals obtained from the dominant roots of the polynomial G(z) and the dominant peaks of the spectra $S_{POP-Euc}(n,\theta)$, and $S_{ROC-Euc}(n,\theta)$ are tabulated in Table 4.4.

Remarks

As it was mentioned earlier, theoretically there are no limitations to the POP-MUSIC method. If the exact cross spectral density matrix is available, POP-MUSIC spectrum can resolve two signals however close they are in angles of arrivals. This can also be observed in Fig. 4.5. However, when the conditions are non-ideal, POP-MUSIC spectrum may not be able to resolve the incoming signals as shown in Fig. 4.4. From Fig. 4.4, it can be seen that the ROC-MUSIC can be used to correct the errors introduced and as a result the two signals are resolved in the ROC-MUSIC spectrum whereas the POP-MUSIC-Euc spectrum has failed. ROC-MUSIC spectrum with the criterion that we have chosen contains some bias in the bearing estimates. It is not very clear why the bias in the direction of arrival estimate of one signal is considerably larger than that of the other signal. Even though the POP-MUSIC spectrum fails to resolve the signals, POP-MUSIC polynomial G(z) could resolve the signals by providing two dominant roots, and this can be observed in Table 4.4. Bias in the bearings of both the signals, obtained by POP-MUSIC polynomial G(z), appears to be considerably large.

(b) Coherent Signals

Here, we consider the case where two incoming signals are coherent. Rest of the environment conditions are assumed to be the same as in section (a).

Example 3

In this example we again have the directions of arrivals of the two coherent signals to be $\sin^{-1}(0.0)$ and $\sin^{-1}(0.2)$. The POP-MUSIC-Euc spectral estimate $S_{POP\text{-}Euc}(n,\theta)$, after one hundred snapshots is shown in Fig. 4.6. The POP-MUSIC-Euc spectrum preceded by an adaptive spatial data smoothing preprocessing, $S_{P\text{-}POP\text{-}Euc}(n,\theta)$ is shown in Fig. 4.7. AIC and MDLC for POP-MUSIC and preprocessed POP-MUSIC are shown in Table 4.5. The bearing estimates based on the dominant roots of the polynomial G(z) and the dominant peaks of the POP-MUSIC-Euc spectrum preceded by the adaptive data smoothing preprocessing scheme are shown in Table 4.6.

Remarks

When the incoming signals are coherent, the input data matrix or the cross spectral density matrix becomes rank deficient. It is very clear from Table 4.5 that both AIC and MDLC show a minimum at the value of $K = 1$ for POP-MUSIC whereas for preprocessed POP-MUSIC minimum occurs at $K = 2$. Further, it is noteworthy that the adaptive spatial data smoothing preprocessing scheme fails to perform successfully at low signal to noise ratios. Therefore, when the incoming signals are coherent, preprocessing scheme provides a solution to the bearing estimation at high signal to noise ratios.

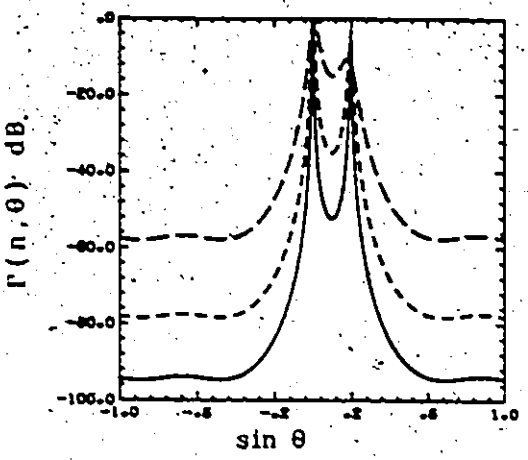

Fig. 4.1 POP-MUSIC-Euc, $S_{POP-Euc}(n,\theta)$ Uncorrelated Signals

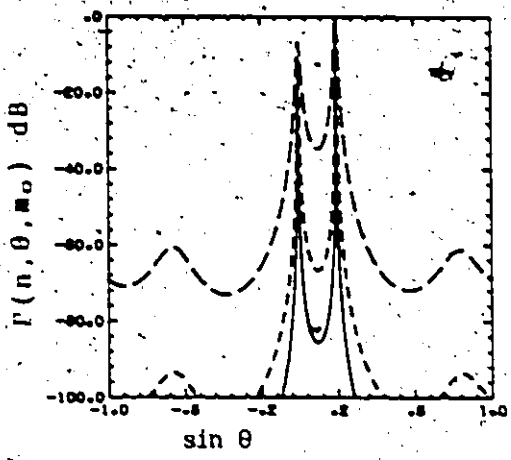

Fig. 4.2 POP-MUSIC-Elem, $S_{POP-Elem}(n,\theta,m_0)$ Uncorrelated Signals

SNR = 20 dB
SNR = 10 dB
SNR = 0 dB

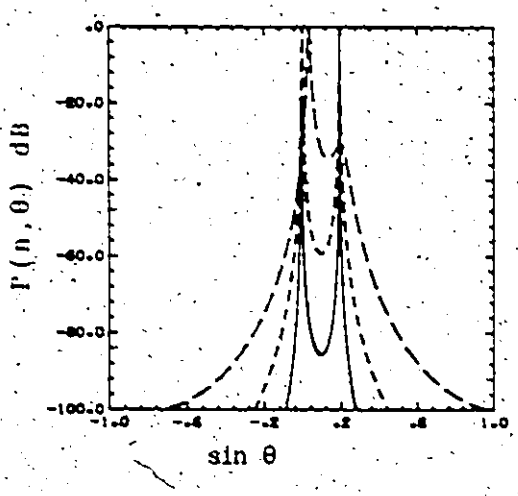

Fig. 4.3 Preprocessed POP-MUSIC-Euc, Uncorrelated Signals

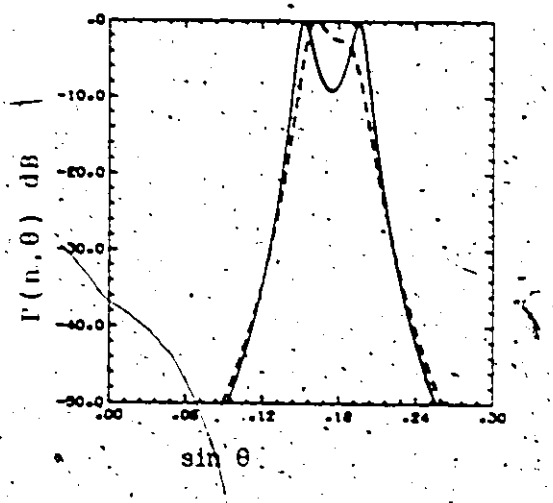

Fig. 4.4 ROC-MUSIC-Euc Uncorrelated signals

SNR = 20 dB
SNR = 10 dB
SNR = 0 dB

SNR = 20 dB
POP-MUSIC
ROC-MUSIC

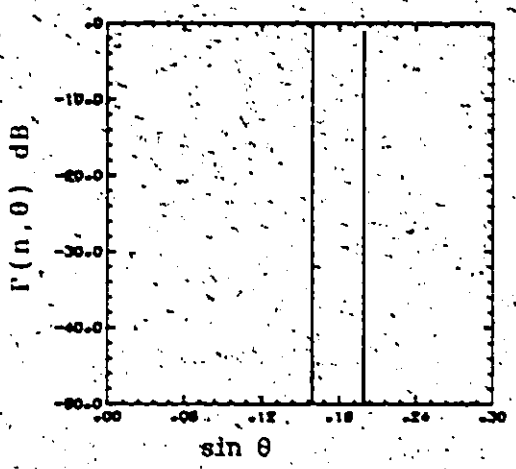

Fig. 4.5 POP-MUSIC-Euc, $S_{POP-Euc}(n,\theta)$
Under known signal and noise environment

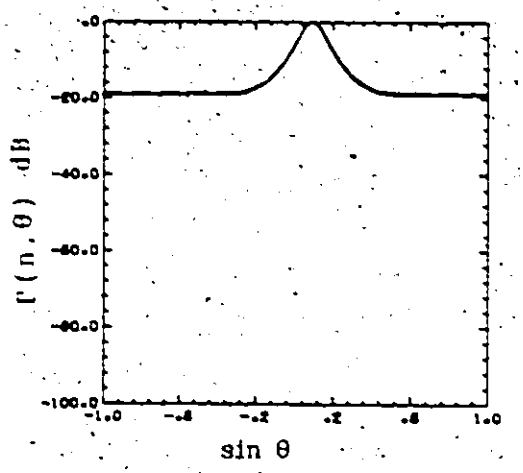

Fig. 4.6 POP-MUSIC-Euc, $S_{POP-Euc}(n,\theta)$, Coherent signals

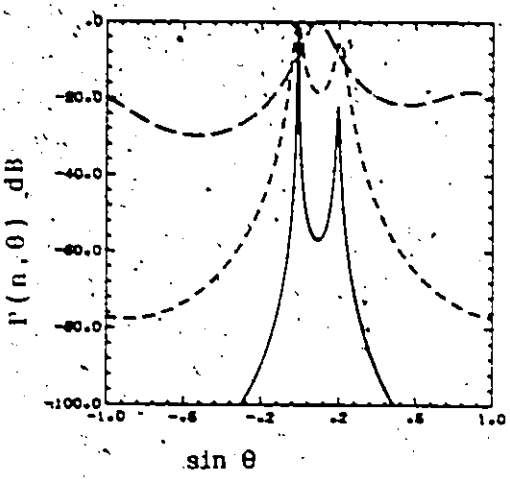

Fig. 4.7 Preprocessed POP-MUSIC-Euc, Coherent signals

——————— SNR = 20 dB
- - - - - - - - - - SNR = 10 dB
— — — — — — — SNR = 0 dB

Table 4.1 Locations of poles in POP-MUSIC-Euc (G(z)) and POP-MUSIC-Elem (H(z))

SNR in dB	G(z) |r|	G(z) sin θ	H(z) |r|	H(z) sin θ
	0.994	0.001*	1.000	0.200*
	0.991	0.199*	0.999	-0.001*
	0.452	-0.133	0.720	0.347
	0.452	0.333	0.718	-0.148
20	1.007	0.001		
	1.008	0.199		
	2.211	-0.133		
	2.212	0.333		
	0.980	0.004*	0.999	0.201*
	0.970	0.197*	0.995	0.003*
	0.453	-0.133	0.721	0.346
	0.453	0.333	0.716	-0.150
10	1.021	0.004		
	1.031	0.197		
	2.208	-0.133		
	2.209	0.333		
	0.934	0.007*	0.979	0.201*
	0.877	0.189*	0.969	0.004*
	0.463	-0.140	0.738	0.343
	0.462	0.333	0.723	-0.160
0	1.071	0.007		
	1.140	0.189		
	2.162	-1.140		
	2.164	0.333		

$z = |r| \exp(j\pi \sin\theta)$, and * denotes the roots corresponding to the incoming signals.

Table 4.2 Bearing estimates (sin θ) based on the roots of the polynomials and spatial spectra

SNR dB	True Bearings	POP-MUSIC-Euc G(z)	POP-MUSIC-Euc $S_{POP-Euc}(n,\theta)$	POP-MUSIC-Elem H(z)	POP-MUSIC-Elem $S_{POP-Elem}(n,\theta,m_o)$
20	0.000	0.001	0.000	0.001	0.000
	0.200	0.199	0.200	0.200	0.200
10	0.000	0.004	0.004	0.003	0.004
	0.200	0.197	0.197	0.201	0.200
0	0.000	0.007	0.008	0.004	0.004
	0.200	0.189	0.180	0.201	0.200

Table 4.3 MDLC and AIC

SNR dB	k	MDLC $L_D(k)$	AIC $L_A(k)$
	0	718	1436
	1	553	1106
20	2	19 *	38 *
	3	23	46
	4	24	48
	0	422	844
	1	269	538
10	2	19 *	38 *
	3	23	46
	4	24	48
	0	156	312
	1	66	132
0	2	19 *	38 *
	3	22	44
	4	24	48

* denotes the minimum and the corresponding
K denotes the number of signals

Table 4.4 Bearing estimates (sin θ) from POP-MUSIC-Euc and ROC-MUSIC-Euc

SNR	True	POP-MUSIC-Euc		ROC-MUSIC-Euc	
dB	Bearings	G(z)	$S_{POP-Euc}(n,\theta)$	G(z)	$S_{ROC-Euc}(n,\theta)$
20	0.160	0.161	unresolvable	0.152	0.153
	0.200	0.192		0.199	0.198

Table 4.5 MDLC and AIC under coherent signals

SNR dB	K	POP-MUSIC-Euc MDLC $L_D(k)$	POP-MUSIC-Euc AIC $L_A(k)$	Preprocessed POP-MUSIC-Euc MDLC $L_D(k)$	Preprocessed POP-MUSIC-Euc AIC $L_A(k)$
20	0	1024	2048	375	750
	1	17 *	34 *	66	132
	2	20	40	8 *	16 *
	3	21	42		
	4	24	48		
10	0	629	1258	260	520
	1	17 *	34 *	11	22
	2	20	40	8 *	16 *
	3	21	42		
	4	24	48		
0	0	264	528	113	226
	1	17 *	34 *	5 *	10 *
	2	20	40	8	16
	3	21	42		
	4	24	48		

* denotes the minimum and the corresponding
K denotes the number of signals

Table 4.6 Bearing estimates (sin θ) from POP-MUSIC-Euc and Preprocessed POP-MUSIC-Euc for coherent signals

SNR dB	True Bearings	POP-MUSIC-Euc	Preprocessed POP-MUSIC-Euc G(z)	Preprocessed POP-MUSIC-Euc $S_{P\text{-}POP\text{-}Euc}(n,\theta)$
20	0.200	unresolvable	0.199	0.200
	0.000		-0.006	-0.008
10	0.200	unresolvable	0.212	0.208
	0.000		-0.013	-0.012
0	0.200	unresolvable	unresolvable	
	0.000			

4.6 Discussion

The spectral estimates POP-MUSIC-Euc and POP-MUSIC-Elem that are derived based on the proper orthogonal projection provide a deeper insight into

the MUSIC method. POP-MUSIC-Euc spectrum does not give rise to any spurious peaks whereas POP-MUSIC-Elem may theoretically give dominant spurious peaks even though it is very rare in practice. It is also shown that the minimum norm technique is a special case of the POP-MUSIC-Elem.

Theoretically there is no limitation to the capabilities of MUSIC method. But in practice due to the errors introduced in using the estimated cross spectral density matrix, estimated signal and noise subspaces may deviate from the true signal and noise subspaces leading to the limitations in the resolution capabilities of the MUSIC method. The rotational correction multiple signal classification (ROC-MUSIC) shows some capability of providing improved resolution capabilities over the POP-MUSIC spectrum. More investigation is necessary to make any conclusion about the capabilities of the ROC-MUSIC. Further, the potential capacity of the ROC-MUSIC is limited due to the nonexistence of an unique criterion in guiding the rotation.

We have considered the array processing under coherent signal environment in a more general framework. A procedure is formulated for estimating the number of signals and the optimal number of subarrays concurrently. Adaptive spatial data smoothing preprocessing (ASDSP) scheme recovers the rank of the signal data matrix under the coherent signal environment. ASDSP scheme is computationally stable and efficient since it does not require the construction of the cross spectral density matrices for each subarray as in the case of cross spectral density matrix smoothing. The given systolic array structure can be used in implementing the ASDSP scheme in VLSI form. In the case of coherent signal environments, the spatial smoothing preprocessing scheme performs successfully at high signal to noise ratios whereas the spatial smoothing preprocessing scheme fails to perform at low signal to noise ratios.

CHAPTER 5

UNIFIED APPROACH TO SPECTRUM REPRESENTATION

Preview There are numerous techniques of spectrum estimation available today and they generally come under the categories of conventional, high resolution and super resolution families. All these spectrum estimation techniques have been developed under different frameworks and each of them has a very distinct origin. Can we bring all these spectrum estimation techniques into a unified framework ?. If we can, not only can we get a deeper understanding of spectrum representation as a whole, but also reveal the mysteries of their relative performance.

Here, we consider the spectrum estimation as the geometric study of the behaviour of the cross spectral density matrix. The idea of the geometric analysis of the cross spectral density matrix is to break it down into a number of subspaces in such a way that the operation on each subspace is particularly simple, and easy to visualize. Proper orthogonal projection matrices are then derived for each of the subspaces separately and they are used to define two out of many possible families of spectrum estimation techniques, namely Euc-Techs, and Elem-Techs. Conventional, high resolution, and super resolution spectrum estimation techniques are unified, and categorized into Euc-Techs and Elem-Techs. This unified approach provides a key to study the relative performance of the spectrum estimation techniques.

Further, if we have any spectrum in the Euo-Techs family, we can also define its corresponding counterpart in the Elem-Techs family. Even though we have defined two families of spectra, it is not limited to two, and one can define as many families as one wishes.

5.1 Introduction

In chapter 4, we have considered only the super resolution spectrum estimation techniques and their geometric relationships. There are other spectrum estimation techniques that have been developed and used successfully in time series as well as in array processing. Almost all the spectrum estimation techniques can be used interchangeably in time series as well as in array processing. In array processing, the direction vector $d(\theta)$ and the cross spectral density matrix $\Phi(n)$ pair $(d(\theta),\Phi(n))$ is used while in time series the frequency vector $d(\omega)$ and the autocorrelation matrix $\Phi(n)$ pair $(d(\omega),\Phi(n))$ is used.

All the classical, high resolution, and the super resolution spectrum estimation techniques have been developed under a different framework. In this chapter, we first provide a unified framework for spectral representation and then we attempt to bring all the existing spectrum estimation techniques together under this unified framework. The basic tool we are going to use is the geometric analysis of operators. Therefore, let us first consider the geometric analysis of operators briefly. We have considered this to some extent in the chapter 2 also. But in chapter 2, our main interest was to break down the cross spectral density matrix into two subspaces whereas here we will go into more basic elements.

5.2 Geometric Analysis of the Cross Spectral Density Matrix

The spectral analysis is basically a geometric study of the behaviour of the cross spectral density matrix. The idea of a geometric analysis is to break up the cross spectral density matrix $\Phi(n)$ in such a way that the operation on each part is particularly simple and easy to visualize.

Subspace decomposition of $\Phi(n)$ can be achieved as we did in chapter 2, i.e.,

$$\underset{V(n)}{\text{minimize}} \quad \text{trace}\,[V^H(n)\Phi(n)V(n)] \tag{5.1}$$

under the constraint $V^H(n)V(n) = I$ (5.2)

where, I is an identity matrix, and $V(n)$, I, $\Phi(n) \in C^{M\times M}$.

The solution is given by,

$$\Phi(n)V(n) = V(n)\Lambda(n) \tag{5.3}$$

where, $V(n) = [v_1(n), v_2(n), \ldots, v_M(n)]$,

$\Lambda(n)$ is a diagonal matrix that contains the Lagrange multipliers as the diagonal elements, and $\Lambda(n) = \text{diag}\,(\lambda_1(n), \lambda_2(n), \ldots, \lambda_M(n))$.

We then identify the eqn. 5.3 as the eigenvalue eigenvector decomposition of the matrix $\Phi(n)$, where $V(n)$ is the eigenvector matrix corresponding to the eigenvalue given by the diagonal elements of the matrix $\Lambda(n)$.

Post multiplying the Eqn. (5.3) by $V^H(n)$, we obtain,

$$\Phi(n) = V(n)\Lambda(n)V^H(n) \tag{5.4}$$

$$= \sum_{m=1}^{M} \lambda_m(n)\, v_m(n)v_m^H(n)$$

Let, $v_m(n)v_m^H(n) = P_m(n)$, then,

$$\Phi(n) = \sum_{m=1}^{M} \lambda_m(n)\, P_m(n) \tag{5.5}$$

Knowing the vector $v_m(n)$, the projection matrix on this vector can be written as,

projection matrix on the m^{th} eigenvector $= v_m(n)(v_m^H(n)v_m(n))^{-1}v_m^H(n)$ (5.6)

But since $V^H(n)V(n) = I$, $v_m(n)$, $m=1,2,....,M$ are orthonormal vectors and therefore,

projection matrix on the m^{th} eigenvector $= v_m(n)v_m^H(n)$ (5.7)

$= P_m(n)$ (5.8)

Therefore, it is clear that the cross spectral density matrix $\Phi(n)$ can be expressed as the weighted sum of the projection matrices, $P_m(n)$, $m=1,2,...,M$ and the weights are the eigenvalues or the power associated with the eigenvectors.

By taking the Hermitian transpose on both sides of the eqn. (5.2), and substituting from eqns. (5.7) and (5.8), we obtain,

$$\sum_{m=1}^{M} P_m(n) = I \tag{5.9}$$

Further, it easy to see that,

$P_m^H(n)P_j(n) = 0$, $m \neq j$ and

$= P_m(n)$, $m=j$ (5.10)

Therefore, a family of projections $\{P_1(n),P_2(n),....P_M(n)\}$ is a resolution of identity [Naylor and Sell (1971)].

Let us assume that the number of incoming signals are K. The knowledge of K is not available in practice, and it can be estimated using the eigenvalues of the cross spectral density matrix $\Phi(n)$ as we mentioned in chapter 2.

Then, we can partition the eigenvector matrix V(n), into the signal subspace, and the noise subspace, so that,

$$V(n) = [V_S(n),V_N(n)] \tag{5.11}$$

$V_S(n) = [v_1(n),v_2(n),....,v_K(n)]$, $V_N(n) = [v_{K+1}(n),v_{K+2}(n),....,v_M(n)]$.

where, K is the number of signals.

Then the projection matrices $P_s(n)$ and $P_N(n)$ for the signal subspace and noise subspace respectively can be written as,

$$P_s(n) = V_s(n)[V_s^H(n)V_s(n)]^{-1}V_s^H(n) \quad (5.12)$$

$$P_N(n) = V_N(n)[V_N^H(n)V_N(n)]^{-1}V_N^H(n) \quad (5.13)$$

But from the constraint eqn. (5.2), we know that,

$$\begin{bmatrix} V_s^H(n) \\ \hline V_N^H(n) \end{bmatrix} [V_s(n), V_N(n)] = I^{(K)}$$

i.e. $V_s^H(n)V_s(n) = I^{(K)}$, and $V_N^H(n)V_N(n) = I^{(M-K)}$, where, $I^{(M)}$, $I^{(K)}$, and $I^{(M-K)}$ are the identity matrices and, $I^{(M)} \in C^{M\times M}$, $I^{(K)} \in C^{K\times K}$, and $I^{(M-K)} \in C^{(M-K)\times(M-K)}$.

Therefore, the projection matrices $P_s(n)$ and $P_N(n)$ reduce to the form,

$$P_s(n) = V_s(n)V_s^H(n) \quad (5.14)$$

$$= \sum_{m=1}^{K} P_m(n) \text{ , and}$$

$$P_N(n) = V_N(n)V_N^H(n) \quad (5.15)$$

$$= \sum_{m=K+1}^{M} P_m(n).$$

Additionally,

$$P_s(n) + P_N(n) = \sum_{m=1}^{M} P_m(n) \quad (5.16)$$

$$= I$$

where I is an identity matrix.

Therefore, it is clear that we can obtain the projection matrices $P_s(n)$ and $P_N(n)$ as the weighted sum of the basic projection matrices, $P_m(n)$, m=1,2,...M. Also, we can obtain the M^{th} order signal subspace cross spectral density matrix $\Phi_{ss}^{(K)}(n)$, and the M^{th} order noise subspace cross spectral density matrix

$\Phi_{NN}^{(\infty)}(n)$ as linear combinations of the basic elements $P_m(n)$, m=1,2,...,M, i.e.,

$$\Phi_{ss}^{(\infty)}(n) = \sum_{m=1}^{K} \lambda_m(n) P_m(n), \text{ and} \tag{5.17}$$

$$\Phi_{NN}^{(\infty)}(n) = \sum_{m=K+1}^{M} \lambda_m(n)\, P_m(n) \tag{5.18}$$

Further, by adding eqns. (5.17) and (5.18), we obtain,

$$\Phi_{ss}^{(\infty)}(n) + \Phi_{NN}^{(\infty)}(n) = \sum_{m=1}^{M} \lambda_m\, P_m(n)$$

$$= \Phi(n) \tag{5.19}$$

Therefore, it is clear that the basic elements, scalar matrix pairs $(\lambda_m(n), P_m(n))$, m=1,2,...,M, play an important role in geometric representation of the cross spectral density matrix. Even though it is difficult to visualize the operation of the matrix $\Phi(n)$, the scalar-matrix pair $(\lambda_m(n), P_m(n))$ is particularly simple and easy to visualize.

Further, it can also be shown that,

$$\Phi^{-1}(n) = \sum_{m=1}^{M} \lambda_m^{-1}(n)\, P_m(n)$$

$$= \sum_{m=1}^{K} \lambda_m^{-1}(n)\, P_m(n) + \sum_{m=K+1}^{M} \lambda_m^{-1}(n)\, P_m(n)$$

$$= [\Phi_{ss}^{(\infty)}(n)]^{\#} + [\Phi_{NN}^{(\infty)}(n)]^{\#}$$

where $[.]^{\#}$ denotes the pseudoinverse of [.].

So far, we have done the decomposition of the operator $\Phi(n)$ into several smaller subspaces so that the operation on each subspace is simple and easy. Let us now consider how we could use this in spectrum representation.

To start with, we first project our direction vector $\bar{d}(\theta)$ of dimension M onto the m^{th} eigenvector, i.e.,

$$d_m(\theta) = P_m(n)d(\theta) \tag{5.20}$$

where, $d_m(\theta)$ is the projection of $d(\theta)$ on the m^{th} eigenvector.

The scalar-vector pair $(\lambda_m(n),d_m(\theta)),m=1,2,\ldots,M$, can be used as the basic element to define different spectral estimation techniques as we want. We can define as many spectra as possible based on the scalar-vector pair $(\lambda_m(n),d_m(\theta))$. Here, we consider only two families because all the conventional, high resolution, and super resolution spectrum estimation techniques can be shown to belong to those two categories. Let us define the two families.

5.3 Euclidian Norm Techniques (Euc-Techs)

We can define a family of spectrum estimation techniques based on the scalar-scalar pair $(\lambda_m(n),|d_m(\theta)|)$, $m=1,2,\ldots,M$, where $|.|$ denotes the Euclidian norm of a vector. Since this spectral family makes use of the Euclidian norm of the projection vector $d_m(\theta)$, $m=1,2,\ldots,M$, it is named as the Euclidian norm Techniques (Euc-Techs).

In the Euc-Techs family, we define a family of spectra $S_{euc}(n,\theta)$ as a function of $(\lambda_m(n),|d_m(\theta)|)$, $m=1,2,\ldots,M$, i.e.,

$$S_{euc}(n,\theta) = f(\lambda_m(n),|d_m(\theta)|) \tag{5.21}$$

Now, we have a choice in the selection of the function. We consider one particular function, i.e.,

$$S_{euc}(n,\theta,r,s) = \frac{\sum_{m=1}^{M} \lambda_m^{-s}(n)\,|d_m(\theta)|^s}{\sum_{m=i}^{M} \lambda_m^{-r}(n)\,|d_m(\theta)|^s} \tag{5.22}$$

where, r and s are constants and can take any value, i, an integer so that $1 \le i \le M$.

We prefer to name this as the generalized maximum likelihood (GML) spectrum. Why we select this name will be made clear later.

Now let us consider some special cases:

(a1) Let i=1, r=0, and s=-1, then

$$S_{GML}(n,\theta) = \sum_{m=1}^{M} \lambda_m(n)\, |d_m(\theta)|^2 \qquad (5.23)$$

$$= d^H(\theta)\Phi(n)d(\theta)$$

= Bartlett spectrum (BS) [Bartlett (1953)]

$$= S_{BS-GML}(n,\theta).$$

This is generally referred to as a conventional spectrum estimation technique. It is clear that this spectrum depends on the eigenvalues and hence on the variance of the noise.

(a2) Let i=1, r=1, and s=0, then we get,

$$S_{GML}(n,\theta) = [\sum_{m=1}^{M} \lambda_m^{-1}(n)\, |d_m(\theta)|^2]^{-1} \qquad (5.24)$$

$$= [d^H(\theta)\Phi^{-1}(n)d(\theta)]^{-1}$$

= Maximum likelihood (ML) spectrum [Capon (1969)]

$$= S_{ML}(n,\theta).$$

Maximum likelihood spectrum is also referred to as the minimum variance spectrum. This is considered to be a speotrum in the high resolution spectra family. This spectrum depends on the eigenvalues and hence on the variance of the noise. Since the spectrum given in eqn. (5.22) reduces to the maximum likelihood spectrum as a special case, it is named as the generalized maximum likelihood spectrum.

(a3) Let i=1, r=2, and s=1, then we get,

$$S_{Euc}(n,\theta) = \frac{\left[\sum_{m=1}^{M} \lambda_m^{-2}(n)\ |d_m(\theta)|^2\right]}{\left[\sum_{m=1}^{M} \lambda_m^{-2}(n)\ |d_m(\theta)|^2\right]} \qquad (5.25)$$

$$= [S_{ML}(n,\theta) \sum_{m=1}^{M} \lambda_m^{-2}(n)\ |d_m(\theta)|^2]^{-1}$$

$$= \frac{[d^H(\theta)\Phi^{-1}(n)d(\theta)]}{[d^H(\theta)\Phi^{-2}(n)d(\theta)]}$$

= Adaptive angular response (AAR) spectrum [Borgiotti and Kaplan (1979)].

$$= S_{AAR-Euc}(n,\theta)$$

This belongs to the high resolution spectra family, and it depends on the eigenvalues, and hence on the variance of the noise.

(a4) Let i=1, r=2, and s=0, then we obtain,

$$S_{Euc}(n,\theta) = [\sum_{m=1}^{M} \lambda_m^{-2}(n)\ |d_m(\theta)|^2]^{-1} \qquad (5.26)$$

$$= [d^H(\theta)\Phi^{-2}(n)d(\theta)]^{-1}$$

= Thermal noise (TN) spectrum [Gabrial (1980)]

$$= S_{TN-Euc}(n,\theta)$$

This comes under the high resolution category. It depends on the eigenvalues and hence on the variance of the noise.

(a5) Let i=K+1, s=0, and r=1, then,

$$S_{Euc}(n,\theta) = [\sum_{m=K+1}^{M} \lambda_m^{-1}(n)|d_m(\theta)|]^{-1}$$

$$= [d^H(\theta)\{\Phi_{NN}^{(M)}(n)\}^{-2}d(\theta)]^{-1}$$

= Eigenvalue eigenvector Spectrum [Johnson (1982)]

$= S_{EV-Euc}(n,\theta)$

where, $\{\Phi_{NN}^{(M)}(n)\}^{-} = \sum_{m=K+1}^{M} \lambda_m^{-2} P_m(n)$ (5.27)

and K is the number of signals.

Even though it has been the custom to consider this as a super resolution technique, this spectrum depends on the eigenvalues and hence the variance of the noise. If the variance of the noise is same for all sensors, then the $S_{EV-Euc}(n,\theta)$ spectrum becomes asymptotically independent of noise. For finite number of snapshots this spectrum will be affected by the perturbation of both the eigenvalues and eigenvectors.

(a6) So far we have considered a few of the possible spectra in Euc-Techs family, which are functions of both $\lambda_m(n)$ and $|d_m(\theta)|$. Now let us define some Euc-Techs spectra using $|d_m(\theta)|$ alone so that they do not depend on the eigenvalues and hence on the variance of the noise.

Let i=K+1, r=0, and s=0, where K is the number of signals.

Then we obtain,

$$S_{Euc}(n,\theta) = \left[\sum_{m=K+1}^{M} |d_m(\theta)|\right]^{-1} \quad (5.28)$$

$$= [d^H(\theta) P_N(n) d(\theta)]^{-1}$$

$\equiv$ MUSIC [Schmidt (1979)] or more appropriately POP-MUSIC-Euc

$= S_{POP-Euc}(n,\theta)$

where, $P_N(n)$ is the noise subspace projection matrix.

This is a spectrum in the super resolution spectra family. It does not depend on the eigenvalues and hence it is asymptotically independent of the

variance of the noise.

At this point it may be interesting to see the spectrum where i=1 and s=0. Then eqn.(5.22) becomes,

$$S_{Euc}(n,\theta) = [\sum_{m=1}^{M} \lambda_m^{-r}(n) \, |d_m(\theta)|^2]^{-1}$$

$$= [d^H(\theta)\Phi^{-r}(n)d(\theta)]^{-1} \qquad (5.29)$$

$$= S_{MGML-Euc}(n,\theta)$$

Let us call this the more general maximum likelihood (MGML) spectrum. We know that the $\lambda_m(n)$, m=K+1,K+2,....,M are asymptotically repetitive and they represent the variance of the noise.

Let us consider the case where $r \to \infty$, then,

$$S_{MGML-Euc}(n,\theta) \Big|_{r\to\infty} = [\sum_{m=K+1}^{M} |d_m(\theta)|^2]^{-1}$$

$$\equiv \text{POP-MUSIC-Euc Spectrum, } S_{POP-Euc}(n,\theta) \qquad (5.30)$$

One may notice that we have disregarded the multiplication factor in obtaining the relationship given in eqn.(5.30). Therefore, in the maximum likelihood spectrum, if we use the $\Phi^{-r}(n)$, r>1, in the place of the $\Phi^{-1}(n)$, we can always get improved performance compared to the maximum likelihood spectrum, and as r increases the performance tends to reach the performance of the POP-MUSIC-Euc spectrum.

Now let us consider the maximum likelihood spectrum when the signal to noise ratio is infinite, i.e.,

$$S_{ML}(n,\theta) \Big|_{SNR\to\infty} = [\sum_{m=K+1}^{M} |d_m(\theta)|^2]$$

$$\equiv \text{POP-MUSIC-Euc spectrum, } S_{POP-Euc}(n,\theta) \qquad (5.31)$$

It may again be noticed that we have disregarded the multiplication

factor in achieving the relationship given in eqn (5.31). We obtain the relationship given in eqn. (5.31) using the fact that $\lambda_m^{-1}(n)$, m=1,2,...,K is negligible compared to the $\lambda_m^{-1}(n)$, m=K+1,K+2,....,M at large signal to noise ratios.

So far we have considered some possible spectra in the family of Euc-Techs. One can define as many spectra as one wants within the Euc-Techs family. But, with a little understanding of spectrum estimation as a whole, reader will easily be convinced that the very best that can be achieved cannot exceed the POP-MUSIC-Euc spectrum in the Euc-Techs family. Therefore, there is no point in defining any more possible spectra in Euc-Tech family.

5.4 Elemental Norm Techniques (Elem-Techs)

Now let us define another possible family of spectra. To achieve this, we express the M^{th} dimensional space by a set of basis vectors e_m, m=1,2, ...,M, where,

$$[e_1, e_2, \ldots, e_M] = I \tag{5.32}$$

Any vector in the M dimensional space can be represented as a linear combination of the basis vectors e_m, m=1,2,....,M. Therefore, the vector $d_m(\theta)$, i.e. the projection of the vector $d(\theta)$ onto the eigenvector $v_m(n)$ can be written as,

$$d_m(\theta) = \sum_{m_o=1}^{M} d_{m(m_o)}(\theta)\, e_{m_o} \tag{5.33}$$

(please note that the m_o is same as $_{m_o}$)

Therefore, $d_{m(m_o)}(\theta)$ represents the m_o^{th} element of the vector $d_m(\theta)$ or the projection of $d_m(\theta)$ onto the m_o^{th} basis vector e_{m_o} given by eqn. (5.32). We refer to the element $d_{m(m_o)}(\theta)$ as the elemental norm of the vector $d_m(\theta)$. We make use of the eigenvalue $\lambda_m(n)$ and the elemental norm $d_{m(m_o)}(\theta)$, to define another spectral estimate. Since this family of spectra are chosen to make use of

the scalar-scalar pair $(\lambda_m(n),d_{m(mo)})$, we refer this family as the Elemental norm Techniques (Elem-Techs).

In the Elem-Techs family, we define the spectra as a function of $(\lambda_m(n),d_{m(mo)}(\theta))$, m=1,2,...,M, i.e.,

$$S_{Elem}(n,\theta) = f(\lambda_m(n),d_{m(mo)}(\theta)) \tag{5.34}$$

Here again we have a choice within the Elem-Techs family. We can choose the function arbitrarily. But we consider only a few of them which are of real interest to us.

We first consider a function,

$$S_{Elem}(n,\theta) = \frac{|\sum_{m=1}^{M} \lambda_m^{-s}(n)d_{m(mo)}(\theta)|^2}{|\sum_{m=i}^{M} \lambda_m^{-r}(n)d_{m(mo)}(\theta)|^2} \tag{5.35}$$

where, r and s can be any number and |.| denotes the amplitude, i is an integer within the range, $1 \le i \le M$.

This function is equivalent to the function used to define the generalized maximum likelihood spectrum in Euc-Techs family. We name this as the generalized linear prediction (GLP) spectrum. The reason why we refer this by the name GLP will be clarified later.

Now let us consider some special cases:

(a1) Let s=0, r=1, and i=1, m_o=1, then we get,

$$S_{Elem}(n,\theta) = |\sum_{m=1}^{M} \lambda_m^{-1}(n)d_{m(i)}|^{-2} \tag{5.36}$$

$$= |e_1^T\Phi^{-1}(n)d(\theta)|^{-2}$$

$$\equiv \text{linear prediction (LP) spectrum [Yule and Walker (1927), Burg (1967,1968), Haykin (1986)]}$$

$$= S_{LP}(n,\theta)$$

where, $d_{m(1)}(\theta)$ is the projection of $d(\theta)$ on the basis vector e_1.

This belongs to the high resolution spectra family. It depends on the eigenvalues and hence on the variance of the noise.

Since the spectrum given in eqn. (5.35) reduces to the well known linear prediction spectrum as a special case, it is named as the generalized linear prediction (GLP).

(a2) Let i=1, r=2, s=1, then,

$$S_{Elem}(n,\theta) = \frac{\left|\sum_{m=1}^{M} \lambda_m^{-a}(n) d_{m(mo)}(\theta)\right|^a}{\left|\sum_{m=1}^{M} \lambda_m^{-a}(n) d_{m(mo)}(\theta)\right|^a} \qquad (5.37)$$

$$= S_{AAR-Elem}(n,\theta)$$

Comparing eqn. (5.37) with eqn. (5.25), we can see that the spectrum given in eqn. (5.37) is the Elem-Techs family counterpart of the adaptive angular response spectrum. Therefore, it is denoted by $S_{AAR-Elem}(n,\theta)$.

(a3) Let i=1, r=2, s=0, then we obtain,

$$S_{Elem}(n,\theta) = \left|\sum_{m=1}^{M} \lambda_m^{-a}(n) d_{m(mo)}(\theta)\right|^{-a} \qquad (5.38)$$

$$= S_{TN-Elem}(n,\theta).$$

Eqn. (5.38) is the Elem-Techs family counterpart of the thermal noise spectrum given in the Euc-Techs family. Therefore, eqn. (5.38) is referred to as $S_{TN-Elem}(n,\theta)$.

(a4) Let i=K+1, s=0, and r=1, then,

$$S_{Elem}(n,\theta) = \left|\sum_{m=K+1}^{M} \lambda_m^{-1}(n) d_{m(mo)}(\theta)\right|^{-a} \qquad (5.39)$$

$$= |e_{mo}[\Phi_{NN}^{(-1)}(n)]^{a} d(\theta)|^{-a}$$

$$= S_{EV\text{-}Elem}(n,\theta)$$

where, $[\Phi_{NN}^{(-1)}(n)]^{a} = \sum_{m=K+1}^{M} \lambda_m^{-1} P_m(n)$

Due to this similarity between eqn. (5.39) and eqn (5.27), the spectrum given in eqn. (5.39) can be referred to as the Elem-Tech correspondence of the eigenvalue eigenvector spectrum given in the Euc-Techs family. Therefore it is denoted by $S_{EV\text{-}Elem}(n,\theta)$.

(a5) All the functions we have defined so far do depend on the eigenvalues and hence on the variance of the noise. To avoid the dependence of the noise in the spectra, we can define a function based on the $d_{m(mo)}(\theta)$ alone.

Let i=K+1, r=1, and s=0, where K is the number of signals, then we obtain,

$$S_{Elem}(n,\theta) = \left|\sum_{m=K+1}^{M} d_{m(mo)}(\theta)\right|^{-a} \qquad (5.40)$$

$$= |e_{mo}{}^{T} P_N(n) d(\theta)|^{-a}$$

= POP-MUSIC-Elem spectrum, $S_{POP\text{-}Elem}$

We had considered this spectrum in Chapter 4. POP-MUSIC-Elem spectrum does not depend on the eigenvalues and hence it is independent of the variance of noise. This spectrum comes under the super resolution techniques.

After defining the POP-MUSIC-Elem spectrum let us consider a special case of eqn. (5.35), i.e., i=1, and s=0, then we obtain,

$$S_{Elem}(n,\theta) = |\sum_{m=1}^{M} \lambda_m^{-r}(n) d_{m(mo)}(\theta)|^{-a} = |e_{mo}\Phi^{-r}(n)d(\theta)|^{-a}. \quad (5.41)$$

Noting the similarity of this eqn. (5.41) to eqn. (5.29), we may refer to eqn. (5.41) as more general linear prediction (MGLP) spectrum. An interesting observation can be made if we consider the case $r\to\infty$, i.e.,

$$S_{Elem}(n,\theta)\Big|_{r\to\infty} \equiv |\sum_{m=K+1}^{M} d_{m(mo)}(\theta)|^{-a} = \text{POP-MUSIC-Elem spectrum.} \quad (5.42)$$

Therefore, more general linear prediction spectrum, $S_{MGLP-Elem}(n,\theta)$ tends to be equal to the POP-MUSIC-Elem when r tends to infinity.

Now let us consider the linear prediction spectrum given in eqn (5.36), when the signal to noise ratio is infinite, i.e.,

$$S_{LP}(n,\theta)\Big|_{SNR\to\infty} \equiv |\sum_{m=K+1}^{M} d_{m(mo)}(\theta)|^{-a} \equiv S_{POP-Elem}(n,\theta). \quad (5.43)$$

Therefore, at infinite signal to noise ratio, the linear prediction spectrum will be the same as the POP-MUSIC-Elem spectrum.

Further more as we have shown in chapter 4, the minimum norm (MN) spectrum will be a special case of POP-MUSIC-Elem spectrum and it is given by,

$S_{MN}(n,\theta)$ = POP-MUSIC-Elem spectrum, when $m_o = 1$. (5.44)

5.5 Comparative Performance

So far we have presented two possible spectral families, namely Euc-Techs and Elem-Techs. One can define many more spectral families as one wishes using the scalar-vector pair $(\lambda_m(n), d_m(\theta))$, m=1,2,....M. Within a spectral family, one also has a freedom to define a function to represent a spectrum. We have considered a few functions. For a given function one can easily obtain its Euc-Techs family counterpart and also the Elem-Techs family counterpart. The chosen functions are shown to be equivalent to the conventional, high resolution, and super resolution spectrum estimation techniques.

The above generalization can be used to compare the performance of the spectral estimation techniques.

In general, eigenvectors asymptotically do not depend on the variance of the noise σ_v^2 asymptotically. But the eigenvalues will depend on the variance σ_v^2 (Appendix 4a) and hence on the signal to noise ratio. Therefore, any spectrum estimation technique that depends on the eigenvalues is susceptible to the signal to noise ratio. Except for the POP-MUSIC-Euc and the POP-MUSIC-Elem, all the rest of the spectrum estimation techniques depend on the signal to noise ratio. This fact can be utilized to analyze the bias properties of the spectrum estimation techniques. To start with, we define the term unbiased estimate.

Definition 5.1

Unbiased estimate

A spectrum estimate is said to be an unbiased estimate if it can provide the true bearings irrespective of the signal to noise ratio for a given true cross spectral density matrix.

As we have seen before, only the POP-MUSIC-Euc and POP-MUSIC-Elem do not depend on the eigenvalues and hence on the signal to noise ratio. Therefore, it is clear that only the POP-MUSIC-Euc and POP-MUSIC-Elem can provide an unbiased estimates. All the rest of the spectra depend on the eigenvalues and hence on the variance of the noise so that they can provide unbiased estimates only when the signal to noise ratio is infinite.

Since we know that,

$$\Phi^{-1} = \sum_{m=1}^{K} \lambda_m^{-1} P_m + \sum_{m=K+1}^{M} \lambda_m^{-1} P_m$$

we can obtain the relationship,

$$\lim_{SNR \to \infty} \Phi^{-1} = \sum_{m=K+1}^{M} P_m$$

$$= P_N(n) \qquad (5.45)$$

It may be noticed that we have disregarded the multiplication factor in obtaining the relationship given in eqn. (5.45).

Due to this, it is obvious that all the spectrum estimation techniques could provide equal performance at infinite signal to noise ratio.

Further, by generalizing the Theorem 4.2.1, it can be easily shown that the high resolution spectra in the Euc-Techs family is able to provide spectra free of dominant spurious peaks at high signal to nose ratio. It is not possible to guarantee dominant spurious peaks free spectra in the Elem-Techs family. Therefore, it is clear that POP-MUSIC-Euc is the only spectrum that could provide a guaranteed spurious peaks free spectrum. Asymptotic performance of the spectrum estimation techniques and their relationships are shown diagrammatically in Fig. 5.1.

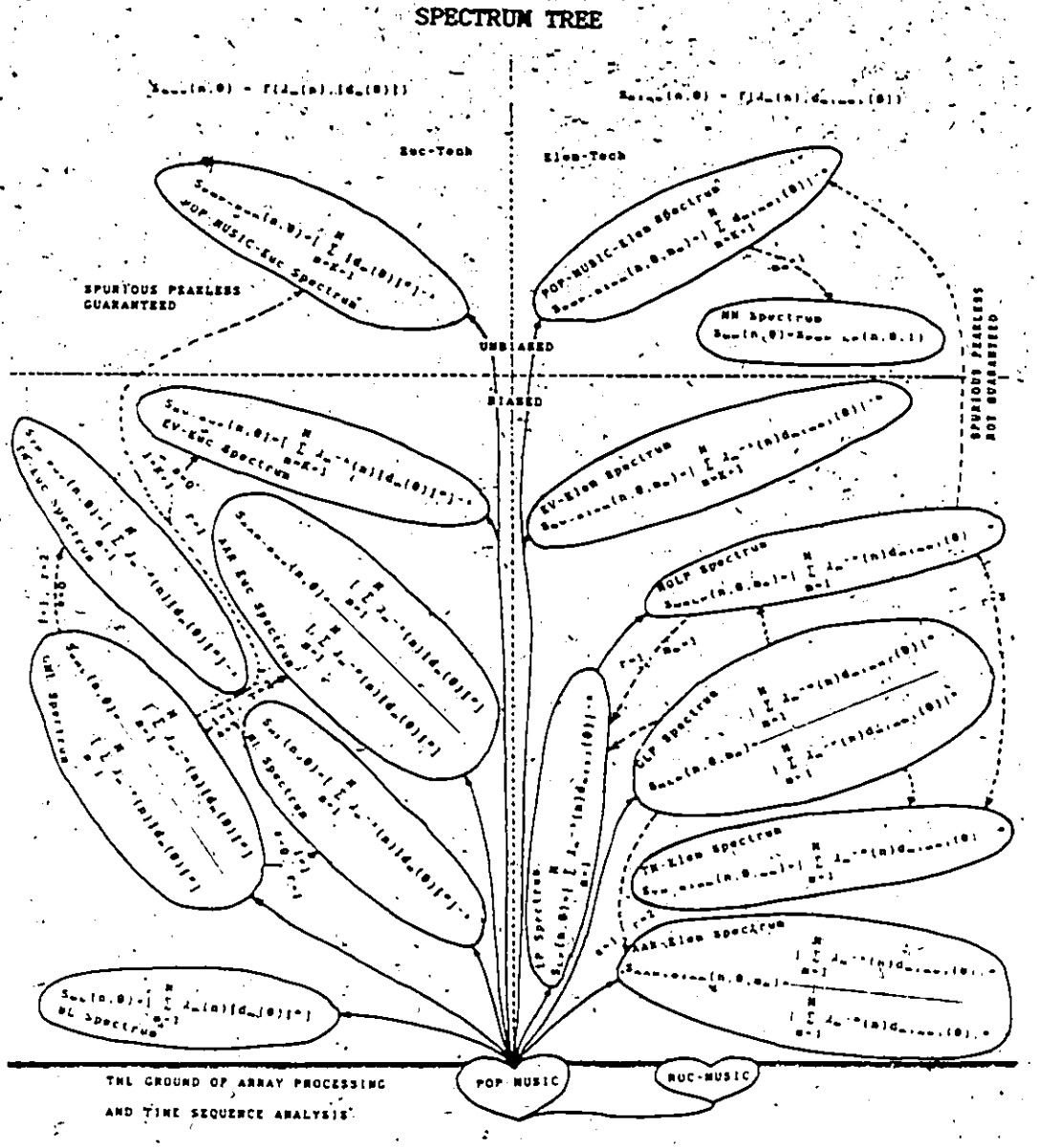

FIG 5.1 UNIFIED APPROACH TO SPECTRUM REPRESENTATION

5.6 Summary

We have presented a unified approach to the spectrum representation based on the scalar-vector pair $(\lambda_m(n), d_m(\theta))$ obtained by using the eigen value eigenvector decomposition of the cross spectral density matrix $\Phi(n)$. Out of many, two possible spectra families, namely, Euc-Techs and Elem-Techs are given. Euc-Techs family makes use of the scalar-scalar pair $(\lambda_m(n), \|d_m(\theta)\|)$, and Elem-Techs family makes use of the scalar-scalar pair $(\lambda_m(n), d_{m(mo)}(\theta))$. Conventional, high resolution, and super resolution spectra are categorized into Euc-Techs and Elem-Techs. Given a spectrum in Euc-Techs, it is possible to obtain its Elem-Techs counterpart and vice versa. Out of the spectra we have considered, only the POP-MUSIC-Euc can provide guaranteed unbiased and spurious peaks free spectrum. At infinite signal to noise ratio, all the spectrum estimation techniques perform equally. All the spectrum estimation techniques can be made asymptotically unbiased by subtracting the minimum eigenvalue from the rest of the eigenvalues.

CHAPTER 6

BEAMFORMING IN ADAPTIVE ARRAY PROCESSING

Preview An array of sensors which acts as a receiver is generally referred as a beamformer. Beamforming can be divided into two main categories, viz;

1. Reception of a signal coming from a known direction while suppressing all the other interferences,
2. Reception of all the signals coming from distinct and unknown directions separately while suppressing the interferences. This can also be considered as a listening device.

Minimum variance distortionless response (MVDR) beamformer is capable of receiving a signal coming from a known and distinct direction adaptively while suppressing all the other interferences. The amount of null of the MVDR beamformer at the interferences, depends on the signal and noise environment and one does not have any control over that. The stronger the interference, the stronger the null has to be in the MVDR beamformer. MVDR beamformer performs successfully provided that the input signals are incoherent. If the signals are coherent, it suppresses the signal in addition to the interference leaving noise as the output of the beamformer. The coherent signal environment can be handled by using the adaptive spatial data smoothing preprocessing (ASDSP) scheme described in chapter 4.

In this chapter we introduce a modified technique of beam-

forming called the flipped minimum variance distortionless response (FMVDR) beamformer based on the flipping technique. The FMVDR beamformer gives improved nulls (by nulls, we mean the notches in the spatial response) at the interference and the improvement is very significant compared to MVDR beamformer. The effect of the angular separation of the incoming signals, i.e. the signal and the interference, is studied for both MVDR and FMVDR beamformers. Nulling capabilities of the MVDR and FMVDR beamformers are studied against the angular separation of the incoming signals.

We also introduce the conditional flipped minimum variance distortionless response (C-FMVDR) beamformer. C-FMVDR beamformer provides an improvement to FMVDR beamformer by making use of the estimated bearing of the interference at each snapshot. The estimated bearing of the interference is then used with the conditional logic in obtaining the best filter weights which provide the strongest null up to n^{th} snapshot which will be used as the filter weight at n^{th} snapshot. The C-FMVDR beamformer gives very stronger nulls compared to the FMVDR beamformer. The computational structures for both beamformers are almost the same except the additional structures such as the conditional logic and the bearing estimator associated with the C-FMVDR beamformer. The nulling capability of the C-FMVDR beamformer is deteriorated when the incoming signals are narrowly separated but is better compared to FMVDR beamformer under the same conditions. Therefore, as far as its nulling capabilities are concerned, the C-FMVDR beamformer will be an attractive alternative to the FMVDR beamformer.

Neither FMVDR nor C-FMVDR is capable of handling the coherent signal environment directly. Both the FMVDR and C-FMVDR beamformers preceded by the adaptive spatial data smoothing preprocessing (ASDSP) scheme can be used under coherent signal environment. None of the MVDR, FMVDR, or C-FMVDR beamformers can be used in receiving the signals coming from distinct and unknown directions while suppressing all the other interferences. Therefore, they do not work as a listening device.

6.1 Flipped Minimum Variance Distortionless Response (FMVDR) Beamformer

6.1.1 Introduction

Minimum variance distortionless response (MVDR) beamformer is generally used to receive a signal coming from a known direction while suppressing all the other interferences. Interference suppression is generally done in frequency domain for each frequency component of the known signal frequency band separately. The filtered output at each beamformers are then collected and inverse fast Fourier transform is performed to recover the desired signal. Systolic array implementation of minimum variance distortionless response beamformer based on the QR decomposition has been considered by Haykin-(1986). MVDR beamformer based on the QR decomposition provides superior nulling capabilities over the rest of the beamformers.

Here, we introduce flipped minimum variance distortionless response beamformer which can be used to receive a signal coming from a desired direction unaltered while suppressing all the other interferences. Minimum variance distortionless response beamformer preceded by the flipping technique is

named as the flipped minimum variance distortionless response (FMVDR) beamformer. Formulation of FMVDR beamformer based on the QR decomposition is given in a form suitable for systolic array implementation. FMVDR beamformer and MVDR beamformer are virtually the same except the flipping network that was incorporated with the FMVDR beamformer. The terms 'figure of convergence (τ)' and the 'steady state convergence time (ρ)' are defined to aid in the comparative analysis of the MVDR beamformer and the FMVDR beamformer. Additionally, computer simulation results are presented.

6.1.2 FMVDR Beamformer and its Systolic Array Structure

Schematic diagram for the FMVDR beamformer is shown in Fig. 6.1. Input data vector u(n) at n^{th} snapshot passes through a flipping network which produces two vectors as its output namely the vector u(n) and its conjugate reverse $u^*(n)$. Then the input data matrix U(2:n) can be formed and used for processing. But as we mentioned in an earlier chapter, the direct use of the data matrix is not suitable for adaptive processing since its dimensions increase with the number of snapshots. Therefore, we transform the matrix $U^*(2:n)$ into an upper triangular matrix of fixed dimensions by using the Jacobi-Givens rotation. This operation is generally performed by using the matrix triangularization systolic array structure as we discussed in chapter 2. The detail of the flipping network is found in chapter 3.

Let the filter weights vector $w^*(n)$ and the output vector $e_n(2:n)$ after n^{th} snapshot be given by,

$$w(n) = (w_{-J}(n), w_{-J+1}(n), \ldots, w_J(n))^T, \tag{6.1.1}$$

$$e_n^*(2:n) = U^*(2:n)w(n) \tag{6.1.2}$$

where,

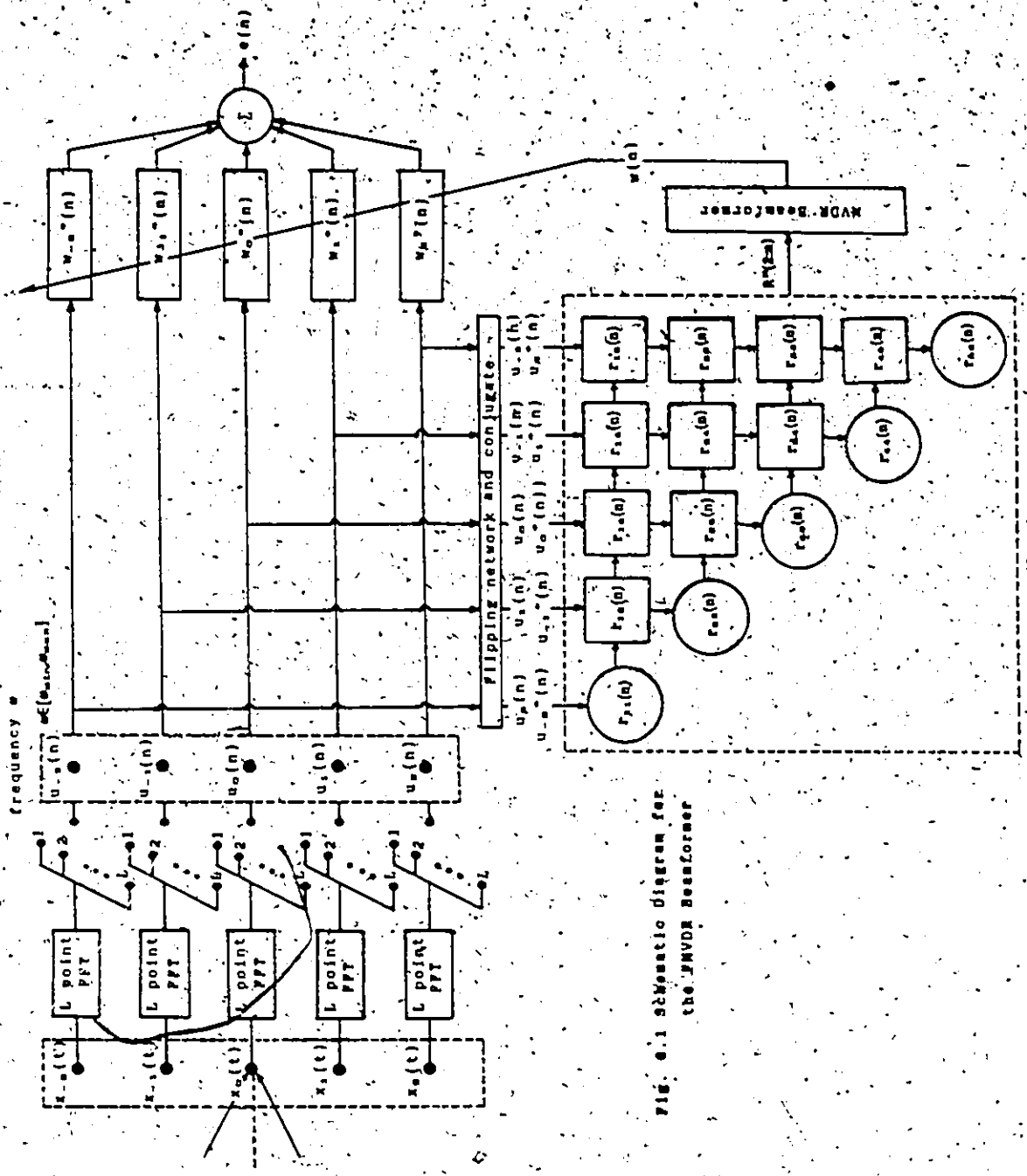

Fig. 6.1 Schematic diagram for the FMVDR Beamformer

$$U(2:n) = [u^H(1),u(1),u^H(2),u(2),\ldots,u^H(n),u(n)], \tag{6.1.3}$$

$J = (M-1)/2$, M is odd, $U(2:n) \in C^{M\times 2n}$, and M is the number of sensors in the array.

Now, operating the Jacobi-Givens rotation Q(2:n) on the eqn. 6.1.2 we obtain,

$$Q^H(2:n)e_n^T(2:n) = Q^H(2:n)U^H(2:n)w(n) \tag{6.1.4}$$

where, $Q(2:n)Q^H(2:n) = I$, (6.1.5)

$Q(2:n) \in C^{2n\times 2n}$, and I is an identity matrix.

The matrix $Q^H(2:n)$ is chosen such that the data matrix $U^H(2:n)$ is transformed to an upper triangular matrix $R^H(2:n)$ (Appendix 2a), i.e.

$$Q^H(2:n)U^H(2:n) = R^H(2:n), \tag{6.1.6}$$

$R(2:n) \in C^{M\times M}$.

Eqn. (6.1.4) then becomes,

$$Q^H(2:n)e_n^T(2:n) = R^H(2:n)w(n) \tag{6.1.7}$$

Q(2:n) is an unitary matrix and hence it is norm preserving so that,

$$\|e_n\| = \|Q^H(2:n)e_n^T(2:n)\| \tag{6.1.8}$$

where, $\|.\|$ denotes the Euclidian norm.

The total output energy, E(n) after n^{th} snapshot is defined by,

$$E(n) = \|e_n^T(2:n)\|^2$$
$$= w^H(n)R(2:n)R^H(2:n)w(n). \tag{6.1.9}$$

Then the development of the FMVDR beamformer is straightforward. We minimize the quantity E(n) after n^{th} snapshot subject to the constraint that the signal coming from a desired direction is unaltered.

i.e. minimize $E(n)$
$w(n)$ (6.1.10)

subject to the constraint, $w^H(n)d(\theta_T) = 1$ (6.1.11)

where, θ_T is the desired direction, $d(\theta_T)$ denotes the direction vector of the

desired signal.

Theorem 6.1

Constraint-minimization problem,

$$\underset{w(n)}{\text{minimize}}\ E(n)$$

subject to the constraint $w^{H}(n)d(\theta_{T}) = 1$ (6.1.12)

leads to the solution:

1. Maximum likelihood spectrum estimate, $S_{ML}(2{:}n,\theta)$ is,

$$S_{ML}(2{:}n,\theta) = |a(2{:}n,\theta)|^{-2} \tag{6.1.13}$$

2. Optimal weight vector $w_{opt}(n)$ is,

$$w_{opt}(n) = S_{ML}(2{:}n,\theta)\ b(2{:}n,\theta) \tag{6.1.14}$$

where, $R(2{:}n,\theta)a(2{:}n,\theta) = d(\theta)$, (6.1.15)

$$R^{H}(2{:}n,\theta)b(2{:}n,\theta) = a(2{:}n,\theta). \tag{6.1.16}$$

Proof

Finding the optimal weight vector, $w_{opt}(n)$ can be accomplished by the method of Lagrange multipliers. By adjoining the constraint in eqn. (6.1.12) to the cost function E(n) using the Lagrange multiplier η, we obtain,

$$\underset{w(n)}{\text{minimize}}\ E'(n)=w^{H}(n)R(2{:}n)R^{H}(2{:}n)w(n)+\eta[w^{H}(n)d(\theta)-1]+\{\eta[w^{H}(n)d(\theta)-1]\}^{H} \tag{6.1.17}$$

Gradient of E'(n) with respect to w(n) is given by,

$$\nabla_{w(n)}[E'(n)] = R(2{:}n)R^{H}(2{:}n)w(n) + \eta\ d(\theta). \tag{6.1.18}$$

A necessary condition for the minimization of E'(n) is that the gradient, $\nabla_{w(n)}[.]$ be equal to zero so that,

$$R(2{:}n)R^{H}(2{:}n)w(n) = -\eta\ d(\theta) \tag{6.1.19}$$

i.e. $w(n) = -\eta\ R^{-H}(2{:}n)R^{-1}(2{:}n)d(\theta)$. (6.1.20)

Combining eqns. (6.1.12) and (6.1.20), we obtain,

$$-\lambda = (d^H(\theta)R^{-H}(2:n)R^{-1}(2:n)d(\theta))^{-1} \quad (6.1.21)$$

$$= \|R^{-1}(2:n)d(\theta)\|^{-2} \quad (6.1.22)$$

By substituting for $-\lambda$ in eqn. (6.1.20) from eqn. (6.1.22), we obtain,

$$w_{opt}(n) = \frac{R^{-H}(2:n)R^{-1}(2:n)d(\theta)}{\|R^{-1}(2:n)d(\theta)\|^{-2}} \quad (6.1.23)$$

Now let,

$R^{-1}(2:n)d(\theta) = a(2:n,\theta)$ and

$R^{-H}(2:n)a(2:n,\theta) = b(2:n,\theta)$,

i.e. $R(2:n)a(2:n,\theta) = d(\theta)$ (6.1.24)

$R^H(2:n)b(2:n,\theta) = a(2:n,\theta)$. (6.1.25)

The optimal weight vector $w_{opt}(n)$ at n^{th} snapshot is then given by,

$$w_{opt}(n) = S_{ML}(2:n,\theta)\ b(2:n,\theta) \quad (6.1.26)$$

where,

$$S_{ML}(2:n,\theta) = \|a(2:n,\theta)\|^{-2} \quad (6.1.27)$$

$S_{ML}(2:n,\theta)$ denotes the minimum value of the quantity $E(n)$ at angle θ and it is equal to the maximum likelihood spectrum estimate.

Eqns. (6.1.24) and (6.1.25) can be solved by using the forward and backward substitution which can be implemented using a linear array as shown in Appendix 2d. Once the optimal weight vector $w_{opt}(n)$ is obtained the beamformer output, $e(n)$ at n^{th} snapshot is given by,

$$e(n) = w_{opt}^H(n)u(n). \quad (6.1.28)$$

Separate beamformers have to be designed for each frequency component of the signal frequency band. The signal can be recovered by using the inverse discrete Fourier transform (IDFT) on the filtered output of all the frequency components. The required systolic array structures can be found in Kung (1986)

and can be listed as follows:

1. Matrix-vector multiplication
2. FFT and IFFT
3. Matrix triangularization
4. Linear arrays for the forward and backward substitutions.

6.1.3 Performance Measures

In order to compare the performance of the FMVDR beamformer and MVDR beamformer we define the followings:

Definition 6.1

Spatial response, $\Gamma(n,\theta)$ of a beamformer is defined as,

$$\Gamma(n,\theta) = |d^{H}(\theta)w_{opt}(n)| \tag{6.1.29}$$

Since the noise is random, $w_{opt}(n)$ is also a random vector which implies that the spatial response $\Gamma(n,\theta)$ is also a random quantity.

Definition 6.2

The plot of $E[\Gamma(n,\theta_x)]$ against the number of snapshots is defined as the 'learning curve', where, E denotes the ensemble average and θ_x is the angle of the interference.

Definition 6.3

We define a term 'figure of convergence (τ)'.

τ = the time taken for a learning curve to reach the null amplitude that is equal to the strength of the interference,

i.e. τ = time index n for $|20 \log \Gamma(n,\theta_x)|$ = INR.

where, INR is the interference to noise ratio in dB, |.| denotes the magnitude.

Definition 6.4

We define a term 'steady state convergence time (ρ)' as the time taken for the learning curve to reach a steady value.

6.1.4 Evaluation of Performance of the FMVDR Beamformer (Simulation example)

To test the performance of the FMVDR beamformer, we carry out a computer simulation, in which we consider the case of two narrow band signals arriving in distinct directions at an array consisting of five equally separated sensors. The target signal and the interference are assumed to be coming from the directions $\sin^{-1}(0.2)$ and $\sin^{-1}(-0.4)$ respectively. We further assume that the incoming signals are uncorrelated and the signals and noise are uncorrelated. We consider the cases where signal to noise ratio is 20 dB and the interferences to noise ratios are 40 dB, 30 dB, and 20 dB. Simulation results are shown after one hundred snapshots.

Spatial Response

Spatial response $\Gamma(n,\theta)$ for MVDR and FMVDR beamformers are shown in Figs. 6.1.2 and 6.1.3 respectively. Strength of the null at the interference for MVDR and FMVDR beamformers are tabulated in Table 6.1.1. Strength of the null at the angle of the interference, $\Gamma(n,\theta_x)$ against the sine-angle of separation of two signals $\Delta(\sin\theta)_{xr}$, for MVDR and FMVDR beamformers are given in Figs. 6.2.4 and 6.1.5 respectively. The sine-angular separation, $\Delta(\sin\theta)_{xr}$ is defined as, $\Delta(\sin\theta)_{xr} = \sin\theta_x - \sin\theta_r$, where, θ_r and θ_x are the incoming angles of the target signal and the interference respectively.

Discussion.

From Figs. (6.1.2) and (6.1.3), it is clear that the FMVDR beamformer produces a strong null at the interference compared to the MVDR beamformer. Improvement achieved in the strength of the null by using the FMVDR beamformer is approximately about 10 dB over the MVDR beamformer. It is noteworthy that the stronger the interference the stronger is the null and that is equally true for both MVDR and FMVDR beamformers. From Figs. 6.1.4 and 6.1.5 we can further conclude that the strength of the null will be reduced when the incoming signals are very close. When the incoming signals are well separated FMVDR beamformer provides superior nulling capabilities over MVDR beamformer. In any beamformer, it is preferable to have the spatial response as small as possible in directions other than the direction of arrival of the target signal. Therefore, the additional null we observe in the spatial response of the FMVDR beamformer given in Fig. (6.1.3), will definitely be an advantage. But, this additional null may create a problem by attenuating the desired signal if the desired direction is ambiguous. On the other hand, from Fig. (6.1.2), it is clear that the MVDR beamformer is quite robust to the ambiguities of the desired direction. Small ambiguities in the desired direction may not have much influence on the desired signal as long as the interference and the signal are well separated.

Table 6.1.1 Strength of the null in dB for MVDR and FMVDR beamformers

INR dB	MVDR	FMVDR
40	-59.41	-69.59
30	-49.47	-60.21
20	-39.68	-52.55

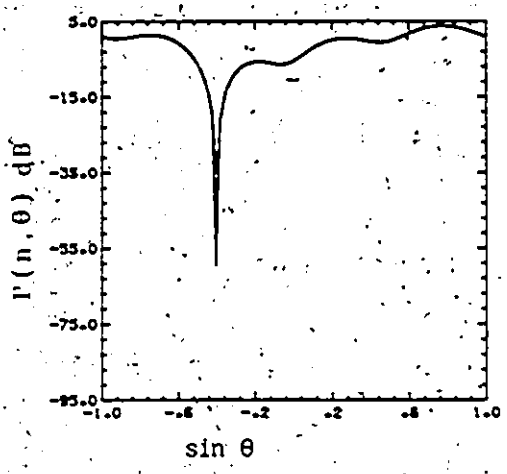

Fig. 6.1.2 Spatial response in dB for the MVDR beamformer

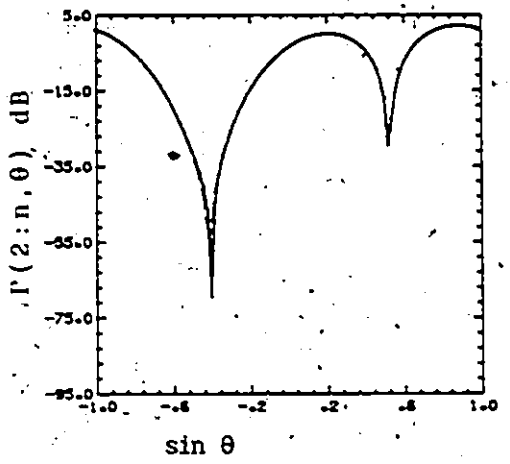

Fig. 6.1.3 Spatial response in dB for the FMVDR beamformer

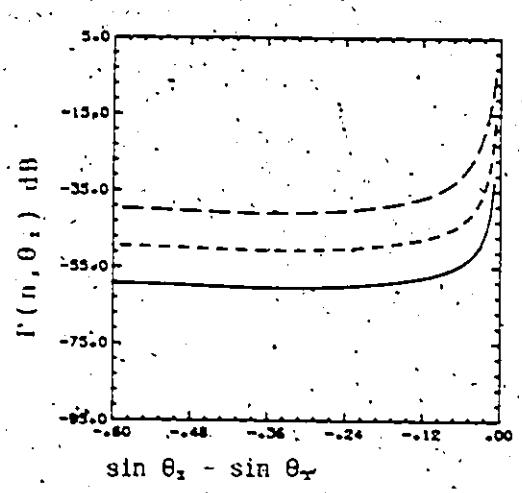

Fig. 6.1.4 20 log $\Gamma(n,\theta_x)$ vs sin-angular separation for MVDR beamformer

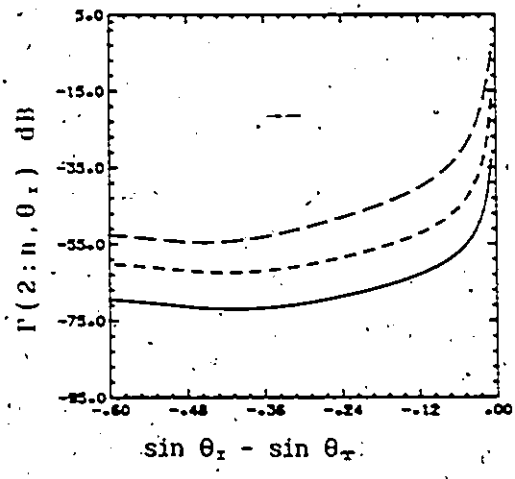

Fig. 6.1.5 20 log $\Gamma(2{:}n,\theta_x)$ vs sin-angular separation for FMVDR beamformer

——————— INR = 40 dB
- - - - - - - - - - INR = 30 dB
— — — — — — INR = 20 dB

Figure of convergence

Learning curves $E[\Gamma(n,\theta_x)]$, and $E[\Gamma(2:n,\theta)]$ for MVDR and FMVDR beamformers respectively are given in Figs. 6.1.6 and 6.1.7. Figure of convergence (τ) for MVDR and FMVDR beamformers are tabulated in Table 6.1.2 for different INR values.

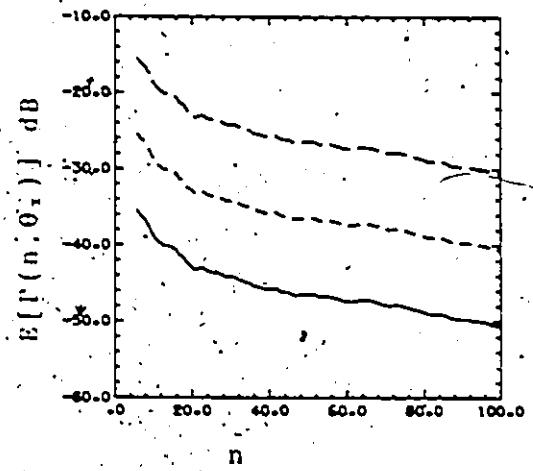

Fig. 6.1.6 20 log $E[\Gamma(n,\theta_x)]$ against n for MVDR beamformer

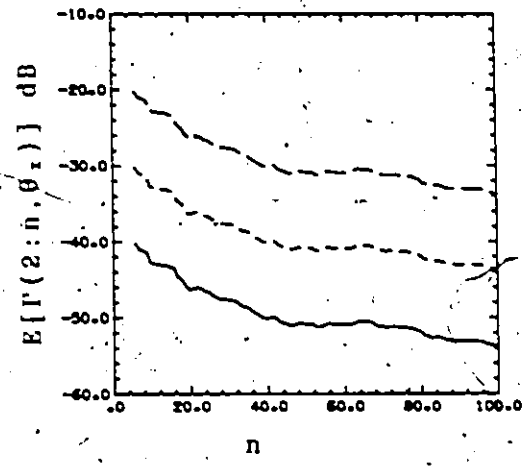

Fig. 6.1.7 20 log $E[\Gamma(2:n,\theta_x)]$ against n for FMVDR beamformer

——————— INR = 40 dB
- - - - - - - - - - INR = 30 dB
— — — — — — INR = 20 dB

Table 6.1.2 Figure of convergence (τ) for MVDR and FMVDR beamformers

INR dB	MVDR	FMVDR
40	14	6
30	14	6
20	14	6

Discussion

Figure of convergence τ is independent of the INR values and the τ for FMVDR, τ_{FMVDR} is less than the τ for MVDR, τ_{MVDR}. Approximate relationship of τ for both MVDR and FMVDR beamformers, obtained through simulation results given in Table 6.1.2, can be written as,

$\tau_{FMVDR} = (3/7)\ \tau_{MVDR}$.

Therefore, FMVDR beamformer produces a specified null amplitude with less number of snapshots than the MVDR beamformer. We could expect this situation since the cross spectral density matrix obtained by flipping is a better estimate to the cross spectral density matrix for finite number of snapshots (chapter 3). In other words, FMVDR beamformer produces stronger nulls at the interference compared to the MVDR beamformer at every snapshot. From Fig. 6.1.6 and 6.1.7, it is also clear that the steady state convergence time (ρ) remains almost unchanged for both MVDR and FMVDR beamformers. The MVDR beamformer appears to be quite robust to the ambiguities of the desired direction compared to the FMVDR beamformer. In the case of both MVDR and FMVDR beamformers, we do not have any control over the strength of null at the interference, and hence they cannot be used to obtain prespecified null at the interference.

By using flipping, we could attain a substantial improvement in the nulling capabilities of the MVDR beamformer. Can we improve the nulls any further? This will be considered in the next section.

6.2 Conditional-Flipped Minimum Variance Distortionless Response (C-FMVDR) Beamformer

6.2.1 Introduction

In any array processor, the structure of the adaptive processor unit is critically dependent on the degree of detailed information about the operational signal and noise environment that is available to the array. As the amount of a priori knowledge concerning signal and noise environment decreases, the adaptive algorithm selected for the adaptive processor becomes critical to a successful design. In general, angle of arrival of the interferences are not known a priori. Even though a priori knowledge of the bearing of the interferences are not available, the bearing information can be obtained adaptively at each snapshot from the input data. This additional information can be used to improve on the performance of the flipped minimum variance distortionless response beamformer.

We introduce the conditional-flipped minimum variance distortionless response (C-FMVDR) beamformer which provides an improvement to the flipped minimum variance distortionless response (FMVDR) beamformer. C-FMVDR beamformer makes use of the estimated bearing of the interferences at n^{th} snapshot in providing improved performance.

In general, the ensemble average of the filter weights at n^{th} snapshot provides improved null at the interference compared to the ensemble average of the filter weights at $n-1^{th}$ snapshot. This fact could also be observed from Figs. (6.1.6) and (6.1.7) given in section 6.1 above. But, for a single realization it is not necessarily true, and the filter weights vector which places improved null at the interference may be somewhere between the first and the n^{th} snapshot. Therefore, in the C-FMVDR beamformer, the filter weights vector that gives rise

to the minimum spatial response at the interference is used as the filter weight at n^{th} snapshot. In addition to the structure for the FMVDR beamformer, the C-FMVDR beamformer requires extra structures for bearing information extraction, and the conditional update of the filter weights vector. Computer simulation results are presented in verifying the performance of the C-FMVDR beamformer.

6.2.2 C-FMVDR Beamformer

We have seen in section 6.1 that the learning curve $E[\Gamma(n,\theta_r)]$ in dB vs n is a monotonically decreasing function. That indicates that the ensemble average of the strength of the null at n^{th} snapshot is stronger than the ensemble average of the null at $n-1^{th}$ snapshot, i.e.

$$|20 \log E[\Gamma(n,\theta)]| > |20 \log E[\Gamma(n-1,\theta)]|; \text{ for all } n. \tag{6.2.1}$$

In general, for a single snapshot this relationship does not necessarily hold. For a single realization the value of n which produces a stronger null may be anywhere between the first and the n^{th} snapshot, which means that the filter weights vector that produces the strongest null may not necessarily be at n^{th} snapshot. This fact can be used in improving the performance of the FMVDR beamformer provided that the a priori knowledge of the direction of arrival of the interference is available. In general, the bearings of the interference is not available in practice. But, one can estimate the bearing of the interference at n^{th} snapshot from the available data by using one of the techniques that we described in chapter 4, which could then be used to improve the performance of the FMVDR beamformer. How we utilize the knowledge of the direction of arrival of the interfering signal to improve the performance of the FMVDR beamformer will be described later. We consider the case where one interfering signal is present in addition to the target signal.

In C-FMVDR beamformer, the filter weights vector that produces the strongest null within n snapshots is used as the filter weights vector at n^{th} snapshot. Let us assume that the strongest null occurs at n_o^{th} snapshot, i.e.

$$\Gamma(n_o,\theta_x) = \inf_{\forall\, n}[\Gamma(n,\theta_x)]$$

Then, the filter weights at n^{th} snapshot $w(n)$ is taken as,

$$\left.\begin{array}{ll} & (6.2.2) \\ w(n) = w(n_o) & (6.2.3) \end{array}\right\}$$

The schematic diagram of the C-FMVDR beamformer is shown in Fig. 6.2.1. The flow chart for the conditional logic used in C-FMVDR beamformer is shown in Fig. 6.2.2.

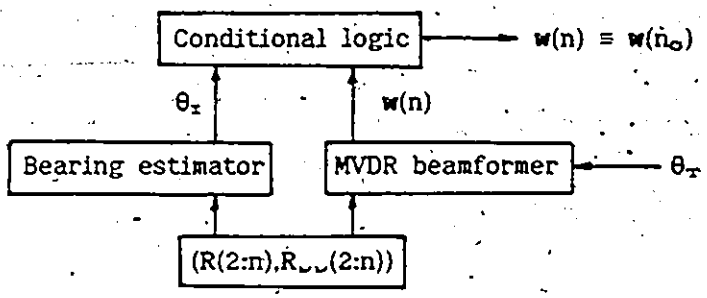

Fig. 6.2:1 Schematic diagram of the C-FMVDR beamformer

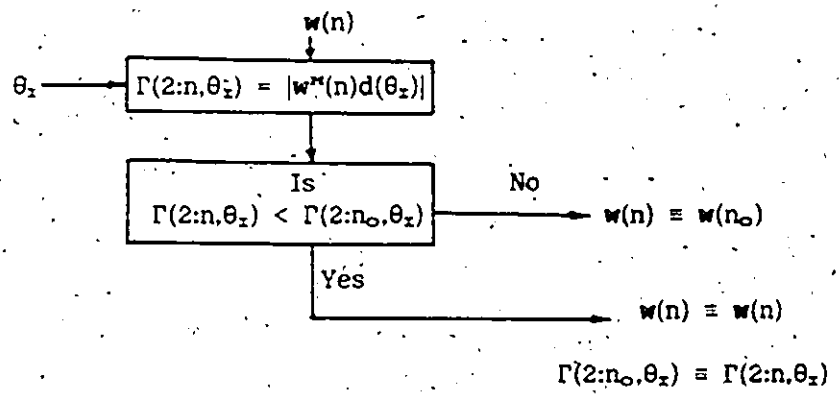

Fig. 6.2.2 Function of the conditional logic

In C-FMVDR beamformer, the spatial response $\Gamma(2{:}n,\theta_x)$ is calculated at each and every snapshot and compared with the $\Gamma(2{:}n_o,\theta_x)$. If $\Gamma(2{:}n,\theta_x)$ is less than $\Gamma(2{:}n_o,\theta_x)$, we replace the quantity $\Gamma(2{:}n_o,\theta_x)$ by $\Gamma(2{:}n,\theta_x)$. At the beginning of the conditional logic, $\Gamma(2{:}n_o,\theta_x)$ is initialized to a very large value so that the conditional logic is adapted very fast to the information obtained from the data. For the case of multiple interferences, the conditional logic has to be chosen according to the user requirement.

6.2.3 Simulation results

We use the same example that was used with the FMVDR beamformer in section 6.1.4. The results are shown after one hundred snapshots. Spatial response of the C-FMVDR beamformer is shown in Fig. 6.2.3 for three different interference to noise ratios, 40, 30 and 20 dB. The signal to noise ratio is assumed to be 20 dB. Strength of the null at the interference of C-FMVDR and FMVDR beamformers are tabulated in Table 6.2.1. Spatial response of the C-FMVDR beamformer against the sin-angular separation of the arrival angles of the signal and interference is shown in Fig. 6.2.4.

Table 6.2.1 Strength of the null in dB for FMVDR and C-FMVDR beamformers

INR dB	FMVDR	C-FMVDR
40	-69.59	-94.61
30	-60.21	-80.04
20	-52.55	-66.00

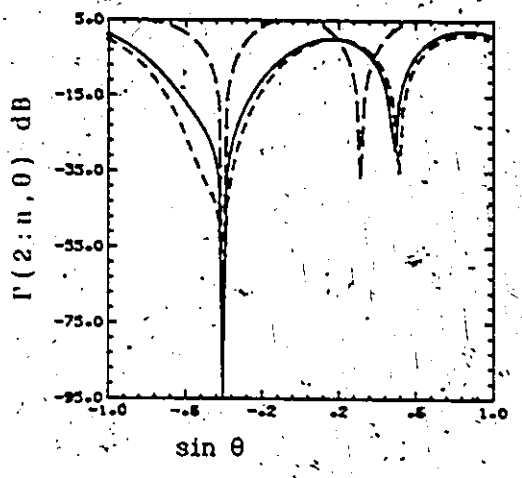

Fig. 6.2.3 Spatial response in dB for C-FMVDR beamformer

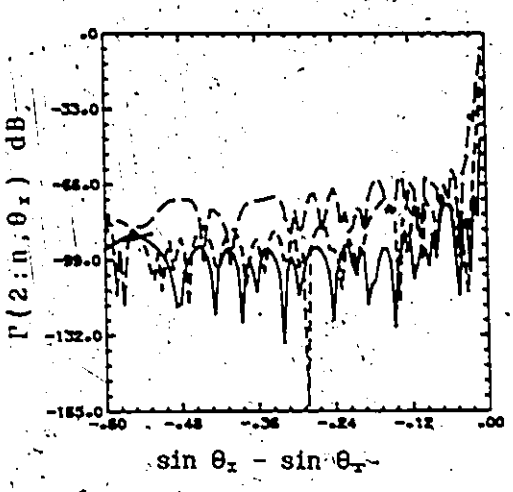

Fig. 6.2.4 20 log $\Gamma(2{:}n,\theta_x)$ vs sin-angular separation for C-FMVDR beamformer

———— INR = 40 dB
- - - - - - - - - - INR = 30 dB
— — — — — — — — INR = 20 dB

Discussion

From Fig. 6.2.3, it is clear that C-FMVDR beamformer provides improved null at the interference compared to the FMVDR beamformer. The improvement of the null amplitude is approximately 20 dB which is quite a significant amount. As we witnessed in the spatial response of the FMVDR beamformer, the additional null appearing in the C-FMVDR spatial response is also an advantage since it can not have any negative influence on the target signal. But, this additional null may create problems by attenuating the desired signal, if the desired direction is ambiguous.

Like any other MVDR type beamformer, the C-FMVDR beamformer also cannot provide prespecified amount of nulls at the interferences. But, it is noteworthy that the C-FMVDR beamformer is able to provide improved nulling

capabilities over any other MVDR type beamformer even when the incoming signals are very close.

6.3 Summary

Flipped minimum variance distortionless response (FMVDR) beamformer is introduced. A structure is proposed for FMVDR beamformer in a form suitable for systolic array implementation. The FMVDR beamformer is the same as the MVDR beamformer except the additional flipping network used in FMVDR beamformer. Performance measures such as the figure of convergence, and the steady state convergence time are defined to facilitate the comparative analysis of the FMVDR beamformer against the MVDR beamformer. FMVDR beamformer provides improved nulling capabilities over the MVDR beamformer. The figure of convergence of the FMVDR beamformer is small compared to that of the MVDR beamformer. The steady state convergence times of MVDR and FMVDR beamformers remain almost the same. Low value of figure of convergence further justifies the superiority of the FMVDR beamformer. One disadvantage of the FMVDR beamformer is that it is not as robust as the MVDR beamformer for the uncertainties in the desired direction. However, the FMVDR beamformer provides quite an attractive alternative to the MVDR beamformer.

Conditional-flipped minimum variance distortionless response (C-FMVDR) beamformer which provides improved performance compared to the FMVDR beamformer is presented. C-FMVDR beamformer provides improved performance by making use of the estimated angle of arrival of the interference in obtaining the filter weights at each snapshot. The estimated bearing of the interference is used in the conditional logic of the C-FMVDR beamformer. Even though we have considered the case of single interference, it can also be used for multiple inter-

ference environment by suitably selecting the conditional logic of the C-FMVDR beamformer. C-FMVDR beamformer is same as the FMVDR beamformer except for the additional conditional logic and the bearing estimation stage used in the C-FMVDR beamformer. Due to its strong nulling capabilities, C-FMVDR beamformer may be an attractive alternative to the FMVDR beamformer.

Beamformers such as MVDR, FMVDR, and C-FMVDR require the a priori knowledge of the desired signal direction. The direction of incoming signal is dependent on the propagation medium and hence the true knowledge of the desired signal direction may not be available in practice. In such situations the performance of the MVDR, FMVDR, and C-FMVDR beamformers will be deteriorated. Especially the additional null appearing in the spatial response of the FMVDR and C-FMVDR beamformers may cause signal attenuation when the direction of the desired signal is ambiguous. As we could observe from the spatial response, MVDR beamformer appears to be somewhat robust to the uncertainties in the desired direction. Further, using MVDR, FMVDR, and C-FMVDR beamformers, a considerable reduction in the interference can only be achieved provided that the strength of the desired signal is smaller than the strength of the interference. Minimum variance distortionless response type beamformers cannot be used to obtain prespecified amount of null at the interference, and they fail to perform successfully when the signal and the interference are comparable in strength.

The MVDR, FMVDR, and C-FMVDR beamformers are generally used under the assumption that the incoming signals are incoherent. If the signals are coherent, these beamformers suppress the desired signal in addition to the interferences leaving noise as the output. When the incoming signals are coherent, MVDR, FMVDR, and C-FMVDR beamformers preceded by the adaptive

spatial data smoothing preprocessing (ASDSP) scheme described in chapter 4, destroys the coherence between the signals leaving the desired signal as the output of the beamformer.

As we have seen, MVDR, FMVDR, and C-FMVDR beamformers can be used in receiving the signals coming from a known direction. None of those beamformers could be used as a listening device, i.e. in receiving the signals coming from unknown directions. This problem remains as a major disadvantage of these beamformers.

CHAPTER 7

ADAPTIVE BEAMFORMING AS A JOINT PROCESS OF BEARING ESTIMATION AND INTERFERENCE CANCELLATION

Preview As we have mentioned earlier, in general, the classical problem of array processing can be divided into three categories, viz.,

1. Locating sources or targets,
2. Reception of a signal coming from a known direction while suppressing all the other interferences,
3. Reception of all the signals coming from distinct but unknown directions separately while suppressing all the other interferences. This can also be considered as a listening device.

We have already presented a solution to the first task, i.e. the locating sources or targets, in Chapter 4. The second and third tasks belong to the adaptive beamforming in array processing. MVDR beamforming techniques that we considered in chapter 6, can provide an approximate solution to the second task, i.e., the reception of a signal coming from a known direction while suppressing all the other interferences. MVDR techniques demand the knowledge of the desired signal direction and in addition, the use of these techniques does not provide exact interference cancellation or the cancellation by a prespecified amount. MVDR beamforming techniques cannot provide a solution to the

third task given above, i.e. the reception of all the signals coming from distinct directions separately while suppressing all the other interferences, and this is because of the fact that the desired direction is unknown.

Most of the techniques available for computing the beamformer filter weights vector, do so by maximizing the overall signal to noise ratio at the system output, where the noise includes the sensor noise and directional interferences. This overall signal to noise ratio maximization provides an optimal solution as long as the sensor noise and the directional interferences are equally detrimental to the system performance. However, there exist situations where jamming signals may be more damaging to the system performance than the sensor noise. This kind of situation may be experienced in war time jamming. The true measure of the system performance is our ability to demodulate the received signals and determine the information being sent and this performance measure is not a function of array SNR alone. Sometimes the structure of the interfering signals is also germane. In these cases, it is necessary to model the interference or jammers and sensor noise or the thermal noise separately.

Here we propose a method named blind reception (BR) beamformer which provides a solution to both the second and third tasks described earlier. BR beamformer treats the sensor noise and interferences separately and places the exact or required amount of null at the interferences. BR beamformer does not demand the knowledge of the desired signal and hence it can be used to receive any signal which is present at the array without being affected by the rest of the

signals considered to be the interferences. BR beamformer is specially suitable for removing the interferences from point-to-point communication system. MVDR type beamformers can be considered as a special case of BR beamformer. Computer simulation results are presented.

If the estimates of the bearings are biased, the performance of the BR beamformer will be drastically deteriorated. This is mainly due to the fact that it contains very sharp nulls. Therefore, the performance of the BR beamformer will be highly dependent on the accuracy of the bearing estimates.

We introduce robust blind reception (R-BR) beamformer in overcoming the deterioration of the BR beamformer, to some extent, due to the bias in the bearing estimates. Structure of the R-BR beamformer is almost the same as the BR beamformer. R-BR beamformer is more robust to the bias in the bearing estimates than BR beamformer. In R-BR beamformer, we keep the gradient of the spatial response at the interference to be equal to zero while maintaining the required amount of null at the interference. The gradient constraint we impose at the interference will make the R-BR beamformer somewhat robust to the bias in the bearing estimates. Computer simulation results are presented.

7.1 Blind reception (BR) beamformer

7.1.1 Introduction

MVDR type beamforming methods are not capable of receiving the signals coming from distinct and unknown directions separately while suppressing the rest of the interfering signals. To achieve that, we introduce a super

precision adaptive array processing technique. We propose this technique based on the joint bearing estimation and interference cancellation and it is capable of providing an exact cancellation of the interferences or cancellation by a prespecified amount. It directly operates on the input data adaptively and provides optimal solution at each snapshot. The proposed beamformer can receive signals coming from distinct and unknown directions separately and hence it is named as the blind reception (BR) beamformer. Unlike MVDR, FMVDR, and C-FMVDR beamformers, BR beamformer is robust to the uncertainties in the desired direction and also to the strength of the interferences. MVDR type beamformers appear to be a special case of the BR beamformer and hence the BR beamformer can also be considered as the generalized minimum variance distortionless response (GMVDR) beamformer. Computer simulation results are presented.

7.1.2 BR beamformer and its systolic array structure

As we did in the FMVDR beamformer, the processing of the blind reception beamformer will be done in the frequency domain for each frequency component of the incoming signals. Then the inverse discrete Fourier transform is performed at the output of all the beamformers in recovering the signal of interest.

In BR beamformer, we perform the operations in two stages for each snapshot:

1. Estimate the bearings of the incoming signals by using the upper triangular matrix pencil $(R^{u}(n), R_{\ell}^{u}(n))$.
2. If the desired signal is known approximately, the estimated bearing which is closest to the approximately known signal bearing can be taken as the

desired signal. If no a priori knowledge of the desired signal direction is available several beamformers have to be designed to receive the signals coming from each direction separately. We then use the minimum variance distortionless response (MVDR) beamformer with multiple constraint imposed so that the required amount of nulls could be placed at the bearings of the interferences while maintaining the desired signal unaltered. Since multiple constraints are imposed on the MVDR beamformer, it is named as the multiple constraint minimum variance distortionless response (MCMVDR) beamformer.

We consider the case where there are K number of signals at the array. The schematic diagram of the BR beamformer is shown in Fig. 7.1.1. Once the number of signals and their bearings are obtained, the next step in the BR beamformer is to find the filter weights in receiving a selected signal while placing the required amount of nulls at the bearings of the interferences. This can be achieved by applying the minimum variance distortionless response method with various constraints imposed as follows:

Let the filter weights that we have to determine after n^{th} snapshot be $\mathbf{w}^{*}(n)$. In determining the vector $\mathbf{w}^{*}(n)$, we make use of all the data available up to n^{th} snapshot. If we pass all the data starting from first snapshot through the filter $\mathbf{w}^{*}(n)$, the output vector $e_n(n)$ we obtain, can be written as,

$$e_n^{*}(n) = U^{H}(n)w(n) \qquad (7.1.1)$$

where $e_n(n) \in C^{n\times 1}$, $U(n) \in C^{M\times n}$ and $\mathbf{w}(n) \in C^{M\times 1}$.

By applying the Jacobi-Givens rotation $Q^{H}(n)$ to eqn. (7.1.1), we obtain,

$$Q^{H}(n)e_n^{*}(n) = Q^{H}(n)U^{H}(n)w(n) \qquad (7.1.2)$$

where, Q(n) is a unitary matrix and $Q^{H}(n) \in C^{n\times n}$.

We select Q(n) such that,

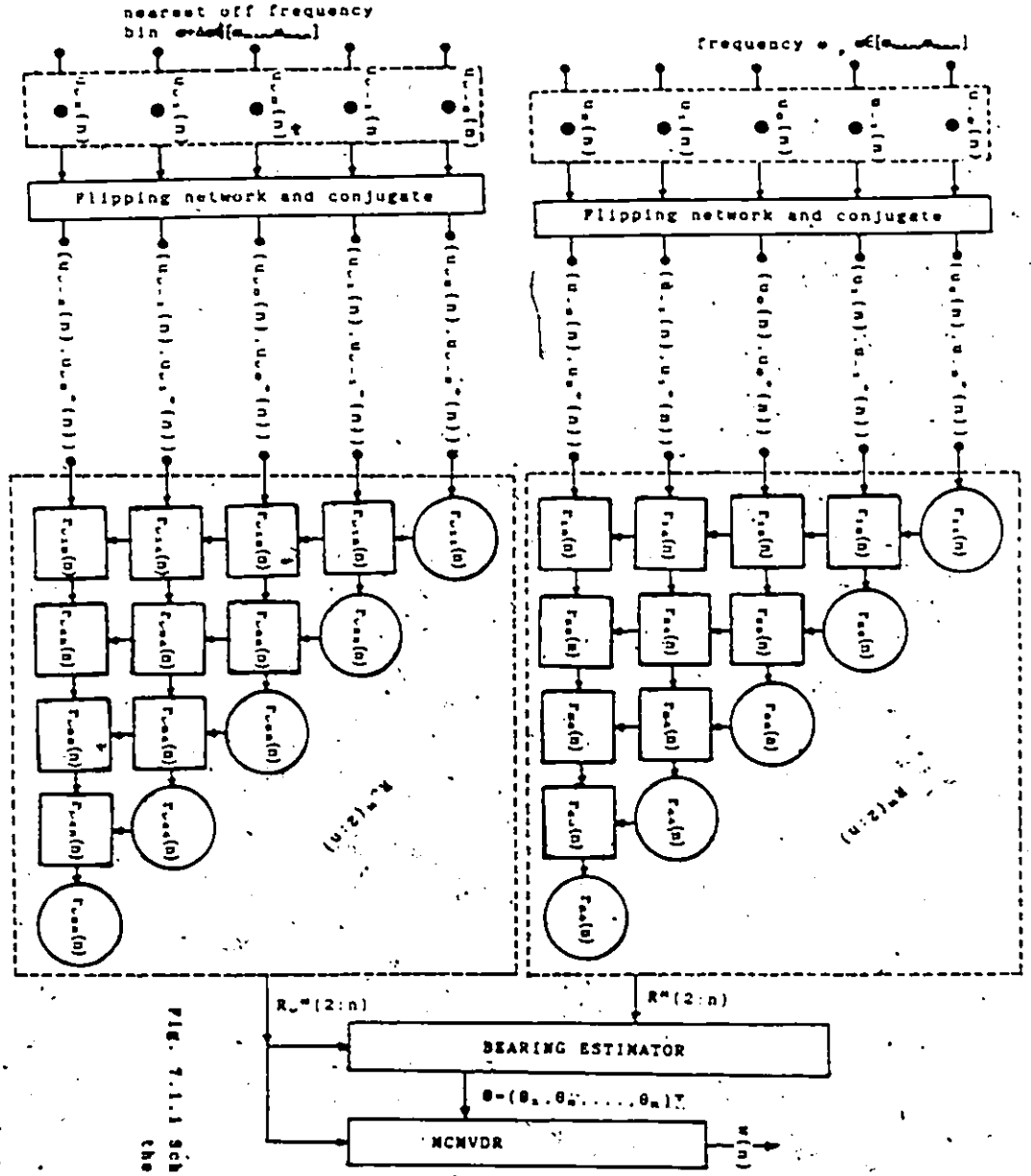

Fig. 7.1.1 Schematic Diagram for the BR Beamformer

$$Q^H(n)U^H(n) = \begin{matrix} R^H(n) \\ \hline 0 \end{matrix} \qquad (7.1.3)$$

where, $R^H(n)$ is an upper triangular matrix and $R(n) \in C^{M\times M}$.

The square of the Euclidian norm of the vector $e_n(n)$ is given by,

$$|e_n(n)|^2 = e_n^H(n)e_n(n) \qquad (7.1.4)$$

Using the property that the unitary transformations are norm preserving, we can write $|e_n(n)|^2$ by using eqn. (7.1.3) as follows:

$$|e_n(n)|^2 = w^H(n)R(n)R^H(n)w(n) \qquad (7.1.5)$$

Now, the optimal filter weight $w_{opt}(n)$ can be obtained by minimizing the square of the Euclidian norm of the vector $e_n(n)$ while maintaining the desired signal unchanged, i.e.

$$\text{minimize}_{w(n)} |e_n(n)|^2$$

subject to the constraint $D^H(\theta)w(n) = c$ (7.1.6)

where, $D(\theta) = [d(\theta_1),d(\theta_2),....,d(\theta_K)]$ (7.1.7)

with θ_k, $k = 1,2,....,K$ being the bearings of the incoming signals, and

$c = (1,\delta,\delta,...\delta)^T$ (7.1.8)

with δ being a specified small quantity, $D(\theta) \in C^{M\times K}$, $c \in C^{M\times 1}$.

Eqn. (7.1.6) specifies the constraints such that the signal from direction θ_1 is unaltered whereas the signals from other directions θ_k, $k = 2,3,....,K$ are suitably suppressed to a small value δ. The extension of the constraint equation to suppress other signals while maintaining only the k^{th} desired signal unaltered is an obvious modification of the constant vector c in eqn. (7.1.8).

The minimization can now be accomplished by using the method of Lagrange multipliers. We define a vector of Lagrange multipliers as,

$$\pi = (\pi_1,\pi_2,....,\pi_K)^T. \qquad (7.1.9)$$

Then the optimal filter weight vector $w_{opt}(n)$ can be obtained by

minimizing the quantity F,

$$F=w^H(n)R(n)R^H(n)w(n)+(w^H(n)D(\theta)-c^T)\lambda+\{(w^H(n)D(\theta)-c^T)\lambda\}^H \quad (7.1.10)$$

A necessary condition for the optimal solution is that the gradient of F with respect to $w(n)$ be zero. Using this,

$$R(n)R^H(n)w_{opt}(n) = -D(\theta)\,\lambda \quad (7.1.11)$$

which yields,

$$w_{opt}(n) = -D_a(\theta)\,\lambda \quad (7.1.12)$$

where, $D_a(\theta) = [b(\theta_1),b(\theta_2),\ldots,b(\theta_K)]$ (7.1.13)

with $b(\theta_k)$ satisfying the relationships,

$$R^H(n)b(\theta_k) = a(\theta_k) \quad (7.1.14)$$

$$R(n)a(\theta_k) = d(\theta_k) \quad (7.1.15)$$

The vector λ can be obtained by substituting eqn. (7.1.12) into the constraint eqn. (7.1.6) so that,

$$-D_1^H(\theta)D_1(\theta)\,\lambda = c \quad (7.1.16)$$

where, $D_1(\theta) \in C^{K\times K}$, is given by,

$$D_1(\theta) = [a_1(\theta),a_2(\theta),\ldots,a_K(\theta)] \quad (7.1.17)$$

with $a(\theta_k)$ satisfying the eqn. (7.1.15).

Multiplying both sides of eqn. (7.1.16) by Jacobi-Givens matrix $Q \in C^{K\times K}$, we obtain,

$$QD_1^H(\theta)D_1(\theta)\,\lambda = -Qc \quad (7.1.18)$$

$$\text{i.e. } R\,\lambda = -Qc \quad (7.1.19)$$

$$= c_a$$

where, $R = QD_1^H(\theta)D_1(\theta)$, (7.1.20)

$R \in C^{K\times K}$, $c_a = -Qc$, and $c_a \in C^{K\times 1}$.

We select Q such that R is an upper triangular matrix. Then the vector λ can be obtain by using the backward substitution on eqn. (7.1.19) (Appendix

2d). The solution to the eqn. (7.1.18) can be obtained by using the QR decomposition based systolic array structure [Gentleman and Kung (1981)] used in solving the least squares problem. The basic nature of the array for K=3 is given in Fig. (7.1.2).

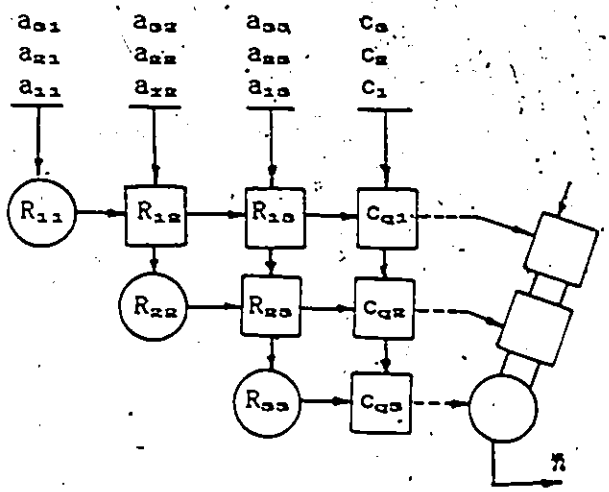

Fig. 7.1.2 Systolic array structure for the least squares solution

$$A\,\underline{h} = c$$

where $A = D_1^H(\theta)D_1(\theta)$

The MCMVDR block shown in the fig. 7.1.1 contains a triangular array and several linear arrays in solving the eqns. 7.1.12 and 7.1.19 while any of the bearing estimation techniques described in chapters 4 and 5 can be used in the bearing estimator block.

Once the filter weights vector is obtained, the filtered output of the BR beamformer at n^{th} snapshot, e(n) is given by,

$$e(n) = \underline{w}^H(n)u(n). \qquad (7.1.21)$$

Then the outputs of all the BR beamformers that was designed for each frequency component of the signal frequency band are collected and inverse

discrete Fourier transform is performed to reconstruct the signal. Systolic array structures required for implementing the BR beamformer can be found in Kung (1986) and can be listed as follows:

1. FFT and IFT
2. Matrix triangularization
3. Forward and backward substitution
4. Matrix and vector products
5. Generalized singularvalue singularvector decomposition

By selecting $\delta = 0$, one can cancel the interferences exactly. The value of δ can be chosen according to the interference rejection required. In many cases, the cancellation of interferences and sensor noise reduction can be compromised by selecting δ such that the system performance is optimised. BR beamformer is capable of removing the interferences according to the user specification. Several beamformers with suitable constraint vectors have to be designed if it is desired that all the incoming signals be received separately. In the development of the BR beamformer we have assumed that the incoming signals are uncorrelated. Under the coherent signal environment, BR beamformer preceded by adaptive spatial data smoothing preprocessing (ASDSP) scheme described in chapter 4 can be used.

7.1.3 Simulation results

For the purpose of simulation we use the same example we used in FMVDR beamformer. The spatial response of the BR beamformer is shown in Fig 7.1.3. We consider the case $\delta = 0$, i.e. the exact cancellation of the interference. Spatial response is shown for interference to noise ratio (INR), 40, 30, and 20 dB.

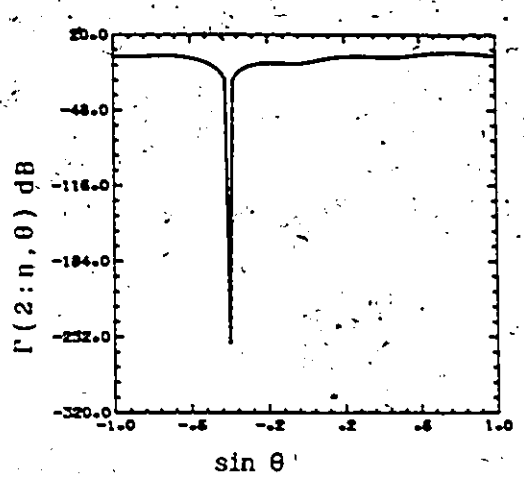

Fig. 7.1.3 Spatial response of the BR beamformer in dB

———— INR = 40 dB
---------- INR = 30 dB
-·-·-·-·- INR = 20 dB

7.1.4 Discussion

BR beamformer provides very sharp and strong null at the interference, and maintains almost flat response in the rest of the directions. The response at the direction from where the signal of interest comes is such that the signal of interest passes unaltered through the beamformer. The performance of the BR beamformer is not dependent on the interference to noise ratio and it is such that even a small amount of bias in the bearing estimate may cause a drastic reduction of the null at the interference. Therefore, the performance of the BR beamformer is highly dependent on the accuracy of the bearing estimate. Real time processing can be made possible by designing the beamformer to perform a cycle of operation within the time interval used to obtain a single snapshot. The BR beamformer and the concept of beamforming as a joint bearing estimation and interference cancellation will provide a new direction towards the super precision adaptive array processing.

7.2 Robust Blind Reception (RBR) Beamformer

7.2.1 Introduction

The blind reception beamformer produces very sharp nulls at the interferences. Owing to the very sharp nulls, any bias in the bearing estimation stage may drastically deteriorate the performance of the blind reception beamformer. To overcome this situation, we will introduce the robust blind reception (RBR) beamformer.

In the robust blind reception beamformer, we impose an additional constraint at each interference to avoid sharp growth of the nulls at the interferences. We constrain the gradient of the beamformer response at the interferences with respect to the bearing angle to be zero, so that the growth of the nulls may not be rapid, producing considerable interference cancellation in the neighborhood of the bearing of the interferences. Therefore, the blind reception beamformer will be rather robust to a fairly small bias in the bearing estimates. The basic structure of the robust blind reception beamformer has absolutely no difference from the blind reception beamformer. Computer simulation results are presented.

7.2.2 RBR Beamformer

The derivation and implementation of the robust blind reception beamformer is very similar to that of the blind reception beamformer. In robust blind reception beamformer we use a new constraint equation in the place of the constraint equation of the blind reception beamformer.

We have seen that the constraint equation of the blind reception beamformer is given by,

$$D^H(\theta)w(n) = c \qquad (7.2.1)$$

where $c = (1,\delta,\delta,\ldots,\delta)^T$ (7.2.2)

In addition to the constraint used to place prespecified strength of nulls at the interferences, we now include the gradient constraint also in constructing the constraint equation.

Since, the spatial response of the BR beamformer $w^H(n)d(\theta)$ is a continuous function of θ, the necessary condition for it to be a minimum is the gradient with respect to θ,

$$\frac{d}{d\theta}\,[w^H(n)d(\theta)] = 0, \qquad (7.2.3)$$

i.e. $w^H(n)d'(\theta) = 0$ (7.2.4)

where, $d'(\theta) = \dfrac{d}{d\theta}\,(d(\theta))$.

The m^{th} element, $d_m'(\theta)$ of $d'(\theta)$ is given by,

$$d_m'(\theta) = j\,\frac{2\pi m\ell}{\lambda}\,\cos\theta.\, d_m(\theta) \qquad (7.2.5)$$

where, $d_m(\theta)$ is the m^{th} element of the direction vector $d(\theta)$, and

$$d_m(\theta) = \exp\left(j\,\frac{2\pi m\ell}{\lambda}\,\sin\theta\right). \qquad (7.2.6)$$

Let the angles of arrival of K signals be given by the vector θ, $\theta=(\theta_1,\theta_2,\ldots,\theta_K)^T$ and the signal of interest is θ_1, then the angles θ_k, $k = 2,3,\ldots,K$ represent the bearings of the interferences.

Now by including the gradient constraint into the constraint eqn. (7.2.1), new constraint equation can be written as,

$$D_{new}^H(\theta)w(n) = c_{new} \qquad (7.2.7)$$

where,

$D_{new}(\theta) = [d(\theta_1), d(\theta_2), d'(\theta_2), d(\theta_3), d'(\theta_3), \ldots, d(\theta_K), d'(\theta_K)]$

and $c_{new} = (1, \delta, 0, \delta, 0, \delta, 0, \ldots, \delta, 0)$, (7.2.8)

$D_{new}(\theta) \in C^{N \times (2K-1)}$

Therefore, in robust blind reception beamformer we perform the optimization,

$$\underset{w(n)}{\text{minimize}} \; \| Q^H(2:n) e_n^*(2:n) \|^2 \qquad (7.2.9)$$

subject to the constraint, $D_{new}^H(\theta) w(n) = c_{new}$ (7.2.10)

The terms used here have the same meanings as in the case of the blind reception beamformer. The solution to the above minimization problem is very similar to the minimization procedure used in the blind reception beamformer. Optimal filter weight vector $w(n)$ for the robust blind reception beamformer can be obtained by substituting the $D_{new}(\theta)$ and c_{new} in the places of $D(\theta)$ and c in the blind reception beamformer respectively.

In order to compare the performance of the RBR beamformer against the BR beamformer we define the following term:

Definition 7.2.1

'ε-robust factor (η_ε) is define as,

$\eta_\varepsilon = -20 \log \Gamma(n, \phi_I + \varepsilon)$

where, $\phi_I = \pi \sin \theta_I$, θ_I is the angle of interference, and ε is a small quantity.

Therefore, the larger is the ε-robust factor, the more robust is the beamformer with respect to the bias in the bearing estimates. Since the spatial response is considered in dB, the η_ε will also be given in dB.

7.2.3 Simulation results

We use here the same example that was used with the FMVDR beam-

former and the BR beamformer. The spatial response of the RBR beamformer is shown in Fig. 7.2.1. As we did in BR beamformer, here also we consider the exact cantellation of the interferences, i.e. $\delta = 0$. Spatial response is shown for interference to noise ratios 40, 30, and 20 dB.

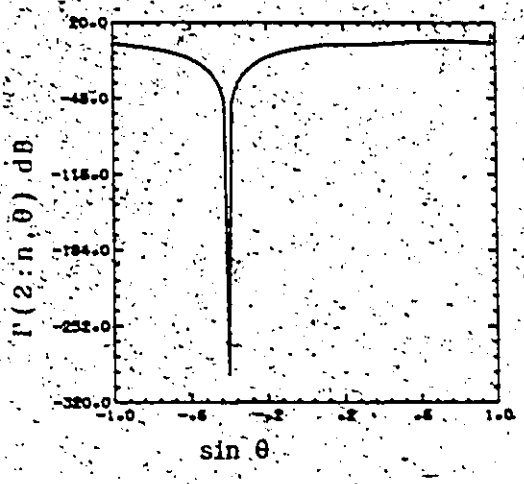

Fig: 7.2.1 Spatial response of the RBR beamformer in dB

——————— INR = 40 dB
- - - - - - - - - - INR = 30 dB
—— — — — — — INR = 20 dB

The null amplitude at the interference is tabulated for both BR and RBR beamformers in Table 7.2.1. The ε-robust factor (η_ε) is also shown in Table 7.2.2 for both BR and RBR beamformers for $\varepsilon = 0.005\pi$.

Table 7.2.1 Performance of the BR and RBR beamformers with respect to the strength of the null in dB

INR dB	BR beamformer	RBR beamformer
40	-268	-290
30	-268	-290
20	-268	-290

Table 7.2.2 ϵ-robust factor (η_ϵ) for BR and RBR beamformers

Beamformer	η_ϵ in dB
BR	-57
RBR	-92

7.2.4 Discussion

It is clear from the above results that the BR beamformer provides improved null at the interferences compared to the BR beamformer within the computer limitations. The ϵ-robust factor of the RBR beamformer is considerably larger than the ϵ-robust factor of the BR beamformer and that is due to the strong and wider null in the RBR beamformer. Therefore, RBR beamformer is more robust to the bias in the bearing estimates. The structures of the BR beamformer and RBR beamformer are the same. In practice, small bias in the bearing estimates is unavoidable since we have only a finite number of snapshots. Therefore, RBR beamformer may provide an attractive alternative to the BR beamformer in overcoming the deterioration of the performance of the BR beamformer due to the bias in the bearing estimates.

7.3 Summary

We have presented a super precision blind reception beamformer and a modular mathematical structure suitable for VLSI implementation. BR beamformer is capable of cancelling the interferences exactly or to the required amount and it recovers the desired signal without altering them. The performance of the BR beamformer does not demand the knowledge of the desired signal and hence it can be used to receive the unknown signal separately (listening device). The bias in the bearing estimates reduce the performance of the blind reception beam-

former drastically. In overcoming this problem, we have introduced the robust blind-reception beamformer. Robust blind reception beamformer is capable of producing fairly strong interference cancellation provided the bias in the bearing estimates are small. Robust blind reception beamformer also fails to perform successfully when the bias in the bearing estimates are large. Performance of both the BR and RBR beamformers depend on the accuracy of the bearing estimates.

CHAPTER 8

A DIRECTION FOR FURTHER RESEARCH (RESTART TO THE ARRAY PROCESSING)

Preview A restart to the array processing problem is initiated. Array processing techniques achieving asymptotically ideal performance are rederived. This is achieved by constructing inphase cross-cross spectral density matrix or interarray cross spectral density matrix and using it in the place of the cross spectral density matrix, which is used in most of the array processing techniques. Inphase cross-cross spectral density matrix is asymptotically independent of the sensor noise and hence of the spatial correlation of the sensor noise. The noise free nature of the inphase cross-cross spectral density matrix is the key to the superior performance of the redefined array processing techniques. Even though it is given in the context of array processing the basic idea can be extended to any digital processing technique which deals with the correlation matrix. In such cases, instead of taking the autocorrelation matrix of one realization, we can take the cross correlation between two independent realizations. The cross correlation between two realizations will be asymptotically same as the noise free autocorrelation matrix. As far as time series concern, in the case where two independent realizations have two independent signal components, this method may breakdown.

8.1 Foundation of the Restart

8.1.1 Introduction

In most of the array processing techniques used to date, the required information is extracted by using the cross spectral density matrix $\Phi(n)$ given by,

$$\Phi(n) = D(\theta)\Phi_{ss}(n)D^{*}(\theta) + \Phi_{vv}(n) \tag{8.1.1}$$

where $\Phi_{ss}(n)$ is the signal only cross spectral density matrix; $\Phi_{vv}(n)$ is the noise only cross spectral density matrix and $D(\theta)$ is the direction vectors matrix.

In general, the noise only cross spectral density matrix $\Phi_{vv}(n)$ is unknown. The use of the matrix $\Phi(n)$ in array processing provides degraded performance in the presence of nonzero noise only cross spectral density matrix $\Phi_{vv}(n)$.

Here we consider beamforming as well as spectrum estimation in array processing. At infinite signal to noise ratio, beamforming techniques such as minimum variance distortionless response beamformers provide perfect nulling capabilities while the high resolution and super resolution bearing estimation techniques such as maximum likelihood, linear prediction, and multiple signal classification (MUSIC) methods perform equally with no resolution limits.

It is time to rethink the use of the cross spectral density matrix in array processing and digital signal processing in general. If we are able to construct a matrix that contains the same information as the cross spectral density matrix without the influence of the noise only cross spectral density matrix $\Phi_{vv}(n)$, it will be the perfect solution to the problems in array processing. It will also be an ideal solution to digital signal processing problems, in general. How could one achieve that?

Here we propose the use of inphase twin array system and generate

what we call inphase cross-cross spectral density matrix $\Phi^{(1,2)}(n)$ between the array 1 and array 2. It is shown that the matrix $\Phi^{(1,2)}(n)$ is asymptotically unaffected by noise. Beamforming techniques such as minimum-variance distortionless response beamformers and bearing estimation techniques such as maximum likelihood, linear prediction and multiple signal classification (MUSIC) are redefined by making use of the inphase cross-cross spectral density matrix $\Phi^{(1,2)}(n)$.

8.1.2 Inphase Cross-Cross Spectral Density Matrix

The twin array system used is shown in Fig. 8. Both the array 1 and array 2 are the same in every aspect. Elements spacing of the array is ℓ. Array 1 and array 2 are in the plane of y-z and they are separated by the distance ℓ_{12} along the y axis. It is assumed that the wave front is reaching the array parallel to the y axis and hence there is no phase difference between the signals received by the m^{th} element of the array 1 and array 2. In other words, the wave front reaches the m^{th} element of the array 1 and array 2 at the same time.

Let the output of the arrays be divided into blocks of L data samples. By taking the Fourier transform of the n^{th} data block and choosing the frequency component ω and noting that by u(n), we obtain the output of the array 1 at n^{th} snapshot $u^{(1)}(n)$,

$$u^{(1)}(n) = (u_1^{(1)}(n), u_2^{(1)}(n), \ldots, u_M^{(1)}(n))^T \qquad (8.1.2)$$

where $[.]^{(1)}$ denotes the measurements related to the array 1, M is the number of elements in the array, and $[.]^T$ denotes the transpose of [.].

If the incoming signals are wideband, we have to process each frequency component within the band separately.

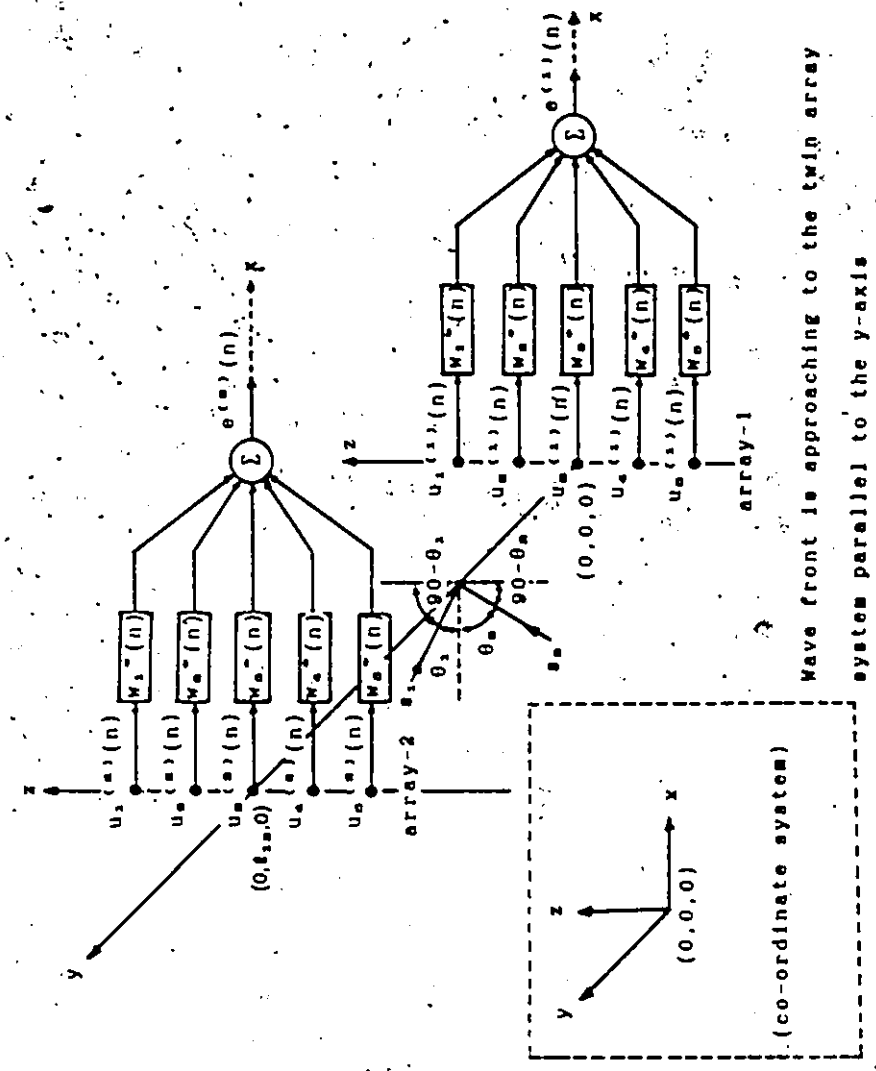

Fig. 6 Twin Array System

The output of the i^{th} array, i=1,2, of frequency ω at n^{th} snapshot $u^{(i)}(n)$ can be expressed as,

$$u^{(i)}(n) = D(\theta)s(n) + \nu^{(i)}(n) \qquad (8.1.3)$$

where, $D(\theta) = [d(\theta_1),d(\theta_2),....,d(\theta_K)]$, $D(\theta) \in C^{M\times K}$, $d(\theta_k) = M^{-1/2}\,(1,z_k,z_k^2,....,z_k^{M-1})^T$, K is the number of signals, $\nu^{(i)}(n)$ is the sensor noise vector of array i, and it is given by,

$\nu^{(i)}(n) = (\nu_1^{(i)}(n),\nu_2^{(i)}(n),....,\nu_M^{(i)}(n))^T$,

s(n) is the signal vector and $s(n) = (s_1(n),s_2(n),....,s_K(n))^T$.

By collecting the information from the previous snapshots, we can form the data matrix $U^{(i)}(n)$ of the i^{th} array at n^{th} snapshot so that,

$$U^{(i)}(n) = [u^{(i)}(1),u^{(i)}(2),....,u^{(i)}(n)]$$
$$= D(\theta)S(n) + N^{(i)}(n) \qquad (8.1.4)$$

where, $D(\theta)$ is a Vandermonde matrix determined by, θ_i, i=1,2,....,K,

$S(n) = [s(1),s(2),....,s(n)]$,

$N^{(i)}(n) = [\nu(1),\nu(2),....,\nu(n)]$, $U^{(i)}(n) \in C^{M\times n}$.

Substituting i=1 and i=2, we obtain the data matrices $U^{(1)}(n)$, and $U^{(2)}(n)$ for the array 1 and array 2 respectively as follows:

For the array 1,

$$u^{(1)}(n) = D(\theta)s(n) + \nu^{(1)}(n),$$
$$U^{(1)}(n) = D(\theta)S(n) + N^{(1)}(n) \qquad (8.1.5)$$

For the array 2,

$$u^{(2)}(n) = D(\theta)s(n) + \nu^{(2)}(n),$$
$$U^{(2)}(n) = D(\theta)S(n) + N^{(2)}(n) \qquad (8.1.6)$$

Now, we obtain the inphase cross-cross spectral density matrix $\Phi^{(1,2)}(n)$ between the array 1 and array 2 such that,

$$\Phi^{(1,2)}(n) = 0.5\{U^{(1)}(n)U^{(2)H}(n)+[U^{(1)}(n)U^{(2)H}(n)]^H\}$$

$$= 0.5\{[D(\theta)S(n)+N^{(1)}(n)][D(\theta)S(n)+N^{(2)}(n)]^H \qquad (8.1.7)$$

$$+\{[D(\theta)S(n)+N^{(1)}(n)][D(\theta)S(n)+N^{(2)}(n)]^H\}^H\}$$

$$= 0.5\{D(\theta)S(n)S^H(n)D^H(\theta)+N^{(1)}(n)S^H(n)D^H(\theta)$$

$$+\{D(\theta)S(n)S^H(n)D^H(\theta)+N^{(1)}(n)S^H(n)D^H(\theta)\}^H$$

$$+D(\theta)S(n)N^{(2)H}(n)+N^{(1)}(n)N^{(2)H}(n)$$

$$+\{D(\theta)S(n)N^{(2)H}(n)+N^{(1)}(n)N^{(2)H}(n)\}^H \}$$

i.e., $\Phi^{(1,2)}(n) = D(\theta)\Phi_{ss}(n)D^H(\theta) + 0.5\{\Phi_{(\nu 1,s)}(n)D^H(\theta)+\Phi_{(\nu 2,s)}(n)D^H(\theta)\}$ (8.1.8)

$$+0.5\{[\Phi_{(\nu 2,s)}(n)D^H(\theta)]^H+[\Phi_{(\nu 1,s)}(n)D^H(\theta)]^H\}$$

$$+0.5\{\Phi_{(\nu 1,\nu 2)}(n)+\Phi_{(\nu 2,\nu 1)}(n)\}$$

$$=D(\theta)\Phi_{ss}(n)D^H(\theta)+\Phi_{(\nu,s)}(n)D^H(\theta)+[\Phi_{(\nu,s)}(n)D^H(\theta)]^H$$

$$+\Phi_{(\nu,\nu)}{}^{(1,2)}(n) \qquad (8.1.9)$$

where, the superscript H denotes the Hermitian transpose.

For sufficiently large number of snapshots, we make the following assumptions:

1. The incoming signals are uncorrelated,

$$\lim_{n\to\infty} \Phi_{ss}(n) = \Phi_{ss}, \quad \text{(full rank)} \qquad (8.1.10)$$

The matrix Φ_{ss} may not be full rank in the presence of the multipath environment or smart jammers. In that case the adaptive spatial data smoothing preprocessing scheme has to be used to recover the rank.

2. Sensor noise of the individual arrays may be coherent. But the noise between the arrays are incoherent. i.e., $\nu^{(1)}(n)$ and $\nu^{(2)}(n)$ are independent and hence,

$$\lim_{n\to\infty} \Phi_{(\nu,\nu)}{}^{(1,2)}(n) = 0 \qquad (8.1.11)$$

where 0 is a null matrix with appropriate dimensions.

We can force this property to be held by selecting the distance ℓ between the array 1 and array 2 sufficiently large while maintaining the coherencies between the arrays.

3. It is also assumed that the signal and noise are uncorrelated, i.e.,

$$\lim_{n\to\infty} \Phi_{(\cdot,\cdot)}(n) = 0 \tag{8.1.12}$$

This assumption is a reasonable one since there is no reasons to assume that the signals and noise are correlated.

With the above assumptions, the inphase cross-cross spectral density matrix $\Phi^{(1,2)}$ can be obtained from eqn. (8.1.8), in the form,

$$\Phi^{(1,2)} = \lim_{n\to\infty} \Phi^{(1,2)}(n) \tag{8.1.13}$$

$$= \lim_{n\to\infty} D(\theta)\Phi_{ss}(n)D^{H}(\theta)$$

$$= D(\theta)\Phi_{ss}D(\theta) \tag{8.1.14}$$

8.1.3 Properties of the Inphase Cross-Cross Spectral Density Matrix

1. $\Phi^{(1,2)}$ is Hermitian,

i.e., $\Phi^{(1,2)H} = \Phi^{(1,2)}$ (8.1.15)

This is an obvious result obtained from eqn. (8.1.14).

2. $\Phi^{(1,2)}$ is completely independent of the sensor noise, and it depends only on the parameters of the signal environments.

Now let us consider the rank of the matrix $\Phi^{(1,2)}$. Since the signals are approaching the arrays from distinct directions, the Vandermonde matrix $D(\theta)$ is the rank of K. Therefore, the rank of $\Phi^{(1,2)}$ is determined by the rank of the matrix Φ_{ss}. But the incoming signals are assumed to be incoherent and hence the rank of the matrix Φ_{ss} is full rank and equal to K. Therefore, the rank of the matrix $\Phi^{(1,2)}$ is equal to the number of incoming signals.

The cross spectral density matrix for the array 1 at n^{th} snapshot can be written as,

$$\Phi^{(1,1)}(n) = D(\theta)\Phi_{ss}(n)D^{H}(\theta) + \Phi_{(\nu,\nu)}{}^{(1,1)}(n) \tag{8.1.16}$$

Limiting value of the cross spectral density matrix $\Phi^{(1,1)}(n)$ is given by,

$$\begin{aligned}\Phi^{(1,1)} &= \lim_{n\to\infty} \Phi^{(1,1)}(n) \\ &= D(\theta)\Phi_{ss}D^{H}(\theta) + \Phi_{(\nu,\nu)}{}^{(1,1)} \\ &= \Phi^{(1,2)} + \Phi_{(\nu,\nu)}{}^{(1,1)}\end{aligned} \tag{8.1.17}$$

Now, let us consider the case where signal to noise ratio (SNR) is infinite. Then we obtain,

$$\lim_{SNR\to\infty} \Phi^{(1,1)} = \Phi^{(1,2)} \tag{8.1.18}$$

Hence, it is clear that the use of the inphase cross-cross spectral density matrix is equivalent to the use of the cross spectral density matrix at infinite signal to noise ratio. In other words, we can briefly state.,

$$\left.\begin{array}{l}\text{Performance of the spectrum} \\ \text{estimation techniques using} \\ \Phi^{(1,2)} \text{ in the place of } \Phi^{(1,1)}\end{array}\right\} = \lim_{SNR\to\infty} \left\{\begin{array}{l}\text{Performance of the} \\ \text{spectrum estimation} \\ \text{techniques with} \\ \Phi^{(1,1)}\end{array}\right.$$

More insight into the inphase cross-cross spectral density matrix or the operator $\Phi^{(1,2)}$ can be obtained by using geometric analysis. The idea of geometric analysis is to break the operator down into a number of parts in such a way that the operation of $\Phi^{(1,2)}$ on each part is particularly simple. This can be achieved by using the eigenvalue eigenvector decomposition on the matrix $\Phi^{(1,2)}$, i.e.,

$$\Phi^{(1,2)} = [V_s|V_N] \begin{bmatrix}\Lambda_s & | & 0 \\ \text{---} & & \text{---} \\ 0 & | & 0\end{bmatrix} \begin{bmatrix}V_s^{H} \\ \text{--} \\ V_N^{H}\end{bmatrix} \tag{8.1.19}$$

where, Λ_s denotes the nonzero eigenvalues which correspond to the signal

subspace, $\Lambda_s \in C^{K\times K}$, $\Lambda_s = \text{diag}(\lambda_1,\lambda_2,....,\lambda_K,0,0,....,0)$, matrix V_s represents the eigenvectors corresponding to the eigenvalue matrix Λ_s, V_N represents the eigenvectors corresponding to the null space and $V_s \in C^{M\times K}$, $V_N \in C^{M\times(M-K)}$.

The matrix P_m which is the resolution of identity is given by,

$$P_m = v_m(v_m^H v_m)^{-1}v_m^H, \quad m=1,2,....,M \tag{8.1.20}$$

where, v_m is the m^{th} eigenvector.

The matrix P_m can easily be shown to have the relationships,

$P_iP_j = 0, \quad i\neq j$

$P_m^H = P_m$, and

$$\sum_{m=1}^{M} P_m = I$$

where, I is an identity matrix.

The family of projections P_m, m=1,2,....,M can be used in unifying the spectrum estimation techniques as we have shown in chapter 5. Further, $\Phi^{(i,s)}$ can be written as,

$$\Phi^{(i,s)} = \sum_{m=1}^{K} \lambda_m P_m$$

In most of the high resolution spectrum estimation and high precision beam forming techniques, we have to use the inverse of the cross spectral density matrix. Therefore, if we are planning to use the inphase cross-cross spectral density matrix we have to consider the inverse of the inphase cross-cross spectral density matrix. The inverse of the inphase cross-cross spectral density matrix can be obtained as follows:

$$\{\Phi^{(i,s)}\}^{-1} = [V_s|V_N]\left[\begin{array}{c|c} \Lambda_s^{-1} & 0 \\ \hline 0 & \Lambda_N^{-1} \end{array}\right]\left[\begin{array}{c} V_s^H \\ \hline V_N^H \end{array}\right] \tag{8.1.21}$$

where, $\Lambda_s^{-1} = \text{diag}(\lambda_1^{-1},\lambda_2^{-1},....,\lambda_K^{-1})$, $\Lambda_N = \text{diag}(0,0,...,0)$

$\Lambda_N^{-1} = \text{diag}(\delta^{-1},\delta^{-1},...,\delta^{-1})$, $\Lambda_N \in C^{(M-K)\times(M-K)}$, and δ^{-1} is the largest number that can be achieved within the limitation of the computer.

The implication of the above inverse is very clear. It tries to give more emphasis to the noise subspace while giving negligible emphasis to the signal subspace. The same effect can also be observed if we substitute $\Lambda_s^{-1} = 0$, and $\Lambda_N^{-1} = I$, where I is an identity matrix, and 0 is a null matrix. This provides an important clue to the question why high resolution and super resolution array processing techniques perform equally with the use of inphase cross-cross spectral density matrix. It is due to the fact that:

$$\{\Phi^{(1,2)}\}^{-1} = P_N$$

where, P_N is the noise subspace projection matrix (refer to chapter 4)

The operator $\Phi^{(1,2)}$ can also be decomposed into signal subspace and noise subspace. The family of projections $\{P_s,P_N\}$ which represents the resolution of identity is then given by,

$$P_s = V_s[V_s^H V_s]^{-1}V_s^H \qquad (8.1.22)$$

$$P_N = V_N[V_N^H V_N]^{-1}V_N^H \qquad (8.1.23)$$

P_s and P_N have the property that,

$P_s^H = P_s$, $P_N^H = P_N$, $P_s + P_N = I$.

The projection matrices P_s or P_N are generally used in the MUSIC method.

After the study of the properties of the inphase cross-cross spectral density matrix, now we consider the use of that in beamforming and bearing estimation in array processing.

8.2 A Beamformer with Perfect Nulling Capabilities

Here, we develop an optimum beamformer using twin array system. Let

us consider the filter weights vector that is used in both arrays at n^{th} snapshot to be $w(n)$.

$w(n) = (w_1(n), w_2(n), \ldots, w_M(n))^T$.

Since the arrays in the twin array system are inphase with the incoming signals, we can use the same filter weights vector $w(n)$ with both the arrays.

If we pass all the data starting from the first snapshot to the n^{th} snapshot through the filter $w(n)$, the output of the i^{th} array can be written as,

$$e_n^{(i)*}(n) = U^{(i)H}(n)w(n) \tag{8.2.1}$$

where, $[.]^*$ denotes the complex conjugate of $[.]$, $e_n^{(i)}(n) \in C^{n\times 1}$, and $U^{(i)}(n) \in C^{M\times n}$, $i=1,2$.

For the array 1 and array 2, we obtain,

$$e_n^{(1)*}(n) = U^{(1)H}(n)w(n) \tag{8.2.2}$$

$$e_n^{(2)*}(n) = U^{(2)H}(n)w(n) \tag{8.2.3}$$

Now, we define a performance index E_{12} such that,

$$\begin{aligned} E_{12} &= \lim_{n\to\infty} 0.5\{(e_n^{(1)*})^H(e_n^{(2)*})+[(e_n^{(1)*})^H(e_n^{(2)*})]^H\} \\ &= \lim_{n\to\infty} 0.5\{[w^H(n)U^{(1)}(n)U^{(2)H}(n)w(n)]+[w^H(n)U^{(1)}(n)U^{(2)H}(n)w(n)]^H\} \\ &= w^H\Phi^{(1,2)}w \end{aligned} \tag{8.2.4}$$

Optimal filter weight vector w can be obtained by minimizing the performance index E_{12} while maintaining the desired signal unaltered, i.e.,

$$\text{minimize}_{w} \; w^H\Phi^{(1,2)}w \tag{8.2.5}$$

subject to the constraint $w^Hd(\theta_T) = 1$ (8.2.6)

where, $d(\theta_T)$ is the direction vector corresponding to the target signal or desired signal reaching at an angle θ_T.

The solution to the above minimization is straight forward and is given by,

$$W_{opt} = S_{ML}(\theta_T)\{\Phi^{(1,2)}\}^{-1}d(\theta_T) \qquad (8.2.7)$$

where, $S_{ML}(\theta)$ is the maximum likelihood spectrum and it is given by,

$$S_{ML}(\theta) = [d^H(\theta)\{\Phi^{(1,2)}\}^{-1}d(\theta)]^{-1} \qquad (8.2.8)$$

The spatial response $\Gamma(\theta)$ of the beamformer is given by,

$$\Gamma(\theta) = |W_{opt}{}^H d(\theta)| \qquad (8.2.9)$$

It has been shown earlier that the matrix $\Phi^{(1,2)}$ is independent of noise. Therefore, the optimal weight vector W_{opt} is also not affected by the noise. Therefore, $\Gamma(\theta)$ provide infinite nulls at the angles of interferences. It can also be seen intuitively that the performance index E_{12} can reach a minimum by placing perfect nulls at the angles of interferences.

8.3 Bearing Estimation without Any Resolution Limits

High resolution and super resolution spectrum estimation techniques provide infinite resolution in the presence of infinite signal to noise ratio (SNR) (chapter 5). The performance of the spectrum estimation techniques highly depend on the amount of noise and the spatial correlation of the noise.

Here, we present a method to overcome the above limitations by using twin array system and rederive the spectrum estimation techniques to achieve asymptotically infinite resolution.

8.3.1 Maximum Likelihood Spectrum Without Any Resolution Limits

In the course of deriving the beamformer given in the section 8.2, we obtained the maximum likelihood spectrum $S_{ML}(\theta)$,

$$S_{ML}(\theta) = [d^H(\theta)\{\Phi^{(1,2)}\}^{-1}d(\theta)]^{-1} \qquad (8.3.1)$$

$S_{ML}(\theta)$ does only depend on the signal environment and hence it can resolve the incoming signals without any resolution limit.

8.3.2 Linear Prediction Spectrum Without Any Resolution Limit

Linear prediction spectrum can be obtained by minimizing the performance index E_{in} under the constraint that the first element of the filter weight vector w is unity, i.e.,

$$\underset{w(n)}{\text{minimize}} \lim_{n\to\infty} 0.5\{(e^{(1)*}(n))^H(e^{(2)*}(n))+[(e^{(1)*}(n))^H(e^{(2)*}(n))]^H\} \tag{8.3.2}$$

subject to the constraint $w^H e_1 = 1$ (8.3.3)

where, $e_1 = (1,0,0,\ldots,0)^T$.

As the solution to the above minimization problem, we obtain the linear prediction spectrum, $S_{LP}(\theta)$ as,

$$S_{LP}(\theta) = [e_1^T\{\Phi^{(1,2)}\}^{-1}d(\theta)]^{-1} \tag{8.3.4}$$

As we see from the above relationship for $S_{LP}(\theta)$, linear prediction spectrum does not depend on noise and hence the spatial correlation properties of the noise. It only depends on the properties of the incoming signals. Therefore, it can resolve the incoming signals without any resolution limit.

8.3.3 POP-MUSIC Spectra

In general, POP-MUSIC method is formulated by using the cross spectral density matrix $\Phi^{(1,1)}$ and the noise only cross spectral density matrix $\Phi_{(v,v)}^{(1,1)}$. Generalized eigenvalue eigenvector decomposition is performed in obtaining the signal and noise subspace basis vectors.

In practice, the noise only cross spectral density matrix is not known and hence the use of the POP-MUSIC spectrum under spatially correlated noise environment will be limited. One way to overcome this difficulty is to estimate the noise only cross spectral density matrix under certain assumptions as we have mentioned in chapter 2. How good the spectral estimate is will depend on

how good the estimate of the noise only cross spectral density matrix is.

Here we propose a method whereby we can avoid the estimation of the noise only cross spectral density matrix. We use our inphase cross-cross spectral density matrix $\Phi^{(1,2)}$ which is not influenced by the noise or the spatial correlation of the sensor noise. As we have shown earlier the inphase cross-cross spectral density matrix can be written as,

$$\Phi^{(1,2)} = \sum_{m=1}^{K} \lambda_m P_m$$

where, P_m, m=1,2,....M is the resolution of identities.

In addition, resolution of identity $\{P_m, P_N\}$ for the signal subspace and noise subspace is related by,

$$P_m + P_N = I.$$

Let us project the direction vector $d(\theta)$ on to the null space to obtain the projection vector $d_N(\theta)$ given by,

$$d_N(\theta) = P_N d(\theta) \qquad (8.3.5)$$

Now we can define two POP-MUSIC spectra based on the Euclidian norm, and the elemental norm of the vector $d_N(\theta)$ as we did before. Then the POP-MUSIC-Euc spectrum and the POP-MUSIC-Elem spectrum can be written as

$$S_{POP-Euc}(\theta) = \|d_N(\theta)\|^{-1}$$

$$S_{POP-Elem}(\theta) = |d_{N(m_o)}|^{-2}$$

where, $d_{N(m_o)}$ is the m_o^{th} element of the vector $d_N(\theta)$, $\|.\|$ and $|.|$ denotes the Euclidian norm and the elemental norm respectively.

8.4 Comments on the Performance Under Finite Number of Snapshots

Under finite number of snapshots the cross spectral density matrix $\Phi^{(1,1)}(n)$ and the inphase cross-cross spectral density matrix $\Phi^{(1,2)}(n)$ are given by,

$\Phi^{(1,1)}(n) = D(\theta)\Phi_{ss}(n)D^{H}(\theta) + \Phi_{(\nu,\nu)}{}^{(1,1)}(n)$

$\Phi^{(1,2)}(n) = D(\theta)\Phi_{ss}(n)D^{H}(\theta) + \Phi_{(\nu,\nu)}{}^{(1,2)}(n)$.

Now let us consider the properties of the matrices $\Phi_{(\nu,\nu)}{}^{(1,1)}(n)$, and $\Phi_{(\nu,\nu)}{}^{(1,2)}(n)$.

1. (a) $\Phi_{(\nu,\nu)}{}^{(1,1)}(n)$ is Hermitian

   (b) $\Phi_{(\nu,\nu)}{}^{(1,2)}(n)$ is Hermitian.

2. $\lim_{n\to\infty} \Phi_{(\nu,\nu)}{}^{(1,1)}(n) = \Phi_{(\nu,\nu)}{}^{(1,1)}$

   $\lim_{n\to\infty} \Phi_{(\nu,\nu)}{}^{(1,2)}(n) = 0$

3. Since ν_1 and ν_2 are two independent processes it is reasonable to assume,

   $$\left[(i,j)^{th} \text{ element of } \Phi_{(\nu,\nu)}{}^{(1,2)}(n)\right] < \left[(i,j)^{th} \text{ element of } \Phi_{(\nu,\nu)}{}^{(1,1)}(n)\right]$$

   $\forall$ i,j and $\forall$ n.

From the above properties, it is clear that the matrix $\Phi^{(1,2)}(n)$ is less corrupted by noise compared to $\Phi^{(1,1)}(n)$. The influence of the noise on the inphase cross-cross spectral density matrix $\Phi^{(1,2)}(n)$ becomes zero when the number of snapshots are increased. The matrix $\Phi_{(\nu,\nu)}{}^{(1,2)}(n)$ can be made less significant for finite number of snapshots by choosing the distance ℓ_{12} between the twin array system properly. The larger is the distance ℓ_{12}, the less is the coupling between the noise vectors ν_1 and ν_2. One has the ability to choose the distance between the array 1 and array 2 as long as the coherencies between the arrays are maintained.

8.5 Summary

Inphase cross-cross spectral density matrix is derived using a twin array system. Properties of the inphase cross-cross spectral density matrix is studied

and it is shown that this matrix is not asymptotically influenced by the sensor noise or the spatial correlation of the sensor noise. Array processing techniques are rederived to make use of the superior properties of the inphase cross-cross spectral density matrix. The minimum variance distortionless response type beamformer that we have derived based on the inphase cross-cross spectral density matrix provides perfect nulling capabilities. The rederived bearing estimation techniques are capable of resolving the incoming signals without any resolution limit. In general, the use of the inphase cross-cross spectral density matrix is not limited to the array processing and it can be suitably extended to time series analysis where the deterministic signals are buried in random noise, very easily. In this case two realizations which have independent noise can be utilized to obtain the cross correlation matrix. Therefore, the use of the inphase cross-cross spectral density matrix provides a restart to the digital signal processing field as a whole.

CHAPTER 9

SUMMARY AND CONCLUSIONS

In adaptive array processing, eigenvalue eigenvector decomposition of the cross spectral density matrix provides the basis vectors of the signal and noise when the sensor noise are spatially uncorrelated. If the sensor noise are correlated, the generalized eigenvalue eigenvector decomposition or the generalized singular-value singularvector decomposition can be used in obtaining the vectors that lie in the noise subspace. The use of upper triangular matrices reduces the computation associated with the generalized singularvalue singularvector decomposition. The number of signals obtained by AIC or MDLC can then be used to partition the eigenvectors into the signal subspace and noise subspace eigenvectors. Based on the signal subspace and the noise subspace basis vectors, the proper orthogonal projection matrices for the signal subspace and noise subspace can be generated. The noise subspace projection matrix projects any vector with suitable dimensions onto the noise subspace while the signal projection matrix projects any vector with suitable dimensions onto the signal subspace. The noise subspace projection matrix or the signal subspace projection matrix provides the foundation for the super resolution bearing estimation techniques.

In bearing estimation, we have derived two spatial spectrum estimates, POP-MUSIC-Euc and POP-MUSIC-Elem, based on the proper orthogonal projection. POP-MUSIC-Euc and POP-MUSIC-Elem bear a very simple geometrical relationship. This relationship further provides an insight into the relation between the maximum likelihood method and linear prediction methods. The POP-

MUSIC-Euc gives strictly dominant spurious peaks free spatial spectrum. As far as POP-MUSIC-Elem is concerned, one cannot strictly guarantee a dominant spurious peaks free spectrum. The geometric relationship between POP-MUSIC-Euc and POP-MUSIC-Elem provides a very good explanation to the question why the signal peaks in POP-MUSIC-Elem are sharper compared to the POP-MUSIC-Euc. But, one should keep in mind that the sharpness is not a criterion for analyzing the performance of the spectrum estimation techniques. In obtaining the bearings from a spatial spectrum without any bias one has to plot the spectrum for infinitesimally small angular sampling which is impossible in practice. The spectrum obtained by interpolating the finite samples may lead to a bias in the bearing estimates. This can be avoided by using the POP-MUSIC-Euc and POP-MUSIC-Elem polynomials, dominant roots of which correspond to the bearings of the incoming signals. The minimum norm technique used in array processing is rediscovered and shown to be a special case of POP-MUSIC-Elem.

Spectrum representation is considered in a more general and unified framework based on the operator decomposition approach. Out of many possible families, we have considered two families of spectra, namely the Euclidian norm techniques (Euc-Techs), and the Elemental norm techniques (Elem Techs). Classical, high resolution, and super resolution spectrum estimation techniques are brought in to the unified framework. This unification shows that most of the spectrum estimation techniques available today only differ by the way they utilize the projection. According to our classification, spectrum estimation techniques are grouped into Euclidian norm techniques (Euc-Tech) and the elemental norm techniques (Elem-Tech). The Euc-Tech guarantee a dominant spurious peaks free spectrum while the Elem-Tech do not guarantee that. It is also clear that the POP-MUSIC-Euc is the only spectrum estimation technique

which provides both unbiased and guaranteed spurious peaks free spectrum. Rest of the spectrum estimation techniques could provide unbiased spectrum, provided that the signal to noise ratio is infinite.

If the true cross spectral density matrix is known, there is no limitation over the resolution capabilities of the POP-MUSIC-Euc and POP-MUSIC-Elem. But in practice, the use of the estimated cross spectral density matrix will cause a rotation in the signal as well as noise subspaces from the true subspaces. This rotation will limit the resolution capabilities of the high resolution and super resolution spectrum estimation techniques. The rotational correction multiple signal classification (ROC-MUSIC) tries to realign the estimated subspaces with the true subspaces. How good one can realign the estimated subspaces depends on the criterion used in guiding the rotation. ROC-MUSIC could not provide expected superiority due to the non availability of such a unique criterion in guiding the rotation. However, the criterion we used could provide improved resolution capabilities over the POP-MUSIC spectrum, at least for the chosen example.

In general, flipping technique provides an improved cross spectral density matrix estimate for symmetric arrays. Therefore, the use of the flipping technique can provide improvement to both the bearing estimation and beamforming. The flipped minimum variance distortionless response (FMVDR) beamformer is capable of placing strong nulls at the interferences. Conditional flipped minimum variance distortionless response (C-FMVDR) beamformer provides further improved nulling capabilities over the FMVDR beamformer. The strength of the null depends on the strength of the interference for both FMVDR and C-FMVDR beamformers. The greater is the strength of the interference, the greater is the strength of the null. Both FMVDR and C-FMVDR beamformers do not provide a

control over the amount of interference cancellation.

The minimum variance distortionless response type beamformers such as MVDR, EMVDR, and C-FMVDR, generally assume that the noise and interferences are equally detrimental to the system performance. But in most of the situations the interferences are more harmful to the system performance. This situation will become more severe when deliberate jammers are present. In this type of situation, it is important to give more weight to the interference cancellation. The blind reception (BR) beamformer is capable of cancelling the interferences more selectively by a prespecified amount. BR beamformer operates as a joint process of bearing estimation and interference cancellation. BR beamformer can also be used to receive any signal present at the array of sensors while rejecting the rest of the signals and hence it also acts as a listening device. The performance of the BR beamformer will be drastically degraded when the bearing estimates are biased. The robust blind reception beamformer is capable of overcoming this difficulty up to some extent. But still the performance of both the blind reception beamformer and robust blind reception beamformer depend on the accuracy of the bearing estimates. [illegible]stification of the blind reception beamformer for large biases in the bearing estimates still remains as an open problem.

Both bearing estimation and beamforming techniques fail to operate when the incoming signals are coherent. The bearing estimation and beamforming techniques preceded by the adaptive spatial data smoothing preprocessing (ASDSP) scheme appear to be preferable alternatives to the cross spectral density matrix smoothing in providing a way out of the problem associated with the coherent signal environments at high signal to noise ratios. Spatial smoothing demands the knowledge of the number of incoming signals and hence the

practical use of the spatial smoothing will be limited. To overcome this problem, we have proposed a methodology to estimate the number of signals and the optimal number of subarrays concurrently. Based on the proposed methodology, spatial smoothing can be performed without the knowledge of the number of incoming signals. Spatial smoothing scheme fails to perform successfully at low signal to noise ratios. The solution to the array processing problem under coherent signal environment at low signal to noise ratios is yet to be found.

We have also initiated a restart to array processing and digital signal processing in general. The array processing techniques are rederived. Under this restart, it is shown that the high resolution and super resolution spectrum estimation techniques perform equally without resolution limit, while the MVDR type beamformers perform with infinite nulling capabilities. This restart is not limited to array processing. It can also be used in time series analysis or more appropriately in time sequence analysis. In time sequence analysis, two realizations which has the same signal component and independent noise can be used to obtain the cross correlation matrix which is asymptotically same as the noise free autocorrelation matrix. A thorough investigation of this restart remains to be done.

APPENDICES

Appendix 2a

Jacobi-Givens rotation and systolic array structure for matrix triangularization:

Jacobi-Givens rotation Q is an elementary orthogonal transformation in the form of plane rotation and it can be used to annihilate the elements of a vector or a matrix more selectively. The matrix $Q_{\ell m}$ which annihilate the $(\ell,m)^{th}$ element of a vector or a matrix can be written as,

$$q_{ik} = \begin{cases} \cos\alpha & i = k = \ell \\ \sin\alpha \exp(j\beta) & i = \ell\ ,\ k = m \\ -\sin\alpha \exp(-j\beta) & i = m\ ,\ k = \ell \\ \cos\alpha & i,k = m \\ 1 & i,k = 1,2,\ldots,\text{excluding } \ell \text{ and } m \\ 0 & \text{otherwise} \end{cases}$$

The product of $Q_{\ell m}U(n)$ can be written as,

$$Q_{\ell m}U(n) = \begin{bmatrix} \cdots & \cdots & \cdots \\ \cdots & \cos\alpha & \sin\alpha\exp(j\beta) \\ \cdots & \cdots & \cdots \\ \cdots & -\sin\alpha\exp(-j\beta) & \cos\alpha \\ \cdots & \cdots & \cdots \end{bmatrix} \begin{bmatrix} \vdots \\ u_{mm}(n) \\ \vdots \\ u_{\ell m}(n) \\ \vdots \end{bmatrix}$$

By selecting,

$$\cos\alpha = \frac{|u_{mm}(n)|}{[|u_{mm}(n)|^2+|u_{\ell m}(n)|^2]^{1/2}}\ , \qquad \sin\alpha = \frac{|u_{\ell m}(n)|}{[|u_{mm}(n)|^2+|u_{\ell m}(n)|^2]^{1/2}}$$

$\theta = \arg(u_{mm}(n)) - \arg(u_{\ell m}(n))$, one can annihilate the element $u_{\ell m}(n)$.

Jacobi-Givens rotation can be used to triangularize a given matrix

adaptively using the systolic array structure shown in Fig. 2.1(chapter 2). Matrix triangularization systolic array structure consists of boundary cells and internal cells which have the following functions:

Boundary cells

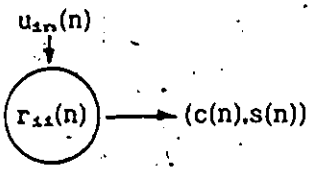

$r_{ii}(n)$ is the $(i,i)^{th}$ component of the upper triangular matrix $R^{M}(n)$.

If $u_{in}(n) = 0$, then $c(n) = 1$, $s(n) = 0$,

Otherwise,

$r_{ii}(n) = [|r_{ii}((n-1))|^{2}+|u_{in}(n)|^{2}]^{1/2}$

$$c(n) = \frac{|r_{ii}((n-1))|}{|r_{ii}(n)|}, \qquad s(n) = \frac{|u_{in}(n)|}{|r_{ii}(n)|}$$

$r_{ii}(n) = |r_{ii}(n)|\exp(j \arg(r_{ii}((n-1))))$

$\beta = \arg[r_{ii}((n-1))] - \arg[u_{in}(n)]$, $s(n) = |s(n)| \exp(j\beta)$, $\forall$ i

Internal cell

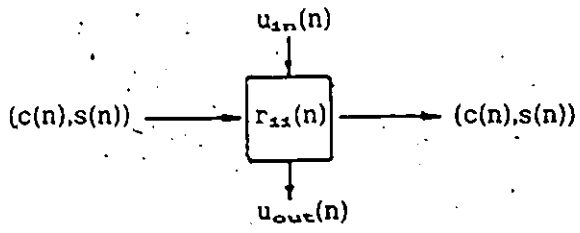

$r_{ij}(n)$ is the $(i,j)^{th}$ component of the upper triangular matrix $R^{M}(n)$.

$u_{out}(n) = c(n)u_{in}(n) - s^{*}(n)r_{ij}((n-1))$

$r_{ij}(n) = s(n)u_{in}(n) + c(n)r_{ij}((n-1))$, Initialization: $r_{ij}(0) = (0,0)$, $\forall$ i,j

The diagram for the assembly of Jacobi-Givens rotation is given as a part of the Fig. 2.1.

Appendix 2b

Solution to the Generalized Eigenvalue Eigenvector Decomposition using Generalized singularvalue singularvector decomposition

When we solve the generalized eigenvalue eigenvector decomposition with the direct use of the data matrices without forming the cross spectral density matrix pencil $(\Phi(n),\Phi_{\downarrow\downarrow}(n))$, it is called the generalized singularvalue singularvector decomposition.

The generalized singularvalue singularvector decomposition directly operates on the data matrices or upper triangularized data matrices $R^{H}(n)$ and $R_{\downarrow}^{H}(n)$ given in eqns. (2.2.2) and (2.2.5) respectively in providing the solution to the generalized eigenvalue eigenvector decomposition of the matrix pencil $(\Phi(n),\Phi_{\downarrow\downarrow}(n))$. The generalized singularvalue singularvector decomposition problem can be stated as the solution to,

$$R(n)R^{H}(n)v(n) = \lambda(n)R_{\downarrow}(n)R_{\downarrow}^{H}(n)v(n) \qquad (2b.1)$$

The generalized singularvectors are equal to the generalized eigenvectors whereas the generalized singularvalues are the square roots of the generalized eigenvalues.

Van Loan (1976) has given a procedure for obtaining the generalized singularvalue singularvector decomposition by using the input data matrices, i.e.

$$U(n)U^{H}(n)v(n) = \lambda(n)U_{\downarrow}(n)U_{\downarrow}^{H}(n)v(n). \qquad (2b.2)$$

The direct use of input data matrices are computationally more involved and not suitable for adaptivity. Therefore we use the same algorithm given by Van Loan (1976) [Speiser and Van Loan (1981)] but instead of the data matrix pencil $(U(n),U_{\downarrow}(n))$, we use the upper triangularized matrix pencil $(R^{H}(n), R_{\downarrow}^{H}(n))$ with fixed dimensions and hence we reduce the computations and achieve a better structure for adaptivity.

The generalized singularvalue singularvector decomposition can be achieved by using the following procedure:

1. Compute the singularvalue decomposition of the matrix G

$$G = \begin{bmatrix} R(n) \\ \hline R_{\smile}(n) \end{bmatrix} = \begin{bmatrix} Q(n) \\ \hline Q_{\smile}(n) \end{bmatrix} \Sigma(n) Z^{H}(n) \qquad (2b.3)$$

where, $\Sigma(n) = \mathrm{diag}(\varepsilon_1(n),\varepsilon_2(n),\ldots,\varepsilon_M(n))$ (2b.4)

$Z(n)$ is a unitary matrix, $Q(n)$ and $Q_{\smile}(n)$ satisfy the equality,

$$Q^{H}(n)Q(n) + Q_{\smile}^{H}(n)Q_{\smile}(n) = I \qquad (2b.5)$$

with I being a identity matrix.

2. Compute unitary matrices $X(n), X_{\smile}(n)$ and $Y(n)$ such that,

$$X^{H}(n)Q(n)Y(n) = \mathrm{diag}(c_1(n),c_2(n),\ldots,c_M(n)), \quad c_m(n)\geq 0 \qquad (2b.6)$$

$$X_{\smile}^{H}(n)Q_{\smile}(n)Y(n) = \mathrm{diag}(s_1(n),s_2(n),\ldots,s_M(n)), \quad s_m(n)\geq 0 \qquad (2b.7)$$

where, $\{c_m(n)\}^2 + \{s_m(n)\}^2 = 1$, $m = 1,2,\ldots,M$, $X(n)$, $Y(n) \in C^{M\times M}$

3. Set, $V(n) = [v_1(n),v_2(n),\ldots,v_M(n)]$ (2b.8)

$$= Z(n)\Sigma^{-1}(n)Y(n) \qquad (b4.9)$$

and $[\lambda_m(n)]^{\frac{1}{2}} = c_m(n)/s_m(n)$. (b4.10)

Then $[\lambda_m(n)]^{\frac{1}{2}}$, $m = 1,2,\ldots,M$ denotes the generalized singularvalues. The columns of $V(n)$ consist of the generalized singularvectors after n^{th} snapshot. The above algorithm is applied irrespective of whether the matrices in the matrix pencil $(\Phi(n),\Phi_{\smile\smile}(n))$ are ill-conditioned or not.

Appendix 2c

Computation of the Hermitian Matrix used in the Alternative Formulation

In the alternative formulation given in the array processing we have the

computational task of $\Phi'(n)$, given by,

$$\Phi'(n) = [R_{\nu}(n)]^{-1}\Phi(n)[R_{\nu}^{H}(n)]^{-1}$$
$$= [R_{\nu}(n)]^{-1}[\phi_1(n),\phi_2(n),....,\phi_M(n)][R_{\nu}^{H}(n)]^{-1} \quad (2c.1)$$
$$= [a_1(n),a_2(n),....,a_M(n)][R_{\nu}^{H}(n)]^{-1}$$

where $\phi_m(n)$ is the m^{th} column of the matrix $\Phi(n)$ and $a_m(n)$ is given by the relationships,

$$[R_{\nu}(n)]^{-1}\phi_m(n) = a_m(n)$$

i.e. $$R_{\nu}(n)a_m(n) = \phi_m(n) \quad (2c.2)$$

Since $R_{\nu}(n)$ is lower triangular, eqn (2c.2) can be solved by forward substitution (Appendix 2d).

Now we can write eqn. (2c.1) as,

$$\Phi'(n) = A(n)[R_{\nu}^{H}(n)]^{-1} \quad (2c.3)$$

where $A(n) = [a_1(n),a_2(n),....,a_M(n)]$.

By taking Hermitian transpose on both sides of eqn. (2c.3) we get,

$$\Phi'^{H}(n) = [R_{\nu}(n)]^{-1}A^{H}(n)$$
$$= [R_{\nu}(n)]^{-1}[a_1'(n),a_2'(n),....,a_M'(n)] \quad (2c.4)$$
$$= [b_1(n),b_2(n),....,b_M(n)]$$

where $a_m'(n)$ is the m^{th} column of $A^{H}(n)$, and $b_m(n)$ is given by the relation ships,

$$[R_{\nu}(n)]^{-1}a_m'(n) = b_m(n)$$

i.e. $$R_{\nu}(n)b_m(n) = a_m'(n) \quad (2c.5)$$

Once again, eqn. (2c.5) can be solved for $b_m(n)$ by forward substitution.

Let $B(n) = [b_1(n),b_2(n),....,b_M(n)]$, then , by taking Hermitian transpose on eqn. (2c.4), we obtain, $\Phi'(n) = B^{H}(n)$.

Appendix 2d

Systolic array structure for forward and backward substitution

Forward substitution:

Consider the solution to the eqn. (2.2.5).

$R_{\nu}(n)a_m(n) = \phi_m(n)$.

This can be solved by forward substitution. Let $a_{im}(n)$ be the i^{th} element of the $a_m(n)$, and $r_{\nu(ik)}(n)$ be the ik^{th} element of $R_{\nu}(n)$, then we have,

$$a_{im}(n) = \frac{\phi_{im}(n)-\xi_i^{(i)}}{r_{\nu(ii)}}, \text{ for } i = 1,2,\ldots,M$$

where: $\phi_{im}(n)$ is the i^{th} element of $\phi_m(n)$ and $\xi_i^{(i)}$ can be obtained from the following equations,

$\xi_i^{(1)} = 0$

$\xi_i^{(k)} = \xi_i^{(k-1)} + r_{\nu(i,k-1)}(n)a_{(k-1)m}(n)$, $k = 1,2,\ldots,i$.

This structure can be implemented using a linear array. Basic nature of the linear array is given in Fig. 2d shown below.

Backward substitution:

Consider the solution to the eqn. (2.2.6).

$R_{\nu}^{M}(n)b_m(n) = a_m(n)$.

This can be solved by backward substitution. Let $b_{im}(n)$ be the i^{th} element of $b_m(n)$. Then,

$$b_{im}(n) = \frac{a_{im}(n)-\eta_i^{(i)}}{[r_{\nu(ii)}(n)]^*}, \text{ for } i = M,M-1,\ldots,1$$

where, $\eta_i^{(k)}$ can be obtained from the following equations:

$\eta_i^{(M)} = 0$

$\eta_k^{(k-1)} = \eta_k^{(k)} + [r_{x(k)}(n)]^* b_{kk}(n)$; $k = M, M-1, \ldots, 1$.

This structure can be implemented using a linear array. More detail about linear array can be found in Haykin (1986). Basic nature of the linear array is given below.

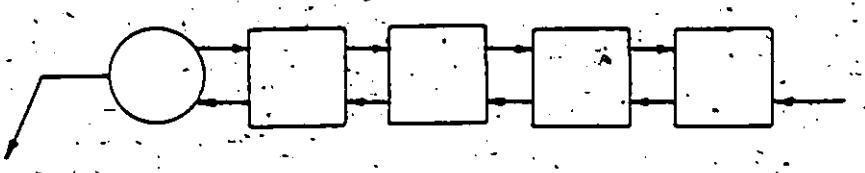

Fig. 2.2 Linear array [Kung and Leiserson (1979)]

Appendix 4a

The effect of the variance of the noise on the eigenvalues and eigenvectors

Let us consider the variance of the noise is σ^2 and the true cross spectral density matrix is Φ. Then the eigenvalue decomposition of Φ and the noise corrupted cross spectral density matrix $\Phi + \sigma^2 I$ can be written as,

$\Phi v = \lambda v$ and (4a.1)

$[\Phi + \sigma^2 I]v' = \lambda' v'$ (4a.2)

where, λ' and v' are the noise corrupted eigenvalues and eigenvectors. λ and v are the true eigenvalues and eigenvectors.

By rearranging the eqn. (4a.2), we obtain,

$\Phi v' = (\lambda' - \sigma^2) v'$ (4a.3)

Comparing eqn. (4a.1) and (4a.2) we get,

$\lambda' = \lambda + \sigma^2$, and $v' = v$.

Therefore the eigenvalues of the cross spectral density matrix is affected by the variance of the noise whereas the eigenvectors are unaffected.

Appendix 4b

Geometric representation of maximum likelihood (ML) and linear prediction (LP) spectra

Maximum likelihood (ML) [Capon (1969)]

The maximum likelihood spectrum, $S_{ML}(n,\theta)$ is generally given by [Haykin (1986)],

$$S_{ML}(n,\theta) = [d^H(\theta)\Phi^{-1}(n)d(\theta)]^{-1} \tag{4b.1}$$

By using the eigenvalue and eigenvector decomposition of the cross spectral density matrix $\Phi(n)$, given by,

$$\Phi(n) = V(n)\Lambda(n)V^H(n)$$

we obtain,

$$S_{ML}(n,\theta) = [d^H(\theta)V(n)\Lambda^{-1}(n)V^H(n)d^H(\theta)]^{-1} \tag{4b.2}$$

where, $V(n) \in C^{M\times M}$ contains the normalized eigenvectors as its columns, and

$\Lambda(n) = \text{diag}(\lambda_1(n),\lambda_2(n),....,\lambda_M(n))$.

Let, $P_m(n) = v_m(n)v_m^H(n)$, (4b.3)

where, $v_m(n)$ is the m^{th} orthonormal eigenvector.

The matrix $P_m(n)$ is Hermitian and idempotent, and hence it represents the projection matrix for the m^{th} basis vector. Now, let us project the direction vector $d(\theta)$ on to the m^{th} basis vector to obtain the projection $d_m(\theta)$.

$$d_m(\theta) = P_m(n)d(\theta). \tag{4b.4}$$

Using eqn. (4b.4), the ML spectrum given in eqn. (4b.2) can be written as,

$$S_{ML}(n,\theta) = [\sum_{m=1}^{M} \lambda_m^{-1}(n)\ d^H(\theta)P_m(n)d(\theta)]^{-1} \tag{4b.5}$$

$$= [\sum_{m=1}^{M} \lambda_m^{-1}(n)\ |d_m(\theta)|^2]^{-1} \tag{4b.6}$$

where, $|.|$ is the Euclidian norm.

Therefore in the maximum likelihood method we first project the direction vector on to the signal and noise space basis vectors separately. Then the square of the Euclidian norm of the projections will be weighted by the reciprocal of their respective eigenvalues. Finally, the reciprocal of the sum of the weighted projections will provide the maximum likelihood spectrum.

Linear prediction (LP) method

The linear prediction (LP) spectrum estimate, $S_{LP}(n,\theta,m_o)$ is expressed as [Haykin (1986)],

$$S_{LP}(n,\theta,m_o) = |e_{m_o}^T \Phi^{-1}(n) d(\theta)|^{-\alpha} \tag{4b.7}$$

where, e_{m_o} is a null vector except the m_o^{th} element being unity.

Again using the eigenvalue eigenvector decomposition of the cross spectral density matrix, we obtain,

$$S_{LP}(n,\theta,m_o) = |\sum_{m=1}^{M} \lambda_m^{-1}(n)\ e_{m_o}^T P_m(n) d(\theta)|^{-\alpha} \tag{4b.8}$$

$$= |\sum_{m=1}^{M} \lambda_m^{-1}(n)\ d_{m(m_o)}(\theta)|^{-\alpha} \tag{4b.9}$$

Therefore, the linear prediction can be interpreted as follows:

First we obtain the projection of the direction vector on to the signal and noise space basis vectors separately. Second, the m_o^{th} elements of the projections are weighted by the reciprocal of the respective eigenvalues. Then the reciprocal of the square of the weighted sum of the m_o^{th} element of the projections represent the linear prediction spectral estimate.

Appendix 4c

The effect of random sensor motion on the cross spectral density matrix and its eigenvector space

Our derivation follows a similar line as that of Wong and Niezgoda (1986). We assume that the sensor motion along the array and perpendicular to the array are independent. Under this assumption, we can study the lateral sensor motion and the perpendicular sensor motion separately. First, we consider the lateral sensor motion or the sensor motion along the axis of the array. Let us consider that there are K number of signals arriving at an array consist of M elements.

The direction vector $d(\theta_k)$ for unperturbed array can be written as,

$$d(\theta_k) = (1, z_k, z_k^2, \ldots, z_k^{M-1})^T , \tag{4c.1}$$

$$z_k = \exp\left(j \frac{2\pi \ell}{\lambda} \sin \theta_k\right) \tag{4c.2}$$

For the perturbed array, the direction vector $d'(n,\theta_k)$ at n^{th} snapshot can be written as,

$$d'(n,\theta_k) = \Xi(n,\theta_k) d(\theta_k) \tag{4c.3}$$

where, $\Xi(n,\theta_k) = \mathrm{diag}(1, z_{k2}'(n), z_{k3}'(n), \ldots, z_{kM}'(n))$, (4c.4)

z_{km}' is the sensor perturbation effect of the m^{th} element of the array and it is given by,

$$z_{km}' = \exp(j\xi_{km}(n)), \quad \xi_{km}(n) = \frac{2\pi}{\lambda} \Delta\ell_m(n) \sin \theta_k,$$

$\Delta\ell_m(n)$ is the perturbation of the m^{th} element at n^{th} snapshot, $m > 1$.

Now, under the assumption that the signal-signal, noise-noise, and signal-noise are uncorrelated, the instantaneous M^{th} order cross spectral density matrix at n^{th} snapshot for the perturbed array can be written as,

$$\Phi^{(M)'}(n) = \sum_{k=1}^{K} s_k s_k^* \, d'(n,\theta_k)[d'(n,\theta_k)]^H + \Phi_{vv}^{(M)}(n) \tag{4c.5}$$

where $[.]^*$ denotes the complex conjugate of $[.]$ and $[.]^H$ denotes the Hermitian transpose of $[.]$.

The M^{th} order cross spectral density matrix $\Phi^{(M)'}$ of the perturbed array is then given by,

$$\Phi^{(M)'} = E[\Phi^{(M)'}(n)] \tag{4c.6}$$

where, $E[.]$ denotes the expectation operator.

Eqn. (4c.6) can also be written as,

$$\Phi^{(M)'} = E[\sum_{k=1}^{K} \Xi(n,\theta_k) d(\theta_k) \, s_k(n) s_k^*(n) \, d^H(\theta_k) \Xi^H(n,\theta_k)] + \sigma_v^2 I \tag{4c.7}$$

where, $E[\Phi_{vv}^{(M)}(n)] = \sigma_v^2 I$ (4c.8)

Eqn. (4c.7) can be written as,

$$\Phi^{(M)'} = E[\sum_{k=1}^{K} \Xi(n,\theta_k) \Phi_{sss_k}(n) \Xi^H(n,\theta_k)] + \sigma_v^2 I \tag{4c.9}$$

where, $\Phi_{sss_k}(n)$ is the k^{th} signal-signal cross spectral density matrix.

More elaborately,

$$\Phi^{(M)} = \sum_{k=1}^{K} \begin{bmatrix} E[\phi_{ssk}^{(1,1)}(n) + \sigma_v^2/K, \\ E[\phi_{ssk}^{(1,2)}(n)\exp(-j\xi_{k2}(n))], \\ E[\phi_{ssk}^{(1,3)}(n)\exp(-j\xi_{k3}(n))], \\ \quad \ldots, \phi_{ssk}^{(1,M)}(n)\exp(-\xi_{kM}(n))] \\ \\ E[\phi_{ssk}^{(2,1)}(n)\exp(j\xi_{k2}(n))], \\ E\phi_{ssk}^{(2,2)}(n)] + \sigma_v^2/K, \\ E[\phi_{ssk}^{(2,3)}(n)\exp(j(\xi_{k2}(n)-\xi_{k3}(n)))], \\ \ldots, E[\phi_{ssk}^{(2,M)}(n)\exp(j(\xi_{k2}(n)-\xi_{kM}(n)))] \\ \\ E[\phi_{ssk}^{(3,1)}(n)\exp(j\xi_{k3}(n))], \\ E[\phi_{ssk}^{(3,2)}(n)\exp(j(\xi_{k3}(n)-\xi_{k2}(n)))], \\ E[\phi_{ssk}^{(3,3)}(n)+\sigma_v^2/K \\ \ldots, E[\phi_{ssk}^{(3,M)}(n)\exp(j(\xi_{k3}(n)-\xi_{kM}(n)))] \\ \\ \\ \\ \\ E[\phi_{ssk}^{(M,1)}(n)\exp(j\xi_{kM}(n))], \\ E[\phi_{ssk}^{(M,2)}(n)\exp(j(\xi_{kM}(n)-\xi_{k2}(n)))], \\ E[\phi_{ssk}^{(M,3)}(n)\exp(j(\xi_{kM}(n)-\xi_{k3}(n)))], \\ \quad \ldots, E[\phi_{ssk}^{(M,M)}(n)] + \sigma_v^2/K \end{bmatrix} \tag{4c.10}$$

Sensor motion at all the sensors are assumed to be independent each other with the same distribution. Further, it is also assumed that the incoming signals are uncorrelated with the sensor motion. Then we obtain,

$$E[\phi_{ssk}^{(i,m)}(n)\exp(j(\xi_{ki}(n)-\xi_{km}(n)))] =$$

$$E[\phi_{ssk}^{(i,m)}(n)]\, E[\exp(j\xi_{ki}(n))]\, E[\exp(-j\xi_{km}(n))]$$

$$= \phi_{ssk}^{(i,m)}\, |E[\exp(j\xi_k)]|^2, \tag{4c.11}$$

$i \neq m$, $i \neq 1$, $m \neq 1$, for all i,m, and

$$E[\phi_{ssk}^{(i,i)}(n)\exp(j\xi_{ki}(n))] = E[\phi_{ssk}^{(i,i)}(n)]\, E[\exp(j\xi_{ki}(n))]$$

$$= \phi_{ssk}^{(i,i)}\, E[\exp(j\xi_k)] \tag{4c.12}$$

$i \neq 1$, for all i,

$$E[\phi_{ssk}^{(i,m)}(n)\exp(-j\xi_{km}(n))] = E[\phi_{ssk}^{(i,m)}(n)]\, E[\exp(-j\xi_{km}(n))]$$

$$= \phi_{ssk}^{(i,m)}\, E[\exp(-j\xi_k)],\ m \neq 1, \text{ for all } m. \tag{4c.13}$$

In eqns. (4c.11), (4c.12), and (4c.13), $\xi_{km}(n)$ is assumed to have the same dis-

tribution for all m and hence $\xi_{km}(n)$ is replaced by ξ_k.

Under the assumption that ξ_k is Gaussian distributed, its characteristic function can be written as,

$$E[\exp(j\rho\xi_k)] = \int_{-\infty}^{+\infty} P(\xi_k)\exp(j\rho\xi_k)\, d\xi_k$$

$$= \exp(-0.5\rho\sigma_{\xi k}^2) \qquad (4c.14)$$

where, $\sigma_{\xi k}^2$ is the variance of the random Gaussian sequence ξ_k, and $P(\xi_k)$ is the probability of the random sequence ξ_k.

Since, $\xi_k = \frac{2\pi}{\lambda} \sin\theta_k \Delta\ell$, (4c.15)

$$\sigma_{\xi k}^2 = (\frac{2\pi}{\lambda} \sin\theta_k)^2 \sigma_s^2 \qquad (4c.16)$$

where, σ_s^2 is the variance of the sensor perturbation.

When $\rho = 1$, $E[\exp(j\xi_k)] = \exp(-0.5\sigma_{\xi k}^2)$ and hence,

$$|E[\exp(j\xi_k)]|^2 = \exp(-\sigma_{\xi k}^2). \qquad (4c.17)$$

Now, M dimensional cross spectral density matrix for the perturbed array can be written as,

$$\Phi^{(M)'} = \sum_{k=1}^{K} \begin{bmatrix} \phi_{mmk}^{(1,1)}+\sigma_v^2/K, & \phi_{mmk}^{(1,2)}\exp(-0.5\sigma_{\phi k}^2), & \phi_{mmk}^{(1,3)}\exp(-0.5\sigma_{\phi k}^2), & \ldots, \phi_{mmk}^{(1,M)}\exp(-0.5\sigma_{\phi k}^2) \\ \phi_{mmk}^{(2,1)}\exp(-0.5\sigma_{\phi k}^2), & \phi_{mmk}^{(2,2)}+\sigma_v^2/K, & \phi_{mmk}^{(2,3)}\exp(-\sigma_{\phi k}^2), & \ldots, \phi_{mmk}^{(2,M)}\exp(-\sigma_{\phi k}^2) \\ \phi_{mmk}^{(3,1)}\exp(-0.5\sigma_{\phi k}^2), & \phi_{mmk}^{(3,2)}\exp(-\sigma_{\phi k}^2), & \phi_{mmk}^{(3,3)}+\sigma_v^2/K, & \ldots, \phi_{mmk}^{(3,M)}\exp(-\sigma_{\phi k}^2) \\ \vdots & \vdots & \vdots & \vdots \\ \phi_{mmk}^{(M,1)}\exp(-0.5\sigma_{\phi k}^2), & \phi_{mmk}^{(M,2)}\exp(-\sigma_{\phi k}^2), & \phi_{mmk}^{(M,3)}\exp(-\sigma_{\phi k}^2), & \ldots, \phi_{mmk}^{(M,M)}+\sigma_v^2/K \end{bmatrix} \quad (4c.18)$$

$$= \Phi^{(M)} + \Delta\Phi_r^{(M)} \quad (4c.19)$$

where, $\Delta\Phi_r^{(M)}$ represents the error introduced due to the random sensor motion and $\Phi^{(M)}$ represents the M^{th} order cross spectral density matrix of the unperturbed array.

From eqn. (4c.18), it can be seen that only the off diagonal elements of the unperturbed cross spectral density matrix are affected by the random sensor motion. The off diagonal elements are modified by the factor $\exp(-\sigma_{\phi k}^2)$ except the first row and the first column which are modified by the factor $\exp(-0.5\sigma_{\phi k}^2)$. This difference is obvious since we have observed the perturbation with respect to the first sensor. The error matrix $\Delta\Phi_r^{(M)}$ in eqn. (4c.19) is non-diagonal irrespective of the number of signals K. Therefore, the eigenvector space of the M^{th} order perturbed cross spectral density matrix will be the rotated version of the eigenvector space of the M^{th} order unperturbed cross spectral density matrix. The amount of rotation depends on the variance of

the random sensor motion.

Now, instead of considering the M^{th} order cross spectral density matrix, let us consider the $M-1^{th}$ order cross spectral density matrix that can be obtained as follows:

By partitioning the M^{th} order cross spectral density matrix $\Phi^{(M)}$ such that,

$$\Phi^{(M)} = \left[\begin{array}{c|c} \phi^{(1,1)'} & c^{M} \\ \hline c & \Phi^{(M-1)'} \end{array}\right] \tag{4c.20}$$

$\Phi^{(M-1)'} \in C^{(M-1)\times(M-1)}$, $c \in C^{(M-1)\times 1}$, and $\phi^{(1,1)'}$ is the $(1,1)^{th}$ element of the matrix $\Phi^{(M)'}$.

By comparing the eqn. (4c.18) and (4c.19), we obtain,

$$\Phi^{(M-1)'} = \sum_{k=1}^{K} \left[\begin{array}{l} \phi_{mmk}{}^{(m,m)}+\sigma_v{}^2/K, \\ \phi_{mmk}{}^{(m,o)}\exp(-\sigma_{\ell k}{}^2), \\ \phi_{mmk}{}^{(m,4)}\exp(-\sigma_{\ell k}{}^2), \\ \qquad \ldots, \phi_{mmk}{}^{(m,M)}\exp(-\sigma_{\ell k}{}^2) \\ \\ \phi_{mmk}{}^{(o,m)}\exp(-\sigma_{\ell k}{}^2), \\ \phi_{mmk}{}^{(o,o)}+\sigma_{\ell k}{}^2/K, \\ \phi_{mmk}{}^{(o,4)}\exp(-\sigma_{\ell k}{}^2), \\ \qquad \ldots, \phi_{mmk}{}^{(o,M)}\exp(-\sigma_{\ell k}{}^2) \\ \\ \phi_{mmk}{}^{(4,m)}\exp(-\sigma_{\ell k}{}^2), \\ \phi_{mmk}{}^{(4,o)}\exp(-\sigma_{\ell k}{}^2), \\ \phi_{mmk}{}^{(4,4)}+\sigma_v{}^2/K, \\ \qquad \ldots, \phi_{mmk}{}^{(4,M)}\exp(-\sigma_{\ell k}{}^2) \\ \\ \qquad \vdots \qquad \vdots \qquad \vdots \\ \\ \phi_{mmk}{}^{(M,m)}\exp(-\sigma_{\ell k}{}^2), \\ \phi_{mmk}{}^{(M,o)}\exp(-\sigma_{\ell k}{}^2), \\ \phi_{mmk}{}^{(M,4)}\exp(-\sigma_{\ell k}{}^2), \\ \qquad \ldots, \phi_{mmk}{}^{(M,M)}+\sigma_v{}^2/K \end{array}\right] \tag{4c.21}$$

$$= \Phi^{(M-1)} + \Delta\Phi_r{}^{(M-1)}. \tag{4c.22}$$

For $K \neq 1$, the perturbation error matrix $\Delta\Phi_r{}^{(M-1)}$ is non diagonal and hence the random perturbation give rise to a rotation of the eigenvector space. The

amount of rotation depend on the variance of the sensor motion.

A very interesting observation can be made if there is only one signal present at the array. For K=1, the perturbed M-1th order cross spectral density matrix given in eqn. (4c.21) can proportionately be written as,

$$\Phi^{(M-1)'} = \begin{bmatrix} \phi^{(1,1)}\exp(-\sigma_{\phi k}^2), & \phi^{(1,2)}, & \phi^{(1,3)}, & \ldots, & \phi^{(1,M)} \\ \phi^{(2,1)}, & \phi^{(2,2)}\exp(-\sigma_{\phi k}^2), & \phi^{(2,3)}, & \ldots, & \phi^{(2,M)} \\ \phi^{(3,1)}, & \phi^{(3,2)}, & \phi^{(3,3)}\exp(-\sigma_{\phi k}^2), & \ldots, & \phi^{(3,M)} \\ \cdot & \cdot & \cdot & \cdots & \cdot \\ \cdot & \cdot & \cdot & \cdots & \cdot \\ \phi^{(M,1)}, & \phi^{(M,2)}, & \phi^{(M,3)}, & \ldots, & \phi^{(M,M)}\exp(-\sigma_{\phi k}^2) \end{bmatrix} \quad (4c.23)$$

$$= \Phi^{(M-1)} + \Delta\Phi_r^{(M-1)} \quad (4c.24)$$

where, $\Delta\Phi_r^{(M-1)} = \text{diag}((\exp(-\sigma_{\phi k}^2)-1)\phi^{(1,1)}, (\exp(-\sigma_{\phi k}^2)-1)\phi^{(2,2)}, \ldots, (\exp(-\sigma_{\phi k}^2)-1)\phi^{(M,M)})$. (4c.25)

From eqn. (4c.24), it is clear that, when there is only one signal present at the array, the effect of the random sensor motion is to modify the perturbed M-1th order cross spectral density matrix by a diagonal matrix $\Delta\Phi_r^{(M-1)}$. Therefore, the eigenvectors of the M-1th order cross spectral density matrix does not affect by the random perturbation of the sensors (Appendix 4a). However, the eigenvectors of $\Phi^{(M)'}$ will not be the same as those of unperturbed $\Phi^{(M)}$.

Up to now we have considered the effect of the random sensor motion in the plane of the array. The effect of the random sensor motion in the plane perpendicular to the array will be the same except that the variance $\sigma_{\phi k}^2$ is substituted by the value $(\frac{2\pi}{\lambda}\cos\theta_k)^2\sigma_{z_k}^2$, where $\sigma_{z_k}^2$ is the variance of the sensor motion perpendicular to the array.

REFERENCES

Akaike, H., (1973), 'Maximum likelihood identification of Gaussian autoregressive moving average models', Biometrica, [illegible] 60.

Akaike, H., (1974),' A new look at the statistical model identification', IEEE Trans. Automatic Control, vol 19.

Bartlett, M. S., (1953), 'An introduction to stochastic process with special reference to methods and applications', Cambridge university press, New York.

Bievenu, G., and L. Kopp, (1983), 'Optimality of high resolution array processing using the eigensystem approach', IEEE Trans. ASSP, vol. ASSP 31, No. 5, October.

Borgiotti, G. V., and L. J. Kaplan, (1979), 'Super resolution of uncorrelated interference sources by using adaptive array techniques', IEEE Trans. on Antennas and Propagation, AP 27, 6, Nov.

Brent, R. P., and F. T. Luck, (1985), 'The solution of singularvalue and symmetric eigenvalue problems on multiprocessor arrays', SIAM J. Sci. Stat. Comput.,vol. 6, no. 1, January.

Bromley, K., and H, J. Whitehouse, (1981), 'Signal processing technology overview', SPIE vol. 298, Real time signal processing IV.

Burg, J. P., (1967), 'Maximum entropy spectral analysis', 37th Ann. Inter. Meeting, Soc. Explor. Geophysics, Oklahoma City, Okle.

Burg, J. P., (1968), 'A new analysis technique for time series data' NATO advanced study institute on signal processing, Enschede, Holland.

Capon, J., (1969), 'High resolution frequency wavenumber spectrum analysis', Proc. IEEE, vol. 57.

Chan, T. F., (1982), 'An improved algorithm for computing the singularvalue decomposition', ACM Trans. on Mathematical Software, vol. 8, no. 1, March.

Citron, T. K., and T. Kailath, (1984), 'An improved eigenvector beamformer', IEEE ICASSP.

Dahanayake, B. W., and K. M. Wong, (1986), 'Proper orthogonal projection multiple signal classification (POP-MUSIC)', IEEE ICASSP, Tokyo.

Dahanayake, B. W., and K. M. Wong, (1986),' A new method of array processing: blind reception beamformer', Signal Processing III: Theories and Applications, I. T. Young et al. (editors), Elsevier science publishers B. V. (North Holland).

Dahanayake, B.W., and K. M. Wong, (1987), 'Unified approach to spectrum estimation', IASTED international symposium on signal processing and its applications (ISSPA)', University of Queensland, Brisbane, Australia.

Dahanayake, B. W., (1987) 'A new method of array processing', IEEE, ICASSP, Dallas, TX.

Dahanayake, B. W., (1987) 'Bearing estimation by QZ and VZ decomposition', IEEE, ICASSP, Dallas, TX.

Evans, J. E., J. R. Johnson, and D. F. Sun, (1982), 'Application of advanced signal processing techniques to angle of arrival estimation in ATC navigation and surveillance', Technical report 582, Lincoln laboratory, Massachusetts Institute of Technology, June.

Gabriel, W. F., (1980), 'Spectral analysis and adaptive array super resolution techniques', Proceedings of the IEEE, 68, June.

Gentleman, W. M., and H. T. Kung, (1981), 'Matrix triangularization by systolic arrays', SPIE vol. 298, Real time signal processing IV.

Haykin, S., (editor) (1985), 'Array processing', Prentice Hall, Inc., Englewood cliffs, New Jersey.

Haykin, S., (1986), 'Adaptive filter theory', Prentice Hall, Englewood cliffs, New Jersey

Johnson, D. H., and S. R. DeGraaf, (1982), 'Improving the resolution of bearing in passive sonar arrays by eigenvalue analysis', IEEE Trans. ASSP, vol. ASSP 30, No. 4, August.

Johnson, D. H., (1982), 'The application of spectral estimation methods to bearing estimation problems' Proceedings of the IEEE, vol. 70, No. 9, September.

Kailath, T. (editor), (1985), 'Modern signal processing', Hemisphere publishing corporation, Washington.

Kaufman, L., (1974), 'The LZ algorithm to solve the generalized eigenvalue problem', SIAM J. Numer. Anal., vol. 11, No. 5, October.

Kaufman, L., (1977), 'Some thoughts on the QZ algorithm for solving the generalized eigenvalue problem' ACM Trans. on mathematical software, vol. 3, No. 1, March.

Kaveh, M., and A. J. Barabell, (1986) 'The statistical performance of the MUSIC and the minimum norm algorithms in resolving plane waves in noise', IEEE Trans. on ASSP, vol. ASSP 34, No. 2, April.

Kaveh, M., H. Wang, and H. Hung, (1987), 'On the Theoretical performance of a class of estimators of the number of narrow band sources', IEEE Trans. on ASSP, vol. ASSP 35, No. 9, September.

Kumaresan, R., and D.W. Tufts, (1983), 'Estimating the angles of arrival of multiple plane waves', IEEE Trans. Aerospace and Electronic Systems,vol. AES 19.

Kung, H. T., and C. E. Leiserson, (1979), 'Systolic arrays (for VLSI)', Sparse matrix proc., Soc. Industrial and Appl. Math.

Kung, H. T., (1982), 'Why systolic architectures', IEEE Computer, vol. 15.

Kung, H. T., H. J. Whitehouse, and T. Kailath, (editors), (1986), 'VLSI and modern signal processing', Prentice Hall, Englewood cliffs, New Jersey.

Kung, S. Y., (1985), 'VLSI array processing', IEEE ASSP magazine, vol. 2, No. 3.

Luk, F.-T., (1980), 'Computing the singularvalue decomposition on the ILLIAC IV', ACM Trans. on Mathematical software, vol. 6, No. 4, December.

Matsuoka, T., and T. J. Ulrych, (1980), 'Information theory measures with application to model identification', IEEE Trans. ASSP, vol. ASSP 34, No. 3, June.

McDonough, R. N., (1974), 'Maximum entropy spatial processing of array data', Geophysics, vol. 39, No. 6, December.

McWhirter, J. G., (1983), 'Recursive least squares minimization using systolic array', Proc. SPIE, vol. 431, Real time signal processing IV.

Mermoz, H. F., (1981), 'Spatial processing beyond adaptive beamforming', J. Acoust. Soc. Amer., 70(1), July.

Moler, C. B., and G. W. Stewart, (1973), 'An algorithm for generalized matrix eigenvalue problems', SIAM J. Numer. Anal., vol. 10, No. 2, April.

Monzingo, R. A., and T. W. Miller, (1980), 'Introduction to adaptive arrays', Wiley-Interscience, New York.

Naylor, A. W., and G. R. Sell, (1971), 'Linear operator theory in engineering and science', Holt, Rinehart and Winston, Inc.

Orfanidis, S. J., (1985), 'Optimal signal processing: An introduction', MacMillan publishing company, New York.

Paige, C. C., and M. A. Saunders, (1981), 'Towards a generalized singularvalue decomposition', SIAM J. Numer. Anal., vol. 18, No. 3, June.

Paulraj, A., R. Roy, and T. Kailath, (1986), 'A subspace rotation approach to signal parameter estimation', Proceedings of the IEEE, July.

Peters, G., and J. H. Wilkinson, (1970), 'Ax=λBx and the generalized eigenproblem', SIAM J. Numer. Anal., vol. 7, No. 4, December.

Pisarenko, V. F., (1972), 'On the estimation of spectra by means of non linear functions of the covariance matrix', Geophys. J. R. astro. soc., 28.

Reilly, J. P., (1986), Personal communication

Schmidt, R. O., (1979), 'Multiple emitter location and signal parameter estimation', RADC spectrum estimation workshop. This paper is reproduced in the 1986 special issue of IEEE Trans. on antennas and propagation.

Schmidt, R. O., (1982), 'A signal subspace approach to multiple emitter location and spectrum estimation', PhD dissertation, Stanford University, Stanford, California.

Shan, T. J., and T. Kailath, (1985), 'Adaptive beamforming for coherent signals and interference', IEEE Trans. on ASSP, vol. ASSP 33, No. 3, June.

Shan, T. J., M. Wax, and T. Kailath, (1985), 'On spatial smoothing for direction of arrival estimation of coherent signals', IEEE Trans. on ASSP, vol. ASSP 33, No. 4, August.

Speiser, J. M., and H. J. Whitehouse, (1981), 'Parallel processing algorithms and architectures for real time signal processing', SPIE vol. 298, Real time signal processing IV.

Speiser, J. M., and H. J. Whitehouse, (1983), 'Techniques for spatial signal processing with systolic arrays', Proceedings of the workshop on the applications of high resolution spatial processing held at Gulfport, MI, October.

Speiser, J. M., and C. Van Loan, (1984), 'Signal processing computations using the generalized singularvalue decomposition', SPIE vol. 495, Real-time signal processing VII.

Stewart, G. W., (1972), 'On the sensitivity of the eigenvalue problem', SIAM J. Numer. Anal., vol. 9, No. 4, December.

Tufts, D. W., and R. Kumaresan, (1982), 'Estimation of frequencies of multiple sinusoides: making linear prediction perform like maximum likelihood', Proc. IEEE, vol. 70.

Van Loan, C. F., (1975), 'A general matrix eigenvalue algorithm', SIAM J. Numer. Anal., vol 12, No. 6, December.

Van Loan, C. F., (1976), 'Generalizing the singularvalue decomposition', SIAM J. Numer. Anal., vol. 13, No. 1, March.

Wang, H., and M. Kaveh, (1985), 'Coherent signal subspace processing for the detection and estimation of angle of arrival of multiple wide band sources', IEEE Trans. on ASSP, vol. ASSP 33, No. 4, August.

Wang, H., and M. Kaveh, (1986), 'On the performance of signal subspace processing - part 1: narrow band systems', IEEE Trans. on ASSP, vol. ASSP 34, No. 5, October.

Ward, R. C., (1975), 'The combination shift QZ algorithm', SIAM J. Numer. Anal., vol. 12, No. 6, December.

Wax, M., and T. Kailath, (1984), 'Determining the number of signals by information theoretic criteria', IEEE, ICASSP, San Diego, CA.

Wong, K. M., and G. Niezgoda, (1986), 'Effects of random sensor motion and finite precision arithmetic on bearing estimation by the MUSIC algorithm', CRL report No. 170, August.

Wong, K. M., (1987), Personal communication.

Zhao, L. C., P. R. Krishnaiah, and Z. D. Bai, (1986), 'On detection of the number of signals in presence of white noise', Journal of multivariate analysis', 20, 1-25.

Zhao, L. C., P. R. Krishnaiah, and Z. D. Bai, (1987), 'Remarks on certain criteria for detection of number of signals', IEEE Trans. on ASSP, vol. ASSP 35, No. 2, February.